

**Potential implication of silver nanoparticles on biological wastewater treatment**

By

**Zhiya Sheng**

A thesis submitted in partial fulfillment of the requirements for the degree of

**Doctor of Philosophy**

in

**Environmental Engineering**

Department of Civil and Environmental Engineering

University of Alberta

© Zhiya Sheng, 2016

## **Abstract**

Nano-silver is the most popular nanomaterial in commercial products. However, its wide use also becomes a concern because Ag-NPs can have potential adverse effects on biological wastewater treatment processes due to its strong antibacterial property. Considerable efforts have been made to study the effects of Ag-NPs on biological wastewater treatment, but great controversy still exists.

The research in this dissertation focused on engineered ecosystems including biofilm and activated sludge used in biological wastewater treatment processes. Ag-NPs were applied to isolated single strains from biological wastewater treatment plants, laboratory mixed cultures with isolated strains, and activated sludge and biofilms, to gain insights on the rules governing the effects of Ag-NPs on microbial communities in complicated ecosystems in biological wastewater treatment. To assess the protective effects of extracellular polymeric substances (EPS), biofilms without loosely bound EPS were also tested. Doses of Ag-NP applied ranged from 1 to 200 mg Ag/L. 1% PBS buffer was used to mimic wastewater environment; real and synthetic wastewater was also tested. 16s rRNA gene based polymerase chain reaction — denaturing gradient gel electrophoresis (PCR-DGGE) was used to analyze the microbial community shift after Ag-NP treatment. Transmission electron microscopy (TEM) was used to examine the biofilm uptake of Ag-NPs. qPCR was used to quantify changes in total bacteria and the abundance of selected bacteria group. GeoChip analysis was done to investigate the effects of Ag-NPs on the functional structure of the microbial community. 16s rRNA gene based

pyrosequencing was used to monitor the compositional change in the bacterial community. The properties of the sludge, accumulation of silver species inside the sludge, and characteristics of the Ag-NPs were examined to explain observed the phenomena.

Results were compared and the tolerance from the lowest to the highest followed the order: single strain < laboratory mixed culture < activated sludge in laboratory reactor < biofilm without loosely bound EPS < original biofilm. Higher tolerance corresponds with higher community diversity and more compact EPS structure. Stimulatory effects of Ag-NPs under low dose were detected under certain conditions, indicating that the effects of Ag-NPs may conform to the hormetic model. Considering the high robustness of full-scale biological wastewater treatment processes, they may be able to stand a relatively high concentration of Ag-NPs and a potentially wider stimulatory dose range can even be observed compared with laboratory systems. However, the higher biomass concentration and community diversity caused by Ag-NPs does not correspond with improved reactor performance and can potentially trigger the appearance of “superbugs” that would pose a significant danger to the health of the public and environment.

## **Preface**

This thesis is an original work by Zhiya Sheng under supervision of Dr. Yang Liu.

Chapter 3 of this thesis has been published as Sheng, Z. and Y. Liu (2011). "Effects of silver nanoparticles on wastewater biofilms." *Water Research* 45 (18): 6039-6050. Chapter 4 of this thesis has been published as Sheng, Z. .; J. D. Van Nostrand; Zhou J.; Liu Y (2015). "The effects of silver nanoparticles on intact wastewater biofilms." *Frontiers in Microbiology* 6: 680. In addition, a version of Chapter 6 has been published as Sheng, Z.; Mohammed, A.; Liu, Y (2016). "Stability of full-scale engineered ecosystem under disturbance: Response of an activated sludge biological nutrient removal reactor to high flow rate condition." *International Biodeterioration & Biodegradation* 109: 88-95. Chapter 5 have also been submitted for publication in refereed journal as original research and a version of Chapter 2 has been submitted as a review for journal publication as well. Appendix C has also been published in the conference proceedings on the 2010 IWA World Water Congress and Exhibition by Ikehata, K., Sun, R.N., Sheng, Z., Stuart, D. and Liu, Y.

## **Acknowledgements**

I would like to thank my supervisor, Dr. Yang Liu for her guidance and support during my entire graduate study. Dr. Liu is the one who brought me into the field of environmental engineering, and I have learned so much from her, not only knowledge in this field but also the way to do research. Her passion in her research and her amazing insights inspired me so much that I would never have been able to complete this work without her. It was a great pleasure to have the opportunity to work under Dr. Liu's supervision.

My appreciation also goes to Dr. David Stuart and Dr. Nicholas Ashbolt for serving on my Ph.D. committee and for providing valuable advices on this research. I would also like to give my special thanks to Dr. Jim Bolton, who not only gives me invaluable guidance on my research and English as my committee member but also is always being there for me as a friend. I am truly thankful for his support when I was in difficult times. I would also like to extend my sincerest thanks and appreciation to Dr. Ian Buchanan and Dr. Joo Hwa Tay for the time and effort they spent on my thesis and oral examination.

I would like to gratefully acknowledge Dr. Joy Van Nostrand and Dr. Jizhong Zhou for their support on GeoChip analysis. In addition, working with Abdul Mohammed at EPCOR was a very valuable experience and I really appreciate Mr. Mohammed's guidance and encouragement in our work in the full-scale wastewater treatment plant.

I would also like to thank Dr. Keisuke Ikehata and Xuejiao Yang who have guided me when I first started here and Dr. Ming Chen, Chen Liang, Jody Yu, Elena Dlusskaya, David Zhao, Jela

Burkus, Dr. Xuejun Sun and Priscilla Gao who have taught me many techniques that I have used in my experiments, assisted our analysis and supported our research. I am also very grateful to all our group members in Dr. Yang Liu's lab. I am sorry that I cannot put all of their names here since the list is too long, but I will never forget any of their help.

I would also like to say thank you to my family and friends. I could never have completed my study without their support. Their help and encouragement means a lot to me, and I will be grateful for that all the time. I am so lucky to have them and would like to thank them from the bottom of my heart.

Finally, my sincerest thanks to the financial supports from the Natural Sciences and Engineering Research Council of Canada (NSERC) Discovery, NSERC Research Tools and Instruments, Canadian School of Energy and the Environment, and the Alberta Ingenuity Graduate Scholarship in Nanotechnology, MSc and the Alberta Innovates Graduate Student Scholarship (PhD in Nanotechnology).

## **Table of contents**

<b>Abstract.....</b>	<b>ii</b>
<b>Acknowledgements .....</b>	<b>v</b>
<b>List of Figures.....</b>	<b>x</b>
<b>List of Tables .....</b>	<b>xiv</b>
<b>List of Abbreviations .....</b>	<b>xv</b>
<b>Chapter 1 Introduction .....</b>	<b>1</b>
1.1 Overview.....	1
1.2 Objectives .....	2
1.3 Organization of the dissertation.....	3
<b>Chapter 2 Literature review .....</b>	<b>5</b>
2.1 Introduction.....	5
2.2 Tests based on bacterial single strains .....	6
2.3 Laboratory mixed cultures .....	11
2.4 Mixed cultures in natural and engineering systems.....	12
2.5 Mechanism of antimicrobial effects and resistance .....	15
2.6 Conclusions and outlook.....	17
<b>Chapter 3 Effects of Silver Nanoparticles on Wastewater Biofilms.....</b>	<b>19</b>
3.1 Introduction.....	19
3.2 Material and Methods .....	22
3.3 Results.....	28

3.4	Discussion .....	41
3.5	Conclusions.....	46
<b>Chapter 4 The effects of silver nanoparticles on intact wastewater biofilms.....</b>		<b>47</b>
4.1	Introduction.....	47
4.2	Materials and methods .....	50
4.3	Results.....	55
4.4	Discussion .....	66
4.5	Conclusions.....	68
<b>Chapter 5 Contradictory effects of silver nanoparticles on activated sludge wastewater treatment.....</b>		<b>70</b>
5.1	Introduction.....	70
5.2	Material and Methods .....	72
5.3	Results.....	75
5.4	Discussion .....	85
5.5	Conclusions.....	89
<b>Chapter 6 Investigation on the stability of full-scale wastewater biological treatments for potential disturbance .....</b>		<b>91</b>
6.1	Introduction.....	91
6.2	Materials and Methods.....	94
6.3	Results.....	98
6.4	Discussion .....	109

6.5	Conclusions.....	111
<b>Chapter 7 Conclusions and recommendations.....</b>		<b>112</b>
7.1	Conclusions.....	112
7.2	Recommendations and future research .....	114
<b>Bibliography .....</b>		<b>116</b>
<b>Appendix A Supporting information for effects of silver nanoparticles on wastewater biofilms.....</b>		<b>145</b>
<b>Appendix B Supporting information for the effects of silver nanoparticles on intact wastewater biofilms .....</b>		<b>152</b>
<b>Appendix C Investigation on other nanoparticles .....</b>		<b>159</b>
<b>VITA.....</b>		<b>170</b>

## List of Figures

- Figure 2-1** Dose-response curve reflecting the effects of Ag-NPs. .... 18
- Figure 3-1** Size distribution of freshly prepared and 24-h-old Ag-NPs in 1% PBS and water suspensions. .... 29
- Figure 3-2** Community profile of wastewater biofilms: (A) phylogenetic tree based on DGGE bands and isolated single strains (Pairwise identities between neighbor branches are indicated on the tree); (B) DGGE profiles of the original biofilm sample (Lane 1) and the R2A media enriched biofilm culture (Lane 2). .... 30
- Figure 3-3** Physical protections in wastewater biofilms: (A) SEM image of original wastewater biofilms; (B) SEM image of wastewater biofilms with loosely bound EPS removed. Bar size: 5  $\mu$ m. (C) peak absorption (400 nm) of remaining Ag-NPs in suspensions during incubation with wastewater biofilms at various initial concentrations (0, 1, 20, 50 mg Ag/L). .... 32
- Figure 3-4** Effects of Ag-NPs (200 mg Ag/L) on wastewater biofilms with (A, C, and E) and without (B, D, and F) loosely bound EPS, compared with the no treatment control (error bars represent one standard deviation): (A) (B) growth of heterotrophic bacteria 24 h after plating; (C) (D) growth of heterotrophic bacteria 4 days after plating; (E) (F) DGGE profile (C represents the no treatment control, while T represents a biofilm community under 200 mg Ag/L Ag-NP treatment. Missing bands are marked with arrows)..... 36

**Figure 3-5** Viability of planktonic bacteria isolated from wastewater biofilms: (A) single culture after different time periods of Ag-NP treatment (1 mg Ag/L); (B) individual strains in mixed cultures (biofilm mixture and artificial mixture) after 24 h of Ag-NP treatment (1 mg Ag/L) compared with the no treatment control. .... 40

**Figure 4-1** Transmission electron microscopy (TEM) images. (A) Ag-NPs in wastewater, (B) Original wastewater biofilms, (C), (D) Wastewater biofilms incubated with Ag-NPs for 45 min, (E), (F) Wastewater biofilms incubated with Ag-NPs for 24 h. Ag-NPs are indicated by white arrows. .... 56

**Figure 4-2** Effects of Ag-NP treatment on gene abundance. (A) Relative abundance of genes in each category, (B) The number of genes detected; the fraction of positive genes detected after Ag-NP treatment is labeled on top of the bar..... 58

**Figure 4-3** Effects of Ag-NP treatment on genes associated with nutrient and pollutant removals. N indicates samples with no treatment and Ag-NP indicates samples with Ag-NP treatment. .... 60

**Figure 4-4** Effects of Ag-NP treatment on genes associated with silver resistance. N indicates samples with no treatment and Ag-NP indicates samples with Ag-NP treatment. Colors are coded according to the lineage; genes from gene variants present only in Ag-NP treated samples are indicated with black arrows. .... 62

**Figure 4-5** Effects of Ag-NP treatment on genes associated with oxidative stress. N indicates samples with no treatment and Ag-NP indicates samples with Ag-NP treatment. Colors are

<p>coded according to the lineage; genes from gene variants present only in Ag-NP treated samples are indicated with black arrows. ....</p>	64
<p><b>Figure 4-6</b> qPCR results. N indicates samples with no treatment and Ag-NP indicates samples with Ag-NP treatment. Error bar indicates standard deviation. ....</p>	65
<p><b>Figure 5-1</b> Performance of each reactor. (A) Effluent COD concentration; (B) Effluent ammonia concentration; (C) COD removal kinetics; (D) Ammonia removal kinetics; (E) Nitrate production kinetics. ....</p>	77
<p><b>Figure 5-2</b> Sludge property in each reactor. (A) MLSS concentration; (B) SVI; (C) Floc size on day 64; (D) Sludge EPS concentration on day 64. ....</p>	79
<p><b>Figure 5-3</b> Microbial diversity analysis. (A) Relative abundance of bacteria families; (B) PCoA analysis of microbial community diversity; (C) 2D projection of PCoA analysis on axis PC2 and PC3; (D) The number of genes detected in each functional category; (E) Detrended correspondence analysis of functional gene diversity; (F) Heatmap of the top 30 abundant functional genes; Sample S0: The initial activated sludge inoculum; S1: Sludge after the thirty-day startup stage; S2: Sludge in reactor with aged Ag-NPs, day 8; S3: Sludge in reactor with fresh Ag-NPs, day 14; S4: Sludge in reactor with only PVP as control, day 64; S5: Sludge in reactor with aged Ag-NPs, day 64; S6: Sludge in reactor with fresh Ag-NPs, day 64; S7: Sludge in reactor with Ag<sup>+</sup> released from fresh Ag-NPs, day 64. ....</p>	81

**Figure 5-4** Silver species accumulation and release. (A) Silver release via effluent; (B) Silver accumulation in activated sludge. Silver concentrations in effluent and sludge from the PVP control reactor were both below the detection limit..... 84

**Figure 6-1** Configuration of Bioreactor #1 and sampling locations numbered in the order from inlet to outlet..... 95

**Figure 6-2** Bioreactor performance during high-flow test. (A)(B)(C)(D), COD, ammonia, orthophosphate, and nitrate in influent and effluent; (E)(F), COD and ammonia removal in each zone; (G) Phosphorous release and removal in the bioreactor (N: Normal flow; H1-5: High flow Day 1-5; Ammonia, nitrate, and orthophosphate were presented as ammonia nitrogen ( $\text{NH}_3\text{-N}$ ), nitrate nitrogen ( $\text{NO}_3\text{ --N}$ ) and phosphorus ( $\text{PO}_4\text{ --P}$ ), respectively; error bars represent one standard deviation). ..... 100

**Figure 6-3** Microbial community changes in the bioreactor. (A) Changes in relative abundance of bacteria at family level during high-flow test; (B) Seasonal variations in relative abundance of bacteria at family level; (C) PCoA analysis of microbial community diversity; (D) Abundance of ammonia-oxidizing bacteria; (E) Abundance of nitrite-oxidizing bacteria; (F) Total bacteria number (N: Normal flow; H1: High flow Day 1; H4: High flow Day 4)..... 105

**Figure 6-4** BioWin model results. (A) Simulated MLSS variation with conditions changed in series; (B) Effluent quality simulation based on the final model (Day 0 indicates normal flow condition). ..... 108

## List of Tables

Table 2-1	Single strain dose-response to Ag-NPs. ....	7
Table 3-1	Sorption of Ag-NPs to wastewater biofilms.....	34
Table 3-2	Colonial morphology and growth rate of isolated biofilm bacteria. ....	39
Table 4-1	qPCR primers and conditions.....	54
Table 4-2	Viability of heterotrophic bacteria in intact wastewater biofilms under Ag-NP treatment. .....	57
Table 5-1	Diversity index of microbial community and functional genes. ....	82
Table 5-2	Particle characterization and silver dissolution. ....	83
Table 6-1	qPCR primers and conditions.....	97
Table 6-2	Biomass change during high-flow test. ....	102

## List of Abbreviations

Ag-NPs	silver nanoparticles
AOB	Ammonia oxidizing bacteria
BOD	biochemical oxygen demand
bTEFAP	bacterial tag-encoded FLX amplicon pyrosequencing
BWTS	biological wastewater treatment system
CFU	colony-forming units
COD	chemical oxygen demand
DCA	detrended correspondence analysis
EPS	extracellular polymeric substances
HPC	heterotrophic plate count
HRT	hydraulic retention time
ICP-MS	inductively coupled plasma mass spectrometry
IFAS	integrated fixed-film activated sludge
LIPUS	low-intensity pulsed ultrasound
MIC	minimum inhibitory concentration
MLSS	mixed liquor suspended solids
MLVSS	mixed liquor volatile suspended solids
MSBR	membrane coupled sequencing batch reactor
NOB	nitrite oxidizing bacteria

OTUs	operational taxonomic units
PCoA	principal coordinate analysis
PCR-DGGE	polymerase chain reaction — denaturing gradient gel electrophoresis
PVP	polyvinylpyrrolidone
R2A	Reasoner's 2A
RBCs	rotating biological contactors
ROS	reactive oxygen species
SEM	scanning electron microscopy
SRT	solid retention time
SVI	sludge volume index
TEM	transmission electron microscopy
T-RFLP	terminal restriction fragment length polymorphism
WWTPs	wastewater treatment plants

## **Chapter 1 Introduction**

### **1.1 Overview**

Nano-silver has been the most commonly used nanomaterial in consumer products for years (2014). It is inevitable that silver nanoparticles (Ag-NPs) could be released into the environment (Benn and Westerhoff, 2008, Hagendorfer et al., 2010). Due to its strong antibacterial property, nano-silver becomes a concern of potential adverse effects on biological wastewater treatment processes.

Considerable efforts have been made to study the effects of Ag-NPs on biological wastewater treatment. However, great controversy still exists in this field as summarized below. First of all, the effects of Ag-NPs are dose dependent, but the minimum inhibitory concentration (MIC) varies significantly in each study (Kim et al., 2007, Raffi et al., 2008, Xiu et al., 2012, Yang et al., 2013). Second, the effects of Ag-NPs vary with the size, shape and coating (Morones et al., 2005, Pal et al., 2007, Kvítek et al., 2008, Vertelov et al., 2008, Choi and Hu, 2008, Zhang et al., 2008a, Arnaout and Gunsch, 2012). The last and the most complicated, the effects of Ag-NPs strongly depends on the system tested, and it is very difficult to compare between different systems. For example, it depends on the strain of bacteria tested, contact time, pH and presence of ligands. It becomes more complex when laboratory mixed culture or engineered ecosystems, such as activated sludge or biofilm are tested (Lok et al., 2006, Smetana et al., 2008, Fabrega et al., 2009a, Anderson et al., 2014, Kumar et al., 2014, Priester et al., 2014).

The research in this dissertation focused on engineered ecosystems, including biofilm and activated sludge used in biological wastewater treatment processes. Ag-NPs were applied to isolated single strains, laboratory mixed cultures, and activated sludge and biofilms, to gain insights on the rules governing the effects of Ag-NPs on microbial communities in complicated ecosystems in biological wastewater treatment.

## **1.2 Objectives**

The overall objective of this study was to elucidate the rules governing the effects of Ag-NPs on biological wastewater treatment processes. To achieve the overall goal, the specific objectives in each section of the study are as follows:

- a) To test different doses of Ag-NPs and to apply Ag-NPs under various conditions to reveal the dose response to Ag-NPs and relationships between treatment conditions and the response.
- b) To explore the effects of Ag-NPs on systems from isolated single strains, laboratory mixed culture to activated sludge and biofilm, and to analyse the effects on Ag-NPs on the microbial community in complicated engineered ecosystems in order to discover the factors that lead to the different impacts of Ag-NPs on various systems.
- c) To study the robustness of full-scale biological wastewater treatment processes under disturbance to gain insights on the scale-up rules on the potential implications of Ag-NPs on real-world biological wastewater treatment.

### **1.3 Organization of the dissertation**

Following the instruction, Chapter 2 summarizes observations in previous publications and generates a possible theoretical model on the effects of Ag-NPs, especially under the low dose range. Evidence of homeotic effects has been collected from pure culture to engineered ecosystems, and factors controlling the dose limits and width of the stimulatory zone have been analyzed.

Chapter 3 contains a paper that examines the effects of Ag-NPs on both original wastewater biofilms and isolated planktonic pure culture bacteria from the biofilms. To assess the protective effects of extracellular polymeric substances (EPS), biofilms without loosely bound EPS were also tested. Ag-NP doses applied range from 1 to 200 mg Ag/L and 1% PBS buffer was used to mimic the wastewater environment. The role of community interactions was also studied, and an artificially mixed community was tested to verify the effects of the community interaction. 16S rRNA gene based polymerase chain reaction — denaturing gradient gel electrophoresis (PCR-DGGE) was used to analyze the microbial community shift after Ag-NP treatment.

Chapter 4 describes the effects of Ag-NPs on intact wastewater biofilms. Tests were performed in wastewater from a local plant to provide the same pH, ionic strength, and natural organic matter present in the plant. Transmission electron microscopy (TEM) was used to examine the biofilm uptake of Ag-NPs. qPCR was used to quantify changes in total bacteria and the abundance of selected bacteria group. GeoChip analysis was carried out to investigate the effects of Ag-NPs on the functional structure of the microbial community in the biofilm. The

abundance of functional genes in 12 categories was monitored. Functional redundancy and its role in the tolerance of wastewater biofilms to Ag-NPs is discussed.

Chapter 5 describes a long-term study under low dose of Ag-NPs on reactors with activated sludge treating synthetic municipal wastewater, which is more similar to the conditions of released Ag-NPs in real wastewater treatment plants. Positive effects were observed and could be repeated stably. 16s rRNA gene based pyrosequencing was used to monitor the bacterial community, and GeoChip was used to examine directly the functional diversity of the microbial community. The properties of the sludge, accumulation of silver species inside the sludge, and characteristics of the Ag-NPs were examined to explain this phenomenon.

Chapter 6 contains an observational study of the stability of a full-scale wastewater treatment bioreactor under flow-rate disturbance and seasonal variation. Both reactor performance and microbial community profile were monitored. Dissolved chemical oxygen demand (COD), ammonia, nitrate, and orthophosphate phosphorus, were monitored in a series of locations in the bioreactor. Biomass concentration and sludge settleability were also examined. Also, 16S rRNA gene-based 454 pyrosequencing was undertaken to track variations in the microbial communities in each zone. A BioWin model was constructed to simulate the performance and biomass dynamics of the full-scale wastewater treatment plant under increased flow rate. The study showed that microbial community in the full-scale bioreactor was stable in terms of both composition and function.

Chapter 7 concludes the research in this dissertation and also provides thoughts for future study.

## **Chapter 2 Literature review**

### **2.1 Introduction**

Nano-silver has been the most commonly used nanomaterial in consumer products (2014) since the boom of nanotechnology in commercial products. It is inevitable that nano-silver will be released into the environment (Benn and Westerhoff, 2008, Hagendorfer et al., 2010). This raises a question: What are the effects of silver nanoparticles (Ag-NPs) on microbes in the environment and biological wastewater treatment processes? Considerable efforts have been made to answer this question, and research has shown that the effects of Ag-NPs depend on the dose, the time period applied, the property of Ag-NPs (size, shape and coating, etc.), and the system to which Ag-NPs are applied. The system can vary from pure culture to complicated engineered ecosystems.

However, substantial controversy exists on how each of these parameters affects the impact of Ag-NPs, and a sophisticated toxicology model has not been built. Previous research covers only a tip of the iceberg of all possible combinations of these parameters. Not to mention that the mechanisms behind the phenomena are poorly understood. In recent years, more and more studies tend to focus on long-term effects of Ag-NPs under real-world conditions, that is, relatively low concentrations of Ag-NPs and the presence of all kinds of ligands.

While the antibacterial activity under sufficient concentration is the major application of Ag-NPs, the most noteworthy gap in our knowledge concerns the effects of Ag-NPs under sublethal concentration. Experiments testing the hormetic effects of many antibiotics under

sublethal concentrations date back to the late 1890s, although the concept has stayed marginalized so far (Calabrese, 2001, 2002). Stimulatory bacterial response to low dose Ag-NP treatment has been detected occasionally but often overlooked. Therefore, it worth to think about the question now: In biological wastewater treatment, does the response of microbes to Ag-NPs conform with the hormetic model as these antibiotics do?

This review summarizes studies on the effects of Ag-NPs on bacteria from simple to complicated systems. Based on previous research, a hypothesis about the effects of Ag-NPs under low dose is presented and a theoretical model is proposed. The conclusion is rationalized based on both experimental phenomena and the potential mechanisms of the observed effects.

## **2.2 Tests based on bacterial single strains**

### **2.2.1 Dose**

Most of the research on single strain bacteria was performed before 2012, and most Ag-NP concentrations tested in these studies are above 1 mg/L (all concentrations are based on silver). Model single strains tested include: model gram-negative strain: *Escherichia coli* (*E. coli*), model gram-positive strain: *Staphylococcus aureus* (*S. aureus*), model ammonia-oxidizing bacterium: *Nitrosomonas europaea* (*N. europaea*), and model biofilm formation bacterium: *Pseudomonas fluorescens* (*P. fluorescens*). Most experiments were carried out in aqueous suspension, and the detection methods was often absorbance (at 600 nm), plate count, inhibition zone or activity observation. To summarize, the effects of Ag-NPs are dose-dependent, and higher concentrations usually lead to more severe adverse effects. Stimulatory response was observed occasionally, but

Table 2-1 Single strain dose-response to Ag-NPs.

Strain	Dose (mg/L)	Response	Reference
<i>Staphylococcus aureus</i> <i>Escherichia coli</i>	0.03-3.6×10 <sup>-3</sup>	Lower cell density at higher dose	(Kim et al., 2007)
<i>Bacillus thuringiensis</i> <i>Bacillus aquimaris</i>	0.25-1	Lower cell viability at higher dose	(Kumar et al., 2014)
<i>Escherichia coli</i> <i>Pseudomonas aeruginosa</i>	2.5-100	Longer lag time and slower growth rate at higher dose	(Priester et al., 2014)
<i>Escherichia coli</i> <i>Proteus mirabilis</i>	20-40	Larger zone of inhibition at higher dose	(Lavakumar et al., 2015)
<i>Escherichia coli</i>	20-100	Lower cell density and counts at higher dose	(Raffi et al., 2008)
<i>Staphylococcus aureus</i> <i>Escherichia coli</i>	300-3000	Majority 100% killed	(Smetana et al., 2008)
<i>Escherichia coli</i> <i>Klebsiella mobilis</i> <i>Staphylococcus aureus</i> <i>Bacillus subtilis</i>	0.5-2	Inhibition ratio increase with dose; inhibition increase slower at higher dose than at lower dose	(Zhang et al., 2008b)
<i>Pseudomonas stutzeri</i> <i>Azotobacter vinelandii</i> <i>Nitrosomonas europaea</i>	4 12 <b>0.0025-5</b>	Minimum inhibitory concentration (MIC) <b>ammonia monooxygenase genes upregulated when 0.0025 mg/L was used</b>	(Yang et al., 2013)
<i>Bacillus subtilis</i> (air)	300-3000	Less CFU at higher concentration; No significant difference at 1000 and 3000 mg/L	(Yoon et al., 2008a)
<i>Arthrobacter globiformis</i> (soil)	0.1-100	Inhibition ratio increase with dose; inhibition-dose curve flattens at higher dose	(Engelke et al., 2014)
<i>Escherichia coli</i>	<b>1-60</b>	<b>stimulated at sub-lethal concentration</b>	(Xiu et al., 2012)
<i>Pseudomonas fluorescens</i>	<b>0.002-2</b>	<b>Growth over 100% at certain doses</b>	(Fabrega et al., 2009a)

\*Positive effects are in bold font.

not much attention was paid to it. Table 2-1 summarizes the reported dose response of bacterial strains to Ag-NPs.

### **2.2.2 Nanoparticle properties**

Over 50 articles have been published on the effects of nanoparticles on bacteria. Over 90% of these studies were carried out after 2008 when the methods to synthesize silver nanoparticle became mature, and various methods and reagents were applied to produce Ag-NPs, producing Ag-NPs with various shapes, sizes and coating. Pal et al. (2007) reported that testing with *E coli* the antibacterial effects from the strongest to the weakest followed the order truncated triangular > spherical > elongated (rod-shaped) > Ag<sup>+</sup> ion. However, it should be noted that many other research claimed that Ag<sup>+</sup> ion has stronger antibacterial effects than Ag-NPs at the same concentration, which will be discussed later in this review. It is well-accepted that smaller Ag-NPs are more toxic (Morones et al., 2005, Lok et al., 2007, Choi and Hu, 2008, Zhang et al., 2008b). Several studies carried out with *N. europaea* showed that smaller Ag-NPs released more Ag<sup>+</sup> ion and thus were more toxic, and the smaller size came from better dispersity (Radniecki et al., 2011, Yuan et al., 2013). Coating affects the toxicity of Ag-NPs because it plays an important role in determining the dispersity and size of Ag-NPs and Ag<sup>+</sup> ion dissolution. Arnaout and Gunsch compared three types of coating: citrate, gum arabic (GA), and polyvinylpyrrolidone (PVP). At a concentration of 2 mg/L, citrate resulted in the highest Ag<sup>+</sup> ion dissolution, and Ag-NPs with GA coating had the smallest size. Citrate and GA coated Ag-NPs caused  $67.9 \pm 3.6\%$  and  $91.4 \pm 0.2\%$  inhibition of nitrification, respectively (Arnaout and Gunsch, 2012). Kvítek et al. (2008) tested several kinds of coating and found out that sodium dodecyl sulfate-SDS,

polyoxyethylenesorbitane monooleate-Tween 80 and PVP 360 had superior Ag-NP stabilization ability which resulted in a Minimum inhibitory concentration (MIC) under 1 mg/L. Combination of Ag-NP with an antibacterial coating can also lower the MIC. Myramistin<sup>®</sup> stabilized Ag-NPs have a lower MIC than citrate capped ones (Vertelov et al., 2008).

### **2.2.3 Treatment conditions**

Similar to other disinfectants, the contact time adopted affects the antibacterial effects of Ag-NPs. Longer time results in more inhibition/killing (Smetana et al., 2008, Kumar et al., 2014). pH and ligands can also affect the toxicity of Ag-NPs. pH can affect Ag<sup>+</sup> ion dissolution, although within the bacterial exposure range (typically pH 6–9), this effect is moderate and does not affect toxicity significantly (Fabrega et al., 2009a). Inorganic ligands, such as Cl<sup>-</sup>, could function as scavengers and increase bacterial survival (Smetana et al., 2008). Tested with *N. europaea*, Mg<sup>2+</sup> and Ca<sup>2+</sup> reduced the adverse effect of Ag-NPs (Anderson et al., 2014), while ammonium accelerated Ag<sup>+</sup> ion dissolution and increased toxicity (Mumper et al., 2013). Organic ligands present in the media or the environment usually bind with Ag-NPs and hinder their contact with cells by forming aggregates so that toxicity is often reduced (Lok et al., 2006). For example, Ag-NPs are more toxic in modified minimal Davis (MMD) media than in LB broth due to the presence of ligands in the LB (Priester et al., 2014). Natural organic matter (NOM) can also help to reduce the toxicity of Ag-NPs (Priester et al., 2014). However, a premix with a low dose of ligands such as bovine serum albumin (BSA) can help with Ag-NP dispersion and avoid aggregation, which can increase toxicity of Ag-NPs in media (Lok et al., 2007).

Different bacterial strains react differently to Ag-NPs. Although the specific mechanism behind their behavior is poorly understood, it appears that the response of each strain highly depends on the properties of Ag-NPs and treatment conditions. The graphene oxide-silver nanocomposite is more toxic to *E. coli* than to *S. aureus* (Tang et al., 2013). *E. coli* was more tolerant to Ag-NPs than was *P. aeruginosa*, especially in MMD (Priester et al., 2014). When tested with various Ag-NPs, *E. coli* was more sensitive than *S. aureus* most of the time, but there were some exceptions (Priester et al., 2014). In air, it took less time to kill *B. subtilis* by Ag-NPs than *E. coli* (10 vs. 60 min) (Yoon et al., 2008b). Sometimes there were no significant differences among various strains regarding their sensitivity to Ag-NPs (Vertelov et al., 2008, Zhang et al., 2008b).

#### **2.2.4 Resistance and recovery**

After 2009, it has been noticed that some bacteria have Ag-NP resistance and occasionally cells can recover from Ag-NP exposure. It has been shown that Ag<sup>+</sup> resistant strains are often tolerant to AgNP as well, and the tolerance may come from EPS (Lok et al., 2007, Khan et al., 2011). Resistance can also be genetically created. Sedlak et al. (2012) reported the silver-tolerance of an engineered *E. coli* strain after the introduction of a silver-binding peptide motif (AgBP2). *Pseudomonas stutzeri* AG259 can produce silver crystals by reducing Ag<sup>+</sup> as a resistance mechanism (Klaus et al., 1999). Besides pre-existing resistance, bacteria can also develop resistance by adapting to Ag-NPs. *E. coli* can develop resistance to Ag-NPs within 225 generations with minimal genomic changes (Klaus et al., 1999). Dhas et al. (2014) isolated five bacterial strains from sewage, and these isolates could stand 2-10 times higher Ag-NP

concentration after 10 days of continuous incubation with Ag-NPs. It was found that the adaption was associated with increased EPS secretion. Recovery after delayed growth was also reported (Schacht et al., 2013).

### **2.3 Laboratory mixed cultures**

Mixed cultures are more complicated than single strain cultures and can be more tolerant to Ag-NPs due to interactions such as mutualism, commensalism, proto-cooperation, and even competition in the symbiotic microbial community. Nitrifying bacteria are the most well studied mixtures regarding the effects of Ag-NPs. 1 mg/L Ag-NPs could inhibit the growth of laboratory-cultivated autotrophic nitrifying bacteria by approximately 80% in laboratory-controlled reactors (Choi and Hu, 2008). Tolerance to Ag-NPs can be improved by a simple combination of different strains. Kumar et al. (2014) reported the behavior of a simple binary consortium from two isolated bacteria strains *B. thuringiensis* and *B. aquimaris*. The viability of the binary consortium in the instance of Ag-NPs exposure was significantly increased in the consortium compared with the viability of each single strain. Sheng and Liu (2011) studied a planktonic mixed culture obtained by inoculating biofilm into Reasoner's 2A (R2A) broth. In the presence of 1 mg/L Ag-NP, some strains in the mixture showed even higher viability than in the case when no Ag-NP was added.

Interactions among bacterial strains within a mixed culture play an important role in its resistance and adaption to Ag-NPs. The silver resistance gene locates on plasmids and can be transferred between bacterial strains (Gupta et al., 2001). Interactions such as mutualism,

commensalism, proto cooperation, and competition contribute to the robustness of a symbiotic microbial community (Allison, 2000). This helps to explain the increased resistance of mixed cultures compared with single strains under Ag-NP treatment (Sheng and Liu, 2011).

## **2.4 Mixed cultures in natural and engineering systems**

### **2.4.1 Natural water**

Das et al. (2012) studied microbial communities from natural water (a stream and a stormwater pond) after exposure to Ag-NPs. Based on DGGE and terminal restriction fragment length polymorphism (T-RFLP) profiles, bacteria in the community were classified into four categories: intolerant, recovering, tolerant, and stimulated. It was found that Ag-NPs selectively affected different types of bacteria in the community. The microbial community diverged 54–56% from the original one after exposure to Ag-NPs. Intolerant bacteria were killed; some others were impacted but recovered from the damage or regrew; tolerant bacteria stayed unchanged under the treatment; stimulated bacteria grew better in the presence of Ag-NPs. Another study on microbes in sediment and streamwater showed that the effects of Ag-NPs on the microbial community can be attenuated by the physical and chemical properties of such an environment (Colman et al., 2012).

### **2.4.2 Activated sludge**

More and more recent studies have focused on activated sludge systems and relatively lower concentrations of Ag-NPs are tested to better mimic the practical condition of silver release in biological wastewater treatments. The effects of Ag-NPs on activated sludge are dose dependent.

However, due to the lower Ag-NP doses used, the inhibition of bacteria is often not as significant as that shown in pure cultures, and the observed recovery becomes more evident and frequent.

With a sufficient Ag-NP dose, selective bacterial inhibition can be observed. Ammonia oxidizing bacteria (AOB) are more sensitive to Ag-NPs than are nitrite oxidizing bacteria (NOB) and organic oxidation heterotrophs (Liang et al., 2010, Sun et al., 2013, Jeong et al., 2014, Yang et al., 2014a). The effects of Ag-NPs on nitrifying bacteria appeared to be an uncompetitive-like inhibition (Nguyen et al., 2012). More attention has been paid to long-term treatment with Ag-NPs. Some researchers found that after long-term (50 days) treatment, the microbial community diversity decreased and the wastewater treatment efficiency was reduced (Nguyen et al., 2012). However, more studies showed recovery of wastewater treatment performance during long-term experiments. Alito and Gunsch reported recovery within three hydraulic retention times (HRTs), although ammonia and COD removal decreased by 30% initially after Ag-NP spikes at 0.2 and 2 mg/L (2014). Zhang et al. (2014) monitored the microbial community in a membrane bioreactor activated sludge system with 0.1 mg/L Ag-NPs in the influent. The results showed that reactor performance was not significantly affected by Ag-NPs during the entire experiment. However, the silver resistance gene (*silE*) increased by 50-fold 41 days after the AgNP exposure, and then declined toward the initial level. Studies based on enhanced biological phosphorus removal found that AgNPs had no significant effect on phosphorous removal when the Ag-NPs dose applied did not exceed 5 mg/L (Chen et al., 2012, Chen et al., 2013). Ag<sup>+</sup> ions can decrease phosphorous removal, but the system recovered within 30–35 days of operation.

Significantly an increase in biomass concentration was even seen when sub-lethal concentration

of Ag-NPs was used and this stimulatory response can be stably repeated (Sheng et al., submitted). Ag-NPs with minimal Ag<sup>+</sup> dissolution helped to maintain the microbial community diversity and function in activated sludge after long term treatment.

Moreover, it has also been well accepted that sulfidation plays an important role on the fate of Ag-NPs in wastewater treatment systems. The majority of Ag-NPs end up as Ag<sub>2</sub>S in wastewater treatment processes, since sulfide concentrations can be high, especially under anaerobic conditions. This can significantly reduce Ag-NP toxicity in wastewater treatments (Kim et al., 2010, Kaegi et al., 2011, Levard et al., 2012, Doolette et al., 2013, Kaegi et al., 2013, Hedberg et al., 2014, Ma et al., 2014). The physical structure of sludge flocs may also play a role in bacterial resistance to Ag-NPs in activated sludge (Sun et al., 2013). Species on the surface of sludge flocs are more exposed to Ag-NPs and at greater risk, whereas bacteria inside the flocs are better protected.

### **2.4.3 Biofilms**

It is well-known that Ag-NPs can inhibit biofilm formation (Juan et al., 2010, Kalishwaralal et al., 2010, Cao et al., 2011, Das et al., 2013, Markowska et al., 2013, Besinis et al., 2014, Wehling et al., 2015). The key point for successful application of Ag-NPs to avoid biofilm formation is sufficient concentration. An example with *P. aeruginosa* AdS biofilm showed that if a sub-inhibitory Ag-NP concentration (4 mg/L) was used, the biofilm mass increased although there was no significant change in cell density (Königs et al., 2015). Both biofilm formation and cell growth were inhibited at higher Ag-NP concentrations.

If Ag-NPs are added to mature biofilms, high biofilm bacterial tolerance is often observed. Sheng and Liu (2011) and Sheng et al. (2015) reported that wastewater biofilms can stand up to 200 mg/L Ag-NPs without significant effect on the biofilm microbial community and function. GeoChip analysis indicated that, under Ag-NP treatment, functional gene distributions in wastewater biofilms are more stable than community composition, which can be attributed to the functional redundancy in such complicated ecosystems (Sheng et al., 2015). Most Ag-NPs cannot reach bacterial cells inside biofilms, since they are trapped in the EPS matrix due to significant aggregation (Fabrega et al., 2009b). When Ag-NPs concentrations were 0.2 and 2 mg/L, biofilm volume and biomass decreased but no significant effects on dominant community were detected (Fabrega et al., 2009b). As the Ag-NP concentration increased, the volume of the biofilm decreased and the uptake of Ag-NPs into the biofilm increased.

## **2.5 Mechanism of antimicrobial effects and resistance**

Ag-NP toxicity arises from two major sources: the intact nanoparticle and the released Ag<sup>+</sup> ions. It is controversial in the literature as to which one plays a more important role. The particle specific toxicity of Ag-NPs falls into three categories: membrane disruption, reactive oxygen species (ROS) production and direct interaction with DNA and proteins. Ag-NPs can damage cell membranes through direct contact (Lok et al., 2006, Rai et al., 2009), and can attack the respiratory chain (Sondi and Salopek-Sondi, 2004). ROS play an important role in Ag-NP toxicity by damaging cell membrane, enzymes and DNA (Song et al., 2006, Kim et al., 2007, Choi and Hu, 2008, Kumar et al., 2014). It has been reported that ROS are produced mainly from

the nanoparticle form (Verano-Braga et al., 2014). However, it has also been reported that a nano-silica silver nanocomposite can exert ROS independent antibacterial activity (Parandhaman et al., 2015). It has been proposed that Ag-NPs can interact with compounds containing phosphorus-containing bases such as DNA (Morones et al., 2005). This has been confirmed in eukaryotic cells. However, no such conglomeration (Ag-NP–DNA binding) has been seen in bacterias and evidence for direct DNA damage is lacking (Morones et al., 2005, Hwang et al., 2008). Evidence for direct Ag-NP–protein interaction in bacteria is also rare (Wigginton et al., 2010). Although under debate, it has been claimed that the majority of Ag-NP toxicity comes from the released Ag<sup>+</sup> ions, and research has shown that Ag<sup>+</sup> ions at a lower concentration than that of Ag-NPs can exert the same level of toxicity. Actually, some research shows that Ag<sup>+</sup> ion can do the same damage as the particle form does on cell membranes, DNA, proteins and the respiratory chain, as well as generate ROS (Feng et al., 2000); also it is easier for Ag<sup>+</sup> to penetrate the cell membrane.

Xiu et al. (2012) has shown that no toxicity was observed under anaerobic condition where no Ag<sup>+</sup> ion was formed, which means that Ag<sup>+</sup> ions have to be there to exert toxicity. It has also been reported that partially oxidized AgNPs are more toxic than the non-oxidized form (Lok et al., 2007). Priester et al. (2014) claimed that the toxicity is due to Ag<sup>+</sup> ions and not the metallic particle since the specific growth rate of the tested bacteria decreased independent of the silver species. However, this statement is a paradox since the Ag<sup>+</sup> ion concentration in the Ag-NP sample is much lower, and the decrease of specific growth rate would be different if the same concentration of silver species is considered. Although relatively rare, there are also research

studies showing that Ag-NPs are more toxic than Ag<sup>+</sup> ion at the same concentration indicating that the role of the particle form in the effects of Ag-NP should not be neglected (Pal et al., 2007, Choi et al., 2008). The reduction of toxicity of the nanoparticle form may result from passivation, adsorption, aggregation, and physical separation under environmental conditions (Bradford et al., 2009, Gao et al., 2011, Colman et al., 2012).

The proposed toxicity mechanism for Ag-NPs indicates that reduced Ag<sup>+</sup> ion dissolution may contribute significantly to the Ag-NP tolerance and resistance. Bacteria resistant to Ag<sup>+</sup> are often resistant to Ag-NP as well, as previously discussed. Bacterial resistance to Ag<sup>+</sup> has been well studied. Since the mechanisms behind the effects of Ag-NPs and resistance to Ag-NPs are both closely associated with Ag<sup>+</sup>, it is possible that resistance and stimulatory response to Ag-NPs exist under sublethal concentrations, just as they exist for the Ag<sup>+</sup> ion. There is evidence for this stimulatory effect of Ag-NPs in systems from pure culture to complicated engineered ecosystems in biological wastewater treatment.

## **2.6 Conclusions and outlook**

- It is possible that the dose-response of bacteria to Ag-NPs conforms to the hormetic model shown in Figure 2-1, and it is worth to systematically examine this hypothesis in future Ag-NP toxicological model development.
- The stimulating zone in Figure 2-1 is fairly narrow compared to the entire dose-response spectrum, and the maximum stimulatory response falls in the 130–160% response range.

Therefore, it is not easy to capture and replicate the stimulatory response; this is why it has been neglected in previous studies.

- The germicidal concentration of Ag-NPs can be 10 times the concentration of the minimum inhibiting dose.
- The width and the exact dose of each zone in Figure 2-1 depend on the Ag-NP properties, the bacterial type, and the environmental conditions of the test.
- The more diverse and stable the microbial system is, the easier it will be to detect and replicate the stimulatory response to Ag-NPs.

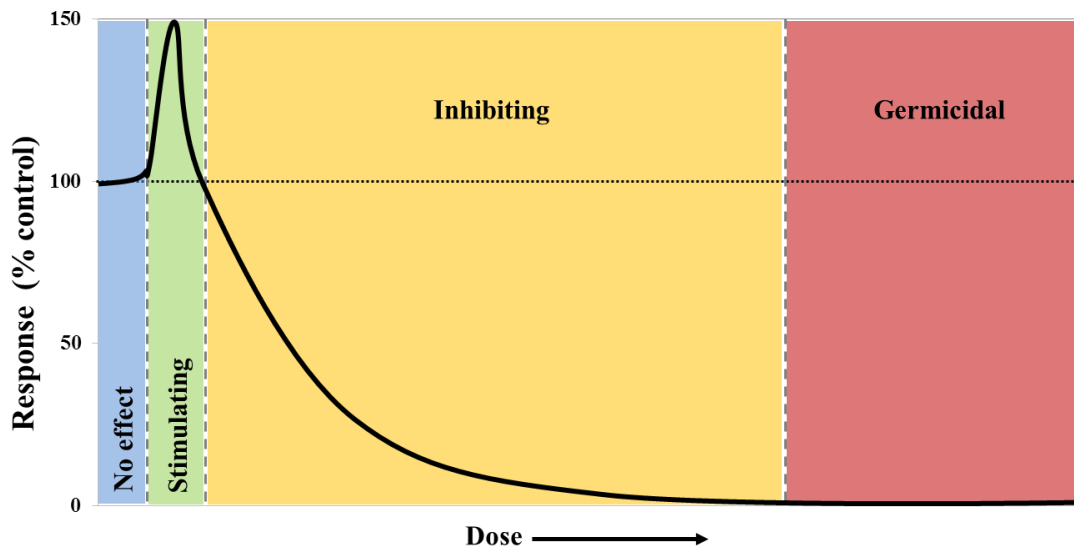


**Figure 2-1** Dose-response curve reflecting the effects of Ag-NPs.

## **Chapter 3 Effects of Silver Nanoparticles on Wastewater Biofilms**

### **3.1 Introduction**

Because of their antimicrobial properties, silver nanoparticles (Ag-NPs) have become the most frequently used nanoparticles in consumer products. By October 2013, there were 383 consumer products containing nano-silver, which ranked first in the “Woodrow Wilson International Centre for Scholars” (2014) study on emerging nanotechnologies. Silver coatings have been widely used to treat chronically infected wounds (McInroy et al., 2009), and to prevent biofilm formation on home appliances such as washing machines. Ag-NP coatings have also been introduced as antimicrobial agents in fabrics (Benn and Westerhoff, 2008). Ag-NP applications have been extensively studied as disinfectants in medical institutions, and an increasing amount of research has been carried out on Ag-NP applications in the food industry and for drinking water treatment and distribution systems (Silvestry-Rodriguez et al., 2008, Konopka et al., 2009, Kumar and Raza, 2009, Zhao et al., 2010).

The explosion of nanotechnology applications makes it inevitable that Ag-NPs will be released into domestic and industrial waste streams (Blaser et al., 2008, Mueller and Nowack, 2008, Benn and Westerhoff, 2008, Geranio et al., 2009, Hagendorfer et al., 2010). Because Ag-NPs are meant to exert toxic effects on microorganisms, their release into wastewater systems may adversely affect the microbial communities found in biological treatment processes. Released Ag-NPs could decrease the effectiveness of contaminant removal in biological treatment processes and cause noncompliance with effluent discharge limits. The antimicrobial

effects of Ag-NPs can be attributed to their capacity to disturb cell membrane functions, to bind with intracellular material such as protein and DNA, and to release Ag<sup>+</sup> ions (Morones et al., 2005). The released Ag<sup>+</sup> ions can attack the thiol groups in enzymes, stop DNA replication and cause the cells to reach a nonculturable state and then cell death (Morones et al., 2005). These mechanisms are closely related to the small size and high surface/volume ratio of Ag-NPs (Marambio-Jones and Hoek, 2010), which equips Ag-NPs with highly active facets and increased catalytic activity. While there are increasing concerns regarding human and animal exposure to nanoparticles as emerging contaminants, little is known about the impact of nanoparticles on biological treatment processes in wastewater treatment plants. Most research has focused on the impact of Ag-NPs on individual or certain types of bacteria cultivated under laboratory conditions. However, the impact of Ag-NPs on wastewater microorganisms is not well understood. The few reported studies on nanoparticle toxicity in wastewater biological processes suggest that Ag-NPs could significantly inhibit both heterotrophic and autotrophic wastewater microorganisms (Choi and Hu, 2008, Choi et al., 2009). Recent studies showed that 1 mg Ag/L Ag-NPs inhibited the growth of laboratory-cultivated autotrophic nitrifying bacteria by approximately 80% in laboratory-controlled reactors (Choi and Hu, 2008, Choi et al., 2009). Nevertheless, these reported studies focused only on the detrimental effects of Ag-NPs on the total number of planktonic (free-floating) bacteria.

To reveal the impact of Ag-NPs in wastewater treatment plants, detailed information regarding nanoparticle toxicity on individual species and microbial communities is needed since different groups of microorganisms are associated with different biological treatment properties

and functionalities. For instance, the nitrification process requires both ammonium-oxidizing nitrifiers (e.g., *Nitrosomonas*) and nitrite oxidizers (e.g., *Nitrospira* and *Nitrobacter*).

Elimination of these microorganisms will lead to reduced nitrogen removal (Choi et al., 2008). To date, little research has been carried out to evaluate the impact of Ag-NPs on microbial communities found in wastewater treatment plants.

In addition, microorganisms in biological wastewater treatment processes are usually in the form of microbial aggregates, such as biofilms in rotating biological contactors (RBCs) and trickling filters. For instance, RBCs are widely used in treatment plants of different scales because of their compact design (high biomass concentration per volume), high pollutant removal efficiency (especially under aerobic conditions), and simple operation (no sedimentation, thus no need for sludge recirculation) (Cortez et al., 2008). Microbial biofilms are highly stratified microbial communities embedded in a matrix of extracellular polymeric substances (EPS) on solid substrata. Previous studies have shown that microbial biofilms are more tolerant to antimicrobial agents than are planktonic bacteria (Rittmann and McCarty, 2001, Davies, 2003, Liu et al., 2007). The physicochemical microenvironments within biofilms also play important roles in shaping the microbial community structure (Rittmann and McCarty, 2001, Davies, 2003, Liu et al., 2007). Therefore, the antibacterial effect of Ag-NPs on wastewater biofilms may be significantly different from the effects of Ag-NPs on planktonic cells. Unfortunately, knowledge regarding the fate and reactivity of Ag-NPs in complex systems such as biofilms is still lagging.

Our hypotheses are (i) Ag-NPs can impact wastewater biofilm microbial community structures, depending on the characteristics of each strain (e.g., its ability to produce EPS and

growth rate) and the community interactions among these strains; and (ii) the effects of Ag-NPs on planktonic cells are different than on wastewater biofilms. To assess these hypotheses, both original wastewater biofilms and isolated planktonic pure culture bacteria from the biofilms were tested under Ag-NP treatment. Possible protective mechanisms in the biofilm were investigated, such as physical exclusion due to the effects of EPS. The role of community interactions was also studied, and an artificially mixed community was tested to verify the effects of the community interaction. 16s rRNA gene based polymerase chain reaction — denaturing gradient gel electrophoresis (PCR-DGGE) was used to analyze the microbial community shift after Ag-NP treatment. Three terms have been used to describe the responses of the samples to Ag-NPs: ‘tolerance’ is defined as the ability of the samples to survive under the treatment of Ag-NPs, while ‘susceptibility’ (or ‘sensitivity’) is defined as their ability to react to Ag-NPs.

## **3.2 Material and Methods**

### **3.2.1 Wastewater biofilm samples**

Wastewater biofilms were collected from the first stage RBC unit in the Devon Wastewater Treatment Plant located in Devon, Alberta, Canada. The average biofilm thickness was 1.5 mm. Biofilm samples were cut with the plastic substratum just before each experiment, kept in a Petri dish on ice during transport, and processed within 30 min of arrival at the laboratory.

### **3.2.2 Isolation and cultivation of heterotrophic bacteria from wastewater biofilms**

To isolate cultivable heterotrophic bacteria from wastewater biofilms, single colonies on Reasoner's 2A (R2A) agar plates were isolated and transferred to new plates based on their

appearance and growth rate (indicated by the time needed to form visible colonies on R2A agar plates). Single colonies on R2A agar plates were then inoculated into R2A broth and shaken at 100 rpm at room temperature (25.5 °C) for 30 h before further studies on planktonic pure culture bacteria. Two types of mixed planktonic wastewater bacterial cultures (i.e., biofilm mixture and artificial mixture) were prepared. The ‘biofilm mixture’ was cultured by directly inoculating wastewater biofilm into R2A broth. The ‘artificial mixture’ was generated by isolating one single colony of each isolated strain from R2A plates and inoculating them into one R2A broth. These liquid R2A cultures of planktonic wastewater bacteria were shaken at 100 rpm at room temperature (25.5°C) for 30 h before the toxicity tests. R2A media are low-nutrient media often used to recover bacteria from environmental samples. Difco R2A agar powder was purchased from Voigt Global Distribution Inc., KS, and 2 × R2A broth was obtained from Teknova, CA.

### **3.2.3 Removal of loosely bound EPS from biofilms.**

Among the biofilm EPS components, those that can be readily removed are defined as ‘loosely bound EPS’, while those that need vigorous removal processes are defined as ‘tightly bound EPS’. Extraction reagents such as ethanol, which can damage bacterial cells, are often applied to remove tightly bound EPS. To eliminate loss of microbial diversity and viability, only loosely bound EPS were removed in this study following the procedure described by Gong *et al.* (2009) as briefly summarized here. Biofilms were scraped off the plastic RBC substratum and suspended in 1% phosphate buffered saline (PBS, 1.65 mM ionic strength). A 30-s vortex was performed to mix biofilm fragments with PBS. The biofilm suspension was vortexed at the maximum speed for 1 min, then centrifuged at 4°C, 4,000 g, for 20 min. The pellets were

resuspended in 10 mL of 1% PBS, vortexed, and centrifuged again. Pellet resuspension, vortexing, and centrifugation were repeated three times. 1% PBS was used to provide a pH (7.0) and chloride concentration (51.4 mg/L) comparable to the first-stage wastewater (neutral pH and 58.0 mg/L chloride) at the Devon Wastewater Treatment Plant. 1% PBS was prepared by dissolving 10.93 mg/L  $\text{Na}_2\text{HPO}_4$ , 3.175 mg/L  $\text{NaH}_2\text{PO}_4 \cdot \text{H}_2\text{O}$ , and 84.75 mg/L NaCl in ultrapure water (PURELAB Maxima system, ELGA LabWater, Mississauga, Canada).

### **3.2.4 Preparation of Ag-NP suspensions**

Self-dispersing silver nanopowder was purchased from SkySpring Nanomaterials, Inc. (Houston, USA). According to the Ag-NP product description, the particle size is less than 15 nm, and the particle composition is 10% silver (99.99% purity) and 90% polyvinylpyrrolidone (PVP), similar to Ag-NPs commonly used in commercial products. Ag-NP suspensions at concentrations of 1, 50, or 200 mg Ag/L were prepared by dispersing Ag-NPs in 1% PBS and mixed by vortex at the maximum speed.

### **3.2.5 Characterization of Ag-NPs**

The particle size distribution of Ag-NPs was characterized using a Malvern Zetasizer Nano-ZS (Model: ZEN3600, Malvern Instruments Ltd, Worcestershire, UK). Since PVP dissolves in water completely, parameters of silver were adopted for the analysis: the refractive index was 2.0 and the absorption coefficient was 0.320 (Gong et al., 2009). A suspension of 1 mg Ag/L Ag-NPs in ultra-pure water was also prepared for particle size analysis. All the 24-h-old suspensions were prepared by shaking the sample at 100 rpm for 24 h in the dark at room temperature (25.5°C), which is the same as that what was done in the toxicity tests.

### **3.2.6 Ag-NP toxicity experiments**

Antimicrobial effects of Ag-NPs were tested on original wastewater biofilms, wastewater biofilms with loosely bound EPS removed, and planktonic bacteria isolated from wastewater biofilms. Biofilms with and without loosely bound EPS were suspended in freshly prepared Ag-NP suspensions (1 g wet original biofilm/5 mL Ag-NP suspension) at 0, 1, 50, and 200 mg Ag/L in sterile glass test tubes. The impact of Ag-NPs on pure and mixed cultures of planktonic bacteria isolated from the wastewater biofilms was tested by adding the appropriate bacterial culture into 0 (no treatment control) and 1 mg Ag/L Ag-NP suspensions (initial cell density: about  $1 \times 10^7$  CFU/mL). Samples and control were shaken at 100 rpm for 24 h in the dark at room temperature (25.5°C). Viability of cultivable bacteria was examined using a heterotrophic plate count (HPC) every 2 h during the first 12 h and every 4 h after 12 h. All toxicity tests were carried out in triplicate. As a comparison, toxicity of Ag<sup>+</sup> ions has also been tested at 200 mg Ag/L using AgNO<sub>3</sub>.

### **3.2.7 Sorption of Ag-NPs to wastewater biofilms**

1 g original biofilm samples were added into 5 mL freshly prepared Ag-NP suspensions at different concentrations (0, 1, 20 or 50 mg Ag/L) and incubated in the dark at 100 rpm and room temperature (25.5°C) for 520 min. 520 min was chosen because saturation was reached in 520 min of incubation and the concentration of free Ag-NPs in the suspension did not change significantly after that. The sample with 0 mg Ag/L was tested as the control. Samples without biofilms were also tested as abiotic controls. To evaluate the sorption of Ag-NPs to wastewater biofilms during the experimental period, aliquots of the Ag-NP suspensions were scanned

periodically to obtain absorption spectra from 250 to 700 nm using a Cary 50 Bio UV-vis spectrophotometer (Varian, USA). Concentration of Ag-NPs in the suspension is directly proportional to the peak absorption at 400 nm on the spectrum (Petit et al., 1993). A decrease of Ag-NPs in the residual suspension can be attributed to their sorption into the biofilm matrix. Concentrations of total silver in biofilm and in liquid suspension were measured by inductively coupled plasma mass spectrometry (ICP-MS) using the ELAN 9000 ICP mass spectrometer (PerKinElmer, Canada). Microwave digestion was performed as described by Wu *et al.* (1997) and briefly summarized here. 10 mL concentrated nitric acid and 2 mL ultra-pure water were added to 1g biofilm (wet weight) or 1 mL suspension and kept at room temperature overnight for pre-digestion. Microwave digestion was then carried out using ETHOS EZ Microwave Solvent Extraction Labstation (Milestone Inc., USA) with the following heating program: heat to 190 °C within 15 min and then hold at 190 °C for 10 min.

### **3.2.8 Bacterial enumeration using HPC**

Bacterial enumeration was performed by HPC using the drop plate method (Zelver et al., 1999, Liu et al., 2007). A series of 10-fold dilutions were performed and 10  $\mu$ L of each dilution was plated on R2A agar in triplicate. Plates were incubated at 31°C for 24 h and held at room temperature for another three days. Counting was performed after 24 h (for fast-growing bacteria) and again after the four-day period (for total number of bacteria). The lower detection limit is 10<sup>2</sup> CFU/mL. For biofilm samples, the result was converted into CFU/cm<sup>2</sup> based on the area of each biofilm sample. T-tests were performed in Microsoft Excel 2007 to examine the statistical significance of the results, and corresponding *p*-values were calculated using Type 3 two-tailed

T-test (unequal standard deviations). A *p*-value less than 0.05 indicates a statistically significant difference.

### **3.2.9 Biofilm community analysis using PCR-DGGE**

A fragment of 16s rRNA gene was analyzed to identify the microbial communities in the original wastewater biofilm, the wastewater biofilm with loosely bound EPS removed, as well as pure and mixed culture planktonic bacteria isolated from wastewater biofilms.

Details on the PCR-DGGE experiment is provided in the supplementary material and briefly described here. For each sample, genomic DNA was extracted and a ~550 bps fragment of 16s rRNA gene from each DNA sample was amplified. The primers were chosen according to Yu and Morrison (2004). The same amount of PCR products (600 ng) was loaded on the DGGE gel for each sample. Selected bands were retrieved from the DGGE gel and sequenced. Each sequence was matched against the NCBI nr nucleotide database using the nucleotide BLAST program. Multiple sequence alignment was built using CLUSTAL W and a neighbor-joining phylogenetic tree was calculated and constructed using TREECON (Van de Peer and De Wachter, 1994). Known strains were also included in the tree for reference.

Details about RBC in the Devon Wastewater Treatment Plant, sample processing and biofilm community analysis using PCR-DGGE are provided in supplementary material. Supplemental experiments on biofilms with the plastic substratum are also described in the supplementary material.

### 3.3 Results

#### 3.3.1 Characterization of Ag-NPs

As shown in Figure 3-1, most Ag-NPs were smaller than 5 nm in freshly prepared water suspensions at a low concentration of 1 mg Ag/L. However, the peak of the size distribution curve moved to 10–15 nm in freshly prepared 1% PBS suspensions at the same concentration, which indicates Ag aggregate formation under increased ionic strength and the presence of chloride in the 1% PBS suspension. After the 1 mg Ag/L suspension was stored at room temperature for 24 h, even more aggregation was observed. The mode size was about 50 nm, and 84% of the particles were in the range of 33–59 nm. In the 1% PBS suspension at 200 mg Ag/L, no significant difference in particle size was detected between newly prepared and 24 h suspensions. Most Ag-NPs were larger than 20 nm when the concentration was as high as 200 mg Ag/L in 1% PBS suspension. In freshly prepared suspensions, 76 % of the particles were in the range of 26–106 nm, and a noticeable proportion of the particles were larger than 200 nm. After 24 h incubation at room temperature, Ag-NP sizes became more uniform. 88% of the particles were in the range of 26–106 nm, while less than 2% were over 200 nm. Similar size distributions under environmental conditions have been reported (Fabrega et al., 2009a).

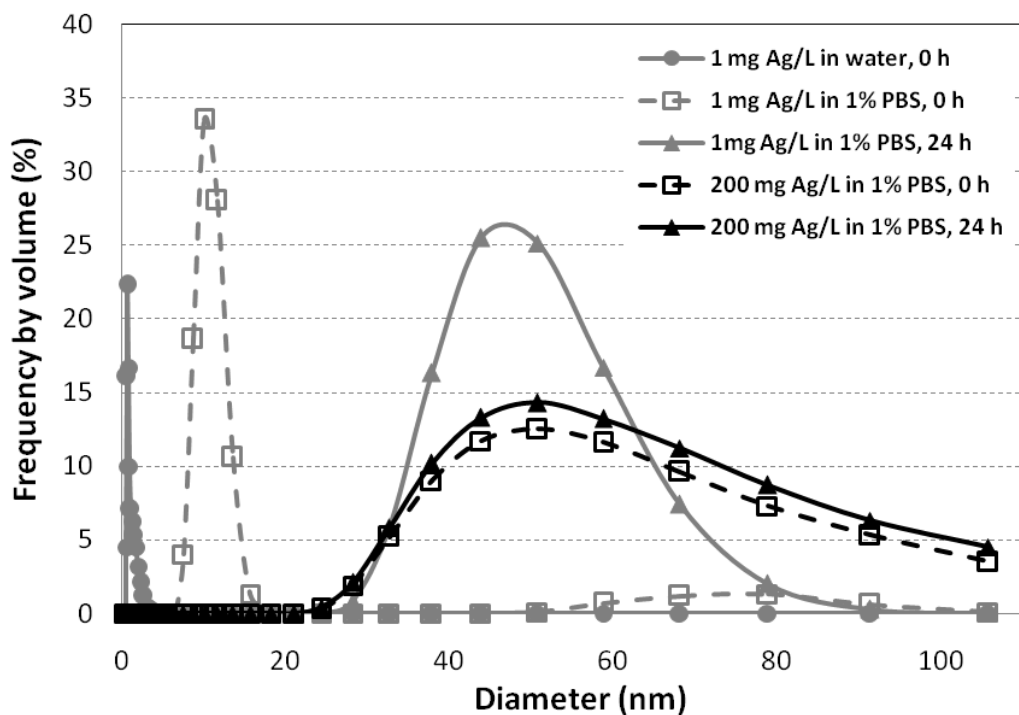


**Figure 3-1** Size distribution of freshly prepared and 24-h-old Ag-NPs in 1% PBS and water suspensions.

### 3.3.2 Microbial communities in wastewater biofilms

Based on the DGGE bands from the original biofilm and isolated single strains, a total of 14 strains were identified in the wastewater biofilm, which fell into three phyla as shown in Figure 3-2A. Six of the eight bands on Figure 3-2B (WWBF-B ~ WWBF-G, corresponding to Bands B ~ G respectively) from the original biofilm were sequenced successfully, as well as eight bands (WWBF-1 ~ WWBF-8) from isolated bacterial strains, which were also loaded onto the same DGGE gel and each formed a single band, confirming the purity (data not shown). Identities between each sequence and the corresponding closest homologue from the database are also shown on Figure 3-2A. The closest homologues to WWBF-C, WWBF-D, WWBF-F are

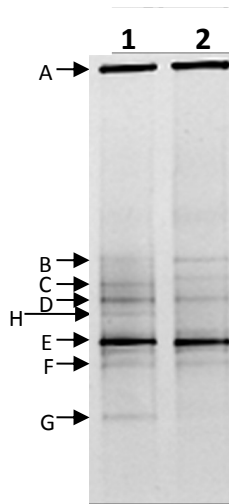
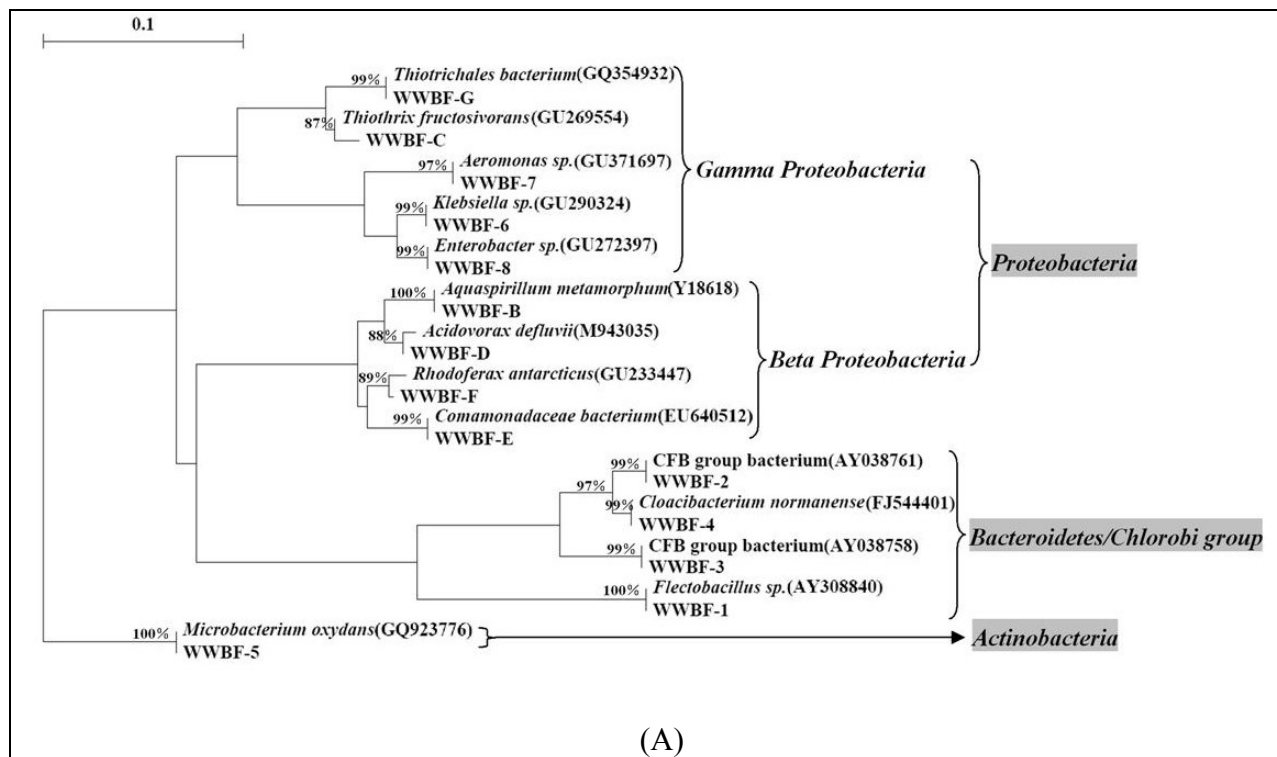


**Figure 3-2** Community profile of wastewater biofilms: (A) phylogenetic tree based on DGGE bands and isolated single strains (Pairwise identities between neighbor branches are indicated on the tree); (B) DGGE profiles of the original biofilm sample (Lane 1) and the R2A media enriched biofilm culture (Lane 2).

*Thiothrix fructosivorans*, *Acidovorax defluvii* and *Rhodoferrax antarcticus* respectively. However, the identities are not high enough to confidently identify these three strains due to the presence of too many 'N's in their sequences. Bands A and H were mixtures of DNA from different strains and were not sequenced successfully. According to the DGGE bands of pure culture bacteria, Band A appeared to be a mixture of WWBF-1 ~WWBF-4, all of which fell into the same phylum (pairwise identities  $\geq 82\%$ ). In fact, WWBF-2 and WWBF-4 share a sequence identity as high as 97% and fell into the same phylum of *Bacteroidetes*. Only WWBF-G was clearly missing in the R2A media enriched biofilm culture, although the intensity of certain bands was slightly lower. This indicates that the majority of the microbial community could be successfully maintained using R2A media. WWBF-C maybe belongs to the same order of *Thiotrichales* as WWBF-G based on the information currently available here.

### **3.3.3 Physical protections in wastewater biofilms**

The biofilm EPS are comprised of polysaccharides, proteins, phospholipids, humic substances, and nucleic acids (Kumar et al., 2011). To some extent, EPS performs as a physical barrier keeping Ag-NPs from reaching the cells. Figure 3-3A and B show the scanning electron microscopy (SEM) images of wastewater biofilms with and without loosely bound EPS, respectively. In Figure 3-3A, it can be seen that bacteria in the original wastewater biofilm were immersed in compact extracellular slimes. By contrast, biofilm cells are much more exposed after the removal of loosely bound EPS (as shown in Figure 3-3B), although tightly bound EPS were still present. The SEM sample preparation process may produce some artifacts on the

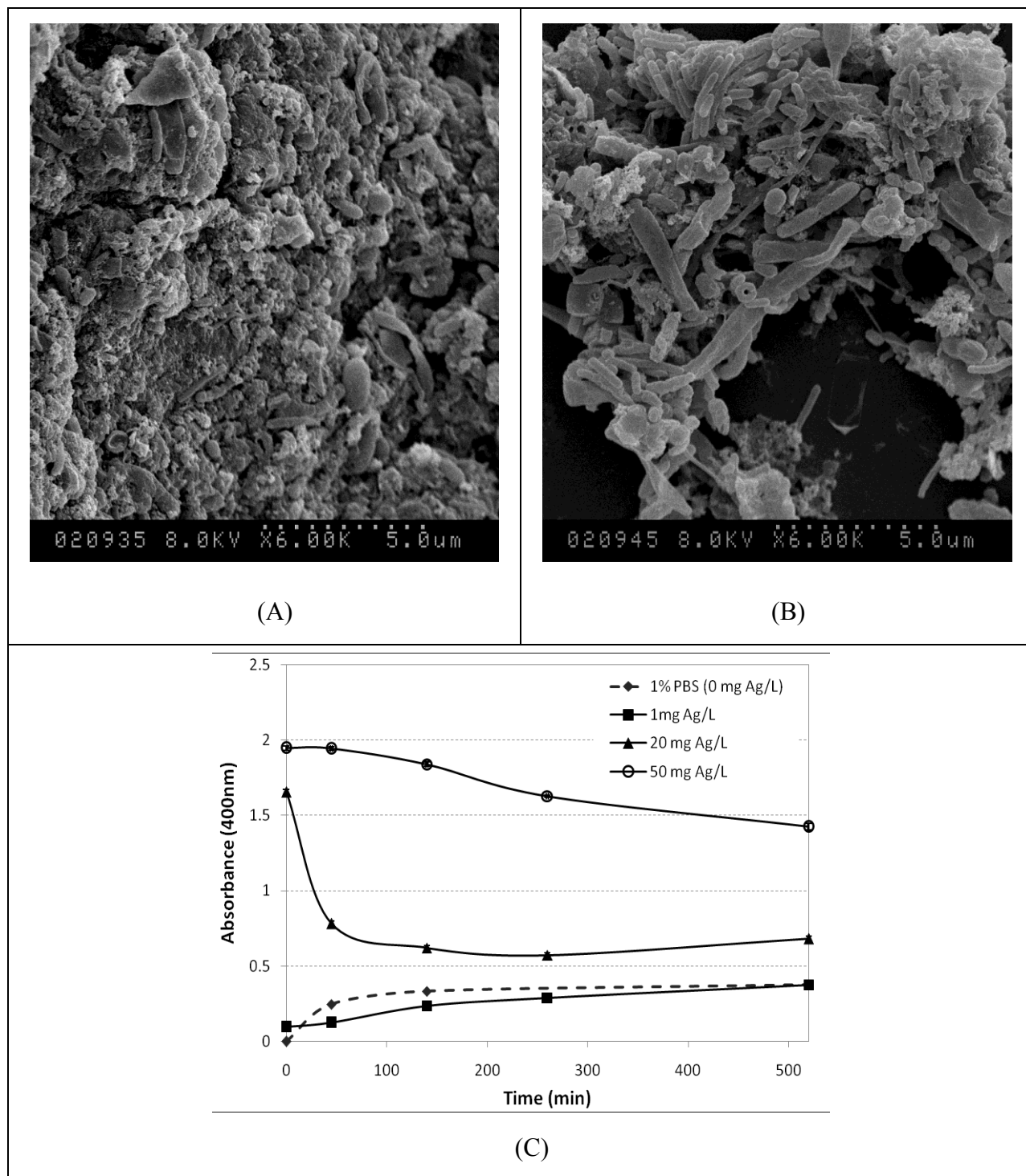


**Figure 3-3** Physical protections in wastewater biofilms: (A) SEM image of original wastewater biofilms; (B) SEM image of wastewater biofilms with loosely bound EPS removed. Bar size: 5  $\mu\text{m}$ . (C) peak absorption (400 nm) of remaining Ag-NPs in suspensions during incubation with wastewater biofilms at various initial concentrations (0, 1, 20, 50 mg Ag/L).

samples. However, both samples went through the same procedure to make sure that they are comparable with each other. As described in the supplemental material, a method that can effectively preserve the macrostructure for hydrated biological samples was used to prepare the SEM samples in this study.

During the incubation of biofilms in Ag-NP suspensions, an evident decrease of free Ag-NPs in the suspension was observed within the first 45 min, but did not change much after further incubation. At an initial concentration of 20 mg Ag/L, a sharp drop from 1.66 to 0.78 in the absorbance of the suspension was detected within 45 min as shown in Figure 3-3C. This result shows that Ag-NPs can be sorbed onto or into the biofilm. However, this does not necessarily mean that these sorbed Ag-NPs can reach the cells. Further, after 520 min incubation, the concentration of free Ag-NPs in the suspension did not change significantly, indicating a saturation of Ag-NPs in the biofilm after 520 min. The mass balance at 45 min with an initial concentration of 20 mg Ag/L is shown in Table 3-1. According to the ICP results, only about 10% of Ag-NPs was sorbed to the biofilm within 45 min when the initial concentration was 20 mg Ag/L.

Table 3-1 Sorption of Ag-NPs to wastewater biofilms.

<b>Biotic sample <sup>a</sup></b>			
<b>Sample</b>	<b>Biofilm</b>	<b>Residual suspension</b>	<b>Abiotic control <sup>b</sup></b>
<b>Total silver (<math>\mu\text{g}</math>)</b>	7.38	68.48	71.76
<b>Sum (<math>\mu\text{g}</math>)</b>		75.86	71.76
<b>Mass balance</b>	Biofilm + Residual = 105.7% (Abiotic control)		

<sup>a</sup> Biotic sample was prepared by adding 1 g wastewater biofilm into 5 mL of Ag-NP suspension (Initial concentration: 20 mg Ag/L), and the total silver in the biofilm and in the residual suspension was measured separately after 45 min of incubation at 100 rpm and room temperature (25.5°C).

<sup>b</sup> Abiotic control was the 5 mL of Ag-NP suspension without wastewater biofilms (Initial concentration: 20 mg Ag/L). The total silver in the suspension was measured after 45 min of incubation at 100 rpm and room temperature (25.5°C).

### 3.3.4 Effects of Ag-NPs on original wastewater biofilms

Figures 3-4A and C show the viability of the cultivable heterotrophic bacteria in the wastewater biofilm. Colony-forming units (CFU)/mL were counted after allowing the bacteria to grow on R2A agar at 31 °C for 24 h (Figure 3-4A), indicating the viability of species that grow rapidly. The number of CFU/mL counted 4 days after bacteria were plated (Figure 3-4C) indicates the total number of viable bacteria. Without Ag-NPs, the HPC was maintained at about

$2 \times 10^8$  CFU/cm<sup>2</sup> during the 24-h treatment for fast-growing bacteria, and at about  $4 \times 10^8$  CFU/cm<sup>2</sup> for the total cultivable heterotrophic bacteria. No significant growth was observed, since no nutrients were provided during the experiments.

After a 24-h treatment with Ag-NPs at 200 mg Ag/L, no significant change ( $p = 0.68$ ) was detected in the viability of cultivable heterotrophic bacteria. This is consistent with the results where the biofilms were not scraped off the substratum (Table A-1), indicating that scraping off the biofilms does not have significant impact on the tolerance of biofilms to Ag-NPs under the conditions tested. Treated samples were not as stable as controls, but the difference in HPC between treated samples and no treatment controls almost never exceeded 0.5 log units. Ag-NP treatment of 1 and 50 mg Ag/L had no pronounced impact on the survival of biofilm microorganisms (Figure A-1). Neither did bulk Ag<sup>+</sup> at 200 mg Ag/L (Figure A-2). In addition, as shown in Figure 3-4E, no significant difference in community profile was detected between samples with and without Ag-NP (200 mg Ag/L) treatment. The slightly higher intensities of several bands in untreated samples may indicate a slight decrease in the viability of these genera under Ag-NP treatment. These results indicate that wastewater biofilms with original EPS are highly tolerant to Ag-NPs.

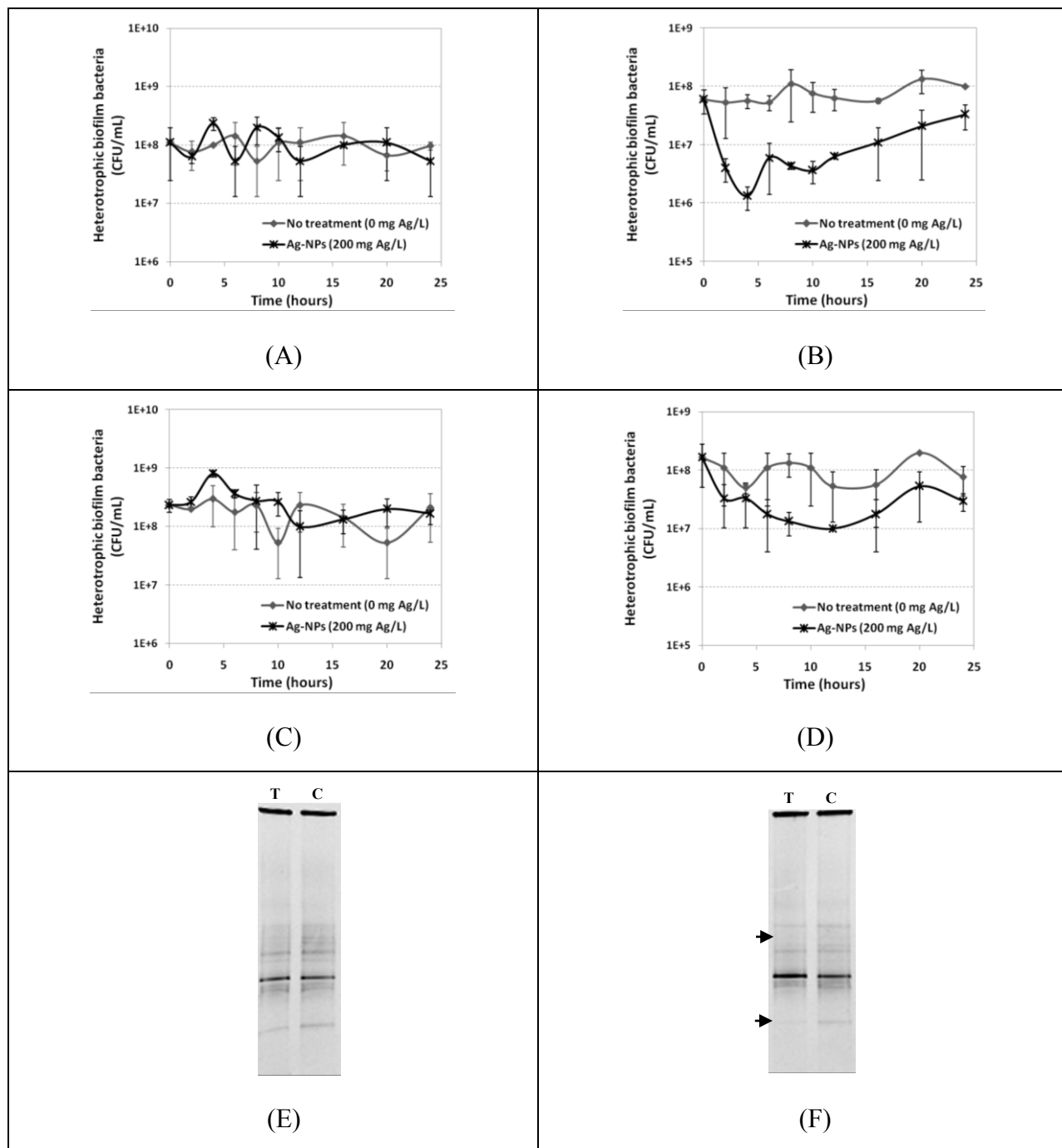


**Figure 3-4** Effects of Ag-NPs (200 mg Ag/L) on wastewater biofilms with (A, C, and E) and without (B, D, and F) loosely bound EPS, compared with the no treatment control (error bars represent one standard deviation): (A) (B) growth of heterotrophic bacteria 24 h after plating; (C) (D) growth of heterotrophic bacteria 4 days after plating; (E) (F) DGGE profile (C represents the no treatment control, while T represents a biofilm community under 200 mg Ag/L Ag-NP treatment. Missing bands are marked with arrows).

### 3.3.5 Effects of Ag-NPs on wastewater biofilms with loosely bound EPS removed

As shown in Figure 3-4B and D, the density of fast-growing bacteria in the no treatment control stabilized at about  $1.7 \times 10^8$  CFU/cm<sup>2</sup> during the 24-h period, and the total HPC stabilized at about  $2.4 \times 10^8$  CFU/ cm<sup>2</sup>. Removal of loosely bound EPS caused only a slight loss of biofilm bacteria (less than 0.2 log units in the HPC).

After the removal of loosely bound EPS, bacteria were more vulnerable to the treatment of Ag-NPs, which is consistent with reported protective effects of EPS on biofilm bacteria (Gong et al., 2009). A decrease in the HPC was detected when biofilms with loosely bound EPS removed were treated with Ag-NPs at 200 mg Ag/L. A comparison of Figure 3-4B and D indicates that Ag-NPs were more toxic to fast-growing bacteria. The maximum HPC reduction for fast-growing bacteria was 1.6 log units ( $p = 0.02$ ), observed 4 h after Ag-NP treatment, while loss in the total HPC never exceeded 1.0 log unit. However, after 4 h treatment, the concentration of heterotrophic bacteria in the treated samples started to recover, and the discrepancy was less than 1.0 log unit after 24 h. No significant decrease was detected for Ag-NP treatments of 1 and 50 mg Ag/L (Figure A-1). Further, our study showed that 200 mg Ag/L Ag<sup>+</sup> was more toxic than Ag-NP (Figure A-2), indicating that the release of Ag<sup>+</sup> might play an important role in the toxicity of Ag-NP to wastewater biofilms, and it may be easier for Ag<sup>+</sup> ions to reach and enter the cells compared to Ag-NPs. However, in our Ag-NP treatment studies, the toxicity of Ag<sup>+</sup> cannot be differentiated from the overall toxicity of Ag-NPs.

Removal of loosely bound EPS did not result in any missing bands, according to the no treatment controls shown in Figure 3-4E and F, but the intensity of several bands decreased

slightly. However, without protection from the intact EPS matrix, Ag-NPs exhibited bactericidal effects on certain bacterial species, although the reduction in HPC was not very pronounced. This may be explained by the fact that these bacteria are not cultivable. WWBF-C and WWBF-G were significantly reduced in the DGGE profile in Figure 3-4F. Since the higher intensity indicates a relatively higher concentration of bacteria (Liu et al., 2010), this may indicate that *Thiotrichales* is more sensitive to Ag-NPs than other strains. The genus of *Thiothrix* in the order of *Thiotrichales* is a group of filamentous bacteria commonly found in wastewater treatment plants (Howarth et al., 1999, Nielsen et al., 2000, Kim et al., 2002, Rossetti et al., 2003). Bacteria in this genus can oxidize reduced sulfur compounds and accumulate sulfur globules inside cells (Howarth et al., 1999). It has been reported that *Thiothrix* is able to sorb heavy metals (Shuttleworth and Unz, 1993). In this case, sorption of Ag-NPs may have led to a reduction in viability.

### **3.3.6 Toxic effects of Ag-NPs on planktonic wastewater bacteria**

Eight bacterial strains were isolated from the wastewater biofilm, distinguished by the appearance and growth rate of their colonies on R2A agar plates, as shown in Table 3-2. Planktonic pure and mixed cultures were tested for viability in the presence of Ag-NPs. As shown in Figure 3-5A, the initial cell density of each strain was about  $1 \times 10^7$  CFU/mL. With the treatment of 1 mg Ag/L Ag-NPs, only three strains (i.e., WWBF-3, WWBF-5 and WWBF-6) were still viable after 1 h. After 24 h, only the WWBF-5 was detected, with a 3 log unit reduction.

Table 3-2 Colonial morphology and growth rate of isolated biofilm bacteria.

Strains	Closest homologes	Color	Shape & surface	Diameter (mm)	Time to form visible colonies on R2A Agar
WWBF-1	<i>Flectobacillus</i> sp.	pink	smooth and shiny	2~3	3 d
WWBF-2	CFB group bacterium	yellow	smooth and shiny	1~2	3 d
WWBF-3	CFB group bacterium	light yellow	smooth	1~2	3 d
WWBF-4	<i>Cloacibacterium normanense</i>	dark yellow	mucoid	2~3	3 d
WWBF-5	<i>Microbacterium oxydans</i>	greenish yellow	smooth and shiny	1	3 d
WWBF-6	<i>Klebsiella</i> sp.	white	round, convex, smooth and shiny	5~7	24 h
WWBF-7	<i>Aeromonas</i> sp.	white	semi-transparent and a little bit wrinkled, with filamentous edges	4~6	24 h
WWBF-8	<i>Enterobacter</i> sp.	white	smoother, less transparent, with curled edges	3~5	24 h

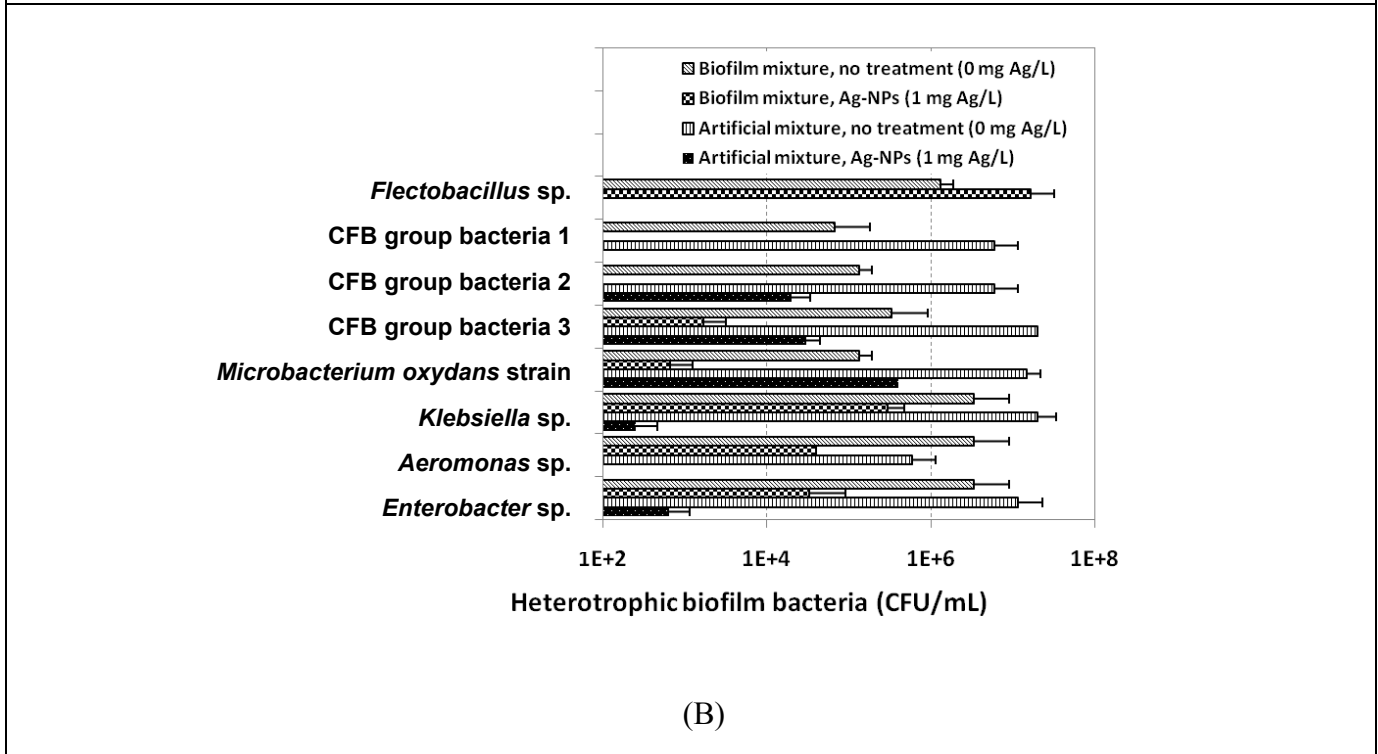
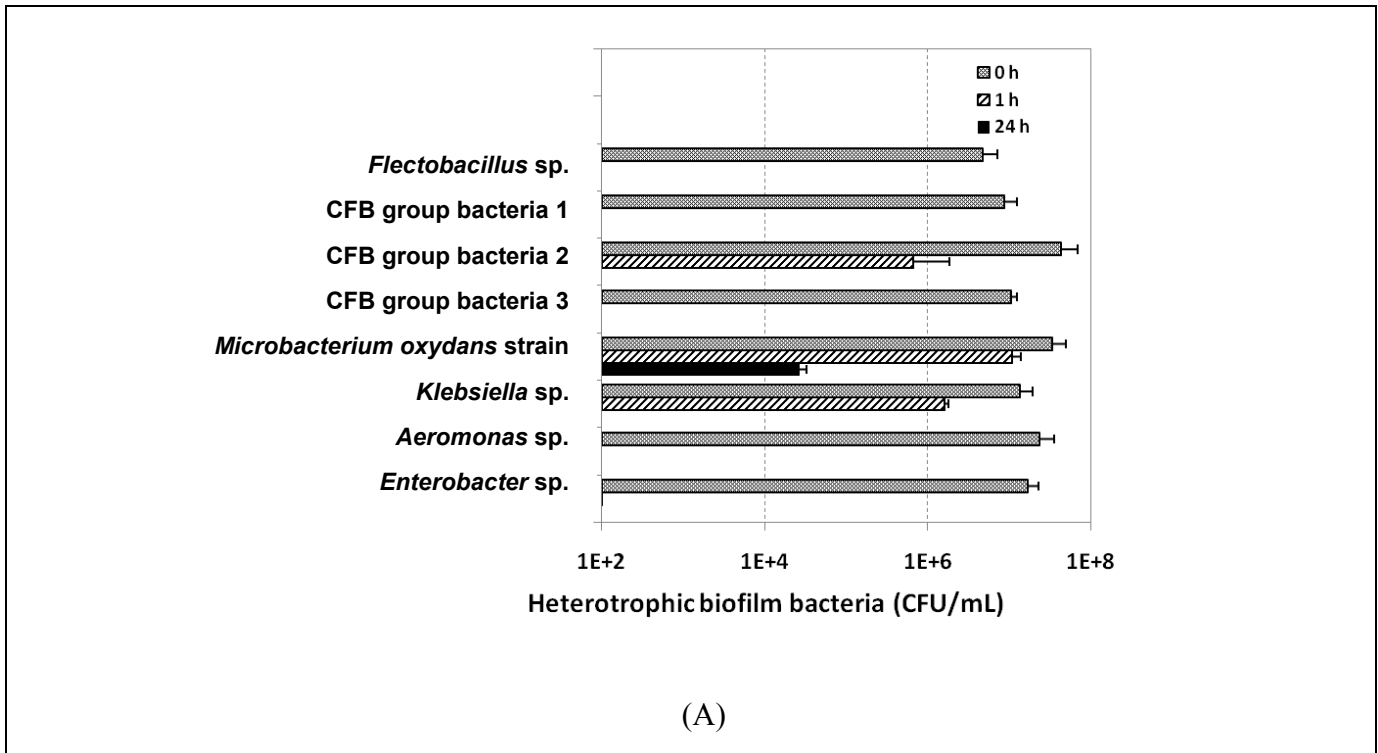


**Figure 3-5** Viability of planktonic bacteria isolated from wastewater biofilms: (A) single culture after different time periods of Ag-NP treatment (1 mg Ag/L); (B) individual strains in mixed cultures (biofilm mixture and artificial mixture) after 24 h of Ag-NP treatment (1 mg Ag/L) compared with the no treatment control.

As shown in Figure 3-5B, however, when treated as biofilm mixture, other strains besides WWBF-5 (WWBF-1, WWBF-4, WWBF-6, WWBF-7 and WWBF-8) survived after 24 h. WWBF-2 and WWBF-3 did not survive after the treatment, and there was a 1–2 log unit reduction in the HPC for WWBF-4, WWBF-6, WWBF-7 and WWBF-8. These results suggest that when treated individually, most of the isolated bacteria are highly sensitive to Ag-NPs, which is consistent with previous research. However, culturing these bacteria as a mixture helps to increase their viability under Ag-NP treatment, although they may be less tolerant to Ag-NPs than they are in the biofilm. This also indicates that the symbiotic effects among bacteria in wastewater biofilms can contribute significantly to their tolerance to Ag-NPs. Similar results were obtained for the artificial mixture, which also support this hypothesis.

### **3.4 Discussion**

#### **3.4.1 Mechanisms of biofilm tolerance**

The high tolerance to Ag-NPs of wastewater biofilms observed in the current study can be explained by several mechanisms: (i) physical protection in the biofilms; (ii) interactions among biofilm microorganisms; (iii) the slow growth rate of certain biofilm microorganisms. More than one mechanism may occur simultaneously.

##### **3.4.1.1 Physical protection**

Physical exclusion of Ag-NPs may be provided by the biofilm. 50–90% of the total organic carbon in a biofilm is usually from EPS, and the EPS matrices in wastewater biofilms are relatively complex (Flemming et al., 2000). The removal of loosely bound EPS (over 80% w/w

of the original biofilm) resulted in a significant increase in the vulnerability of bacteria to Ag-NPs. Furthermore, genera such as *Klebsiella* that produce large amounts of EPS were relatively more tolerant to Ag-NPs when treated individually in the current study. This is consistent with previous research indicating that several species from the genus *Klebsiella*, often present in wastewater treatment processes, have been shown to survive in toxic industrial wastewaters or under antibiotic treatment (Zahller and Stewart, 2002, Chen et al., 2008). Even after the removal of loosely bound EPS, the cells are still much more tolerant to Ag-NPs compared with planktonic cells. This may be associated with physical protection from tightly bound EPS. Similar results were observed in a study by Liu *et al.* (2007), where biofilm bacteria, in the presence of EPS, were found to be much more tolerant to TiO<sub>2</sub> nanoparticles, compared with planktonic cells.

In addition, since mass transfer into a biofilm is driven by diffusion, bacteria inside biofilms may be exposed to substantially lower concentrations of both toxins and nutrients. Furthermore, it is possible that Ag-NPs are trapped in the EPS matrix and cannot reach the microbial cells, due to significant aggregation near the cells (Holbrook et al., 2006). It has also been reported that environmentally relevant pH, ionic strength, and the presence of natural organic matter, had obvious impacts on the size distribution of Ag-NPs and consequently on their toxic effects (Cumberland and Lead, 2009, Fabrega et al., 2009a). In this study, Ag-NPs aggregated under the simulated environment in wastewater biofilms. This may have affected their bactericidal activity, since smaller Ag-NPs are more toxic (Morones et al., 2005, Choi and Hu, 2008). After extended

exposure times, more Ag-NPs may penetrate into the biofilm EPS matrix and bacterial cell membranes. It will be interesting to test these effects after 24h Ag-NP exposure.

#### **3.4.1.2 Biofilm community interaction**

The results in this study indicate that strains sensitive to Ag-NPs when tested individually survived when treated with Ag-NPs in a mixed community. This is consistent with studies showing that bacteria growing as a biofilm are more tolerant to antimicrobial agents due to interactions such as mutualism, commensalism, proto-cooperation and even competition in the symbiotic microbial community (Allison, 2000). In a mature biofilm community, vulnerable bacteria are often protected deep within the spatially organized consortium as a result of these interactions (Allison, 2000).

#### **3.4.1.3 Slow growth rate**

Slow growing bacteria are often more resistant than fast growing bacteria to antibiotics (Mah and O'Toole, 2001). This may explain why slow-growing bacteria WWBF-3 and WWBF-5 were more tolerant to Ag-NPs. A slow growth rate may also explain the increased tolerance to nanoparticles of bacteria in mature biofilms, where nutrients are limited (Brown et al., 1988, Mah and O'Toole, 2001). The protective effects from a slow growth rate may be associated with the expression of stress response genes (Stewart, 2002, Lu et al., 2009).

However, growth rate is not the only reason for the tolerance. Other factors, such as certain EPS components, may play an important role in the tolerance of each strain. It is also possible that starvation may contribute to the results obtained in this study, since there is no carbon source in PBS. No significant change of heterotrophic bacterial number was observed in no-treatment

control throughout the 24 h, indicating the reliability of the results. Further studies are needed to differentiate the potential impact of starvation. It is worth noting that a 1 log unit increase in WWBF-1 was observed in the biofilm mixture. The intensity of WWBF-E from the treated sample was also even higher than the intensity of the corresponding band from the no treatment control. This suggests that certain bacteria started to grow using cell debris of bacteria killed by Ag-NPs, causing recovery of the HPC during treatment.

### **3.4.2 Environmental implications**

Conditions in wastewater treatment plants are generally more complex than in the laboratory. Microorganisms usually congregate in suspended flocs (e.g., in the activated sludge process) or attached biofilms (e.g., in RBCs). The ionic strength in wastewater is usually high because of the presence of charged organic and inorganic ligands. Therefore, in this study, physical exclusion provided by the biofilms and the wastewater conditions were taken into account. Different from previous reports, microorganisms tested here are highly tolerant to Ag-NP treatment, indicating that results from treatment of planktonic bacteria cannot be used to estimate the impact of nanoparticles in environmental systems. These results largely complement previous research which only focuses on planktonic cells.

In addition, results here underlined the importance to understand the impact of nanoparticles on the microbial community structure in addition to counting the total number of bacteria. In this study, one group of filamentous microorganisms was observed to be highly susceptible to Ag-NPs. In the biological treatment process, filamentous microbes account for only 1% of the microorganisms. However, a reduction in filamentous microbes can significantly impact

treatment efficiency, especially in activated sludge systems since filamentous microbes constitute the backbone of activated sludge flocs (Sezgin et al., 1978).

Furthermore, it was found here that Ag-NPs can be sorbed to the biofilm matrix, indicating a potential role for biological removal of nanoparticles from wastewater. Sorption and accumulation in microbial aggregates may increase the concentration of engineered nanoparticles in biological treatment systems and thus pose a significant threat. The concentration of engineered nanoparticles in biological aggregates has not yet been determined, and is an important area for future study, particularly in sludge treatment. Some research has been carried out based on laboratory scale reactors in this direction (Hu, 2010).

### **3.4.3 Future research**

It should be noted that this study only focused on one kind of nanoparticle under aerobic conditions. Research on other kinds of nanoparticles in conditions relevant to various engineered wastewater purification systems would be further helpful. In addition, this study focused only on the protective mechanisms for wastewater biofilms. Further studies on the mechanisms controlling Ag-NPs toxicity will provide valuable information for understanding the potential adverse impact of Ag-NPs. Further, bacterial tolerance to silver may potentially develop during the course of the treatment (Chopra, 2007), which requires further studies to understand its impacts on the bacterial susceptibility to Ag-NPs.

It should also be noted that the HPC result is highly dependent on bacterial cultivability. It is possible that some bacteria are injured but still viable. These injured cells may temporarily lose their colony forming capability but are able to recover from the damage, which may also explain

our observation that for biofilm samples with loosely bound EPS removed, HPC reduced then increased after 200 mg Ag/L Ag-NP treatment. Similar recovery phenomena have been reported for other nanoparticles (Hardman, 2006). Therefore, for future studies, culture-independent methods should be applied to verify bacterial viability. Longer exposure times may also provide the opportunity to observe the return from dormancy.

### **3.5 Conclusions**

- Original wastewater biofilms are highly tolerant to Ag-NPs. However, accumulated Ag-NPs in wastewater biofilms may impact their microbial activity.
- Biofilms can provide physical protection for bacteria under Ag-NP treatment, and EPS may play an important role in this protection. Biofilm bacteria with loosely bound EPS removed are more sensitive to Ag-NPs.
- The effects of Ag-NPs on planktonic cells are different than on wastewater biofilms. Biofilm bacteria treated as isolated pure culture are much more sensitive to Ag-NPs, compared with mixture of bacteria in the biofilm. Even artificially mixed bacteria community can survive better under Ag-NP treatment.
- Susceptibility to Ag-NPs is different for each microorganism in the biofilm microbial community. *Thiotrichales*, in this study, is more sensitive than other biofilm bacteria.

## **Chapter 4 The effects of silver nanoparticles on intact wastewater biofilms**

### **4.1 Introduction**

By October 2013, there were 383 consumer products containing nano-silver, making nano-silver the most commonly used nanomaterial in consumer products for over five years (2014). It is inevitable that silver nanoparticles (Ag-NPs) will be released into domestic and industrial waste streams (Benn and Westerhoff, 2008, Hagendorfer et al., 2010) considering the high rate of use. These Ag-NPs could potentially cause adverse effects on microbial communities in biological wastewater treatment systems due to their antimicrobial properties. Considerable attention has been paid to this since the boom in application of nano-silver in consumer products, particularly after 2010. However, this research has been limited to specific groups of microbes, and most of the studies have been carried out on either pure cultures or lab-scale activated sludge systems. In addition, the characterization of microbial communities affected by Ag-NPs in biological wastewater treatment systems has not been directly linked to community function due to a lack of environmental sample sequence annotation in existing databases. Therefore, the effects of Ag-NPs on functional genes in biological wastewater treatment systems need to be monitored directly, especially the effects on wastewater biofilms, for which so far limited information has been discovered.

Comparatively speaking, the inhibition of nitrification by Ag-NPs has been relatively well-characterized in previous research. It is well-accepted that nitrification can be inhibited by Ag-NPs even at concentrations lower than 1 mg Ag/L; the effects are dependent on the dose, the

particle size, and the Ag-NPs coating (Choi and Hu, 2008, Choi and Hu, 2009, Nguyen et al., 2012, Yuan et al., 2013). The mechanism of Ag-NP toxicity involves membrane disruption, gene expression, enzyme inhibition, and energy production, and is closely associated with silver dissolution (Radniecki et al., 2011, Arnaout and Gunsch, 2012, Yuan et al., 2013). Ammonia oxidizing bacteria (AOB) are more sensitive to Ag-NPs than nitrite oxidizing bacteria (NOB) (Yang et al., 2013, Yang et al., 2014a). An elevated ammonia concentration can increase the toxicity of Ag-NPs (Mumper et al., 2013), while greater water hardness decreases toxicity (Yang et al., 2013, Anderson et al., 2014). At sublethal concentrations, Ag-NPs can upregulate *amoA* (Yang et al., 2013). The few reports that have documented the adverse effects of Ag-NPs on nutrient removal from wastewater are dose dependent, and nutrient removal can recover with time (Chen et al., 2013, Jeong et al., 2014, Alito and Gunsch, 2014). The effects of Ag-NPs on other microbial functional groups in biological wastewater treatment systems are far less well studied.

Biofilms are commonly used in a relatively large proportion of current biological wastewater treatment systems, such as rotating biological contactors (RBCs) and trickling filters. Previous studies have shown that microbial biofilms are more tolerant to antimicrobial agents than planktonic bacteria (Liu et al., 2007, Sheng and Liu, 2011). However, most of the current research has focused on pure-cultured planktonic or activated sludge systems under controlled conditions in the lab, and it is well recognized that full-scale systems are much more complicated than the scaled-down laboratory experimental systems (Wong et al., 2005). Moreover, it has recently been reported that sulfidation plays an important role on the fate of Ag-NPs in

wastewater treatment systems and can significantly reduce Ag-NP toxicity, since sulfide concentrations can be high in the wastewater treatment process, especially under anaerobic conditions (Hedberg et al., 2014, Kent et al., 2014, Liu et al., 2014). It is estimated that microgram per liter concentrations of nano-silver may be reaching wastewater treatment plants in North America (O'Brien and Cummins, 2010, Gottschalk et al., 2010, Tugulea et al., 2014), yet the effective concentration (the concentration actually resulting in toxicity) of Ag-NPs in wastewater treatment plants is likely lower than this estimation due to sulfidation. Therefore, to set regulation limits, it is essential to determine the real-world impacts of Ag-NPs on biofilms in wastewater treatment plants.

While some pyrosequencing of Ag-NP-exposed biological wastewater treatment system microbial communities have been performed (Yang et al., 2014b), direct information on the functional structure of microbial community is lacking. It has also been suggested that microbial communities in complicated ecosystems are functionally redundant (Lawton and Brown, 1993, Yin et al., 2000, Briones and Raskin, 2003). GeoChip analysis makes it possible to carry out systematic studies on the microbial community in terms of functional potential. In addition, microarrays interrogate samples against the exact same probe set, so as long as the appropriate probe set is present, low abundance populations are less likely to be missed. GeoChip 4 contains over 82,000 probes targeting 410 functional gene families (141,995 coding sequences), and covers genes associated with carbon, nitrogen, and sulfur cycling, phosphorus utilization, antibiotic and metal resistance, fungi function, etc. (Lu et al., 2012, Tu et al., 2014).

In this study, intact wastewater biofilms from a local wastewater treatment plant were treated with Ag-NPs. Tests were performed in wastewater from the plant to provide the same pH, ionic strength, and natural organic matter present in the plant. Transmission electron microscopy (TEM) was used to examine the biofilm uptake of Ag-NPs. GeoChip analysis was carried out to investigate the effects of Ag-NPs on the functional structure of the microbial community in the biofilm. The abundance of functional genes in 12 categories was monitored. Functional redundancy and its role in the tolerance of wastewater biofilms to Ag-NPs is discussed.

## **4.2 Materials and methods**

### **4.2.1 Wastewater biofilm samples**

Wastewater biofilms were collected from the first stage rotating biological contactor (RBC) unit in the Devon Wastewater Treatment Plant located in Devon, Alberta, Canada. The total surface area of the first stage RBC unit is 9290 m<sup>2</sup>. The average daily influent flow is about 2500 m<sup>3</sup>, with an average influent biochemical oxygen demand (BOD) of 158 mg/L. All RBC units are run indoors under ambient light. The year-round average room temperature is 20 °C, and the water temperature varies from 10–16 °C. The average biofilm thickness was 1.5 mm. Biofilms were sampled by cutting out a section (1.5 × 1.5 cm, attached to substratum) of the biofilm and substratum just before each experiment. Samples were stored in a Petri dish on ice during transport, and then processed within 30 min of arrival at the laboratory.

#### **4.2.2 Preparation of Ag-NP suspensions**

Self-dispersing silver nanopowder was purchased from SkySpring Nanomaterials, Inc. (Houston, USA). According to the product description, the Ag-NPs have a diameter less than 15 nm, and the particle composition is 10% silver (99.99% purity) and 90% polyvinylpyrrolidone (PVP), similar to Ag-NPs commonly used in commercial products. An Ag-NP suspension of 200 mg Ag/L was prepared by dispersing Ag-NPs in filtered (0.22  $\mu$ m) wastewater and vortexing for 30 s at the maximum speed.

#### **4.2.3 Ag-NP treatment**

For each experiment, replicate biofilms were each placed in either 5 mL of filtered wastewater or a Ag-NP suspension and then incubated with shaking (100 rpm) for 24 h in the dark at room temperature (25.5°C). For TEM imaging, the biofilm was sampled by cutting out small sections (0.5  $\times$  1.5 cm, attached to substratum) at 0 min (before exposure to Ag-NP), 45 min and 24 h. For cell enumeration and DNA extraction, the biofilm was scraped off the RBC substratum after the 24 h incubation. Each experiment was done in triplicate.

#### **4.2.4 Bacterial enumeration using HPC**

Bacterial enumeration was performed by HPC using the drop plate method (Zelver et al., 1999, Liu et al., 2007). A series of 10-fold dilutions were performed and 10  $\mu$ L of each dilution was plated on R2A agar in triplicate. Plates were incubated at 31° C for 24 h and held at room temperature for three days. Counting was performed with a lower detection limit of 10<sup>2</sup> CFU/mL. The result was converted into CFU/cm<sup>2</sup> based on the area of each biofilm sample. T-tests were performed in Microsoft Excel 2007 to examine the statistical significance of the results, and

corresponding *p*-values were calculated using a type 3 two-tailed T-test (unequal standard deviations). A *p*-value less than 0.05 indicated a statistically significant difference.

#### **4.2.5 TEM imaging**

TEM samples were prepared using the method described by (Zelver et al., 1999, Liu et al., 2007). Biofilm samples were fixed immediately after sampling with 2.5% glutaraldehyde in phosphate buffer for 30 min and rinsed with the same buffer three times for 5 min each. Samples were then fixed with 1% OsO<sub>4</sub> in phosphate buffer for 30 min and rinsed briefly with distilled water, followed by staining with 1% uranyl acetate and dehydrated in a series of ethanol solutions (50%, 70%, 90%, and 100%) for 5 min each. After two more additional changes in 100% ethanol, the samples were embedded in epoxy resin and polymerized at 60 °C for 24 h. Polymerized resin blocks were sectioned into ~60 nm slices and post-stained with uranyl acetate and lead citrate. Samples were visualized using a Philips/FEI (Morgagni) transmission electron microscope with a Gatan digital camera.

#### **4.2.6 GeoChip analysis**

The Powersoil<sup>®</sup> DNA Isolation Kit from MO BIO Laboratories, Inc. (Carlsbad, USA) was used to extract genomic DNA from each sample. DNA extracted from the triplicates under each condition (with/without Ag-NPs) were pooled respectively. Pooled DNA (1 μg) was labeled with Cy3 and hybridized to the GeoChip 4 microarray synthesized by NimbleGen (Madison, WI, USA) and processed as previously described by Lu et al. (2012). The signal-to-noise ratio threshold for a spot to be considered positive was  $\geq 2$  as described previously (He et al., 2010). Pearson's correlation coefficient (*r*) was calculated as a measure of the similarity between

selected gene profiles (Pearson, 1896). That is, for two profiles of normalized gene signal intensity:  $X = \{x_i : i = 1, \dots, n\}$  for no treatment control and  $Y = \{y_i : i = 1, \dots, n\}$  for Ag-NP treated sample,

$$r = \frac{\sum_{i=1}^n (x_i - \bar{x})(y_i - \bar{y})}{\sqrt{\sum_{i=1}^n (x_i - \bar{x})^2 \cdot \sum_{i=1}^n (y_i - \bar{y})^2}},$$

where  $\bar{x} = \frac{1}{n} \sum_{i=1}^n x_i$  and  $\bar{y} = \frac{1}{n} \sum_{i=1}^n y_i$ .

#### 4.2.7 qPCR analysis

qPCR was used to quantify total bacteria and bacteria associated with nitrification and denitrification. A CFX 96 real-time PCR system with a C1000 Thermal cycler (Bio-Rad Laboratories, Inc.) was used to run the reactions. 10  $\mu\text{L}$  of SsoFast EvaGreen Supermix (Bio-Rad Laboratories, Inc.), 10 pmol of each primer, 6  $\mu\text{L}$  of sterile water, and 2  $\mu\text{L}$  of DNA template (7  $\mu\text{L}$  of sterile water, and 1  $\mu\text{L}$  of DNA template for total bacteria) were added to each 20  $\mu\text{L}$  reaction system. Primers used and reaction programs are shown in Table 4-1. Calibration was performed with serial dilutions of a known quantity of the target fragments. Triplicate reactions were run for all samples analysed. Melting curves were examined to eliminate primer dimer formation or nonspecific amplification.

Table 4-1 qPCR primers and conditions.

Target	Primers	Program*	Reference
<b>Total Bacteria</b>	341f 5'-CCTACGGGAGGCAGCAG-3' 907r 5'-CCGTCAATTCCTTTRAGTTT-3'	3 min at 95 °C; 35 cycles of 30 s at 94°C, 30 s at 56°C and 30 s at 72°C.	Muyzer et al. 1993
<b>amoA gene</b>	amoA-1F 5'-GGGGTTTCTACTGGTGGT-3' amoA-2R-TC 5'-CCCCTCTGCAAAGCCTTCTTC-3'	1 min at 95 °C; 40 cycles of 5 s 95 °C, 20 s at 57 °C and 45 s at 72 °C	McTavish et al. 1993
<b>Nitrospira spp.</b>	NSR 1113f 5'-CCTGCTTTCAGTTGCTACCG-3' NSR 1264r 5'-GTTTGCAGCGCTTTGTACCG-3'	3 min at 95 °C; 50 cycles of 30 s at 95 °C, 60 s at 60°C	Dionisi et al., 2002
<b>Nitrobacter spp.</b>	Nitro 1198f 5'-ACCCCTAGCAAATCTCAAAAACCG-3' Nitro 1423r 5'-CTTACCCCCAGTCGCTGACC-3'	3 min at 95 °C; 50 cycles of 20 s at 94 °C, 60 s at 58°C and 40 s at 72 °C	Graham et al., 2007
<b>narG gene</b>	narG 1960m2f 5'-TAYGTSGGGCAGGARAAACTG-3' narG 2050m2r 5'-CGTAGAAGAAGCTGGTGCTGTT-3'	30 s at 95 °C; 35 cycles of 15 s at 95 °C, 30s at 58 °C, and 31s at 72 °C	Lo'pez-Gutie'rraz et al., 2004
<b>nirS gene</b>	nirS 1f 5'-TACCACCCSGARCCGCGCGT-3' nirS 3r 5'-GCCGCCGTCRTGVAGGAA-3'	30 s at 95 °C; 30 cycles of 15 s at 95 °C, 20s at 60 °C, and 31s at 72 °C	Braker et al., 1998
<b>nirK gene</b>	nirK 876 5'-ATYGGCGGVCAYGCGCA-3' nirK 1040 5'-GCCTCGATCAGRTRRTGGTT-3'	30 s at 95 °C; 30 cycles of 15 s at 95 °C, 30 s at 58 °C, and 31 s at 72 °C	Henry et al., 2004
<b>nosZ gene</b>	nosZ 2f 5'-CGCRACGGCAASAAGGTSMSSGT-3' nosZ 2r 5'-CAKRTGCAKSGCRTGGCAGAA-3'	30 s at 95 °C; 30 cycles of 15 s at 95 °C, 30 s at 60 °C, and 31s at 72 °C	Henry et al., 2006

\* all the programs included and a final melting curve analysis from 65 to 95 °C, measuring fluorescence every 0.5 °C.

## 4.3 Results

### 4.3.1 Uptake of Ag-NPs into the biofilm and cells

Ag-NPs were incorporated into the biofilms quickly after the incubation started. In the abiotic sample in Figure 4-1A, most Ag-NPs are round with a diameter no more than 20 nm and some formed aggregates larger than 50 nm. No particles similar to the Ag-NPs were seen in the control biofilm (Figure 4-1B). After 45 min, Ag-NPs (Figure 4-1 C, D, white arrows) were observed in the biofilm and only smaller Ag-NPs entered the biofilms. Over 10 areas were observed in each sample and most of the Ag-NPs were in the biofilm extracellular polymeric substances (EPS) matrix and not in the cells. Some Ag-NPs were near cells (Figure 4-1C), but other Ag-NPs aggregated in the EPS matrix far away from cells. This is consistent with previous research (Holbrook et al., 2006). After 24 h, the Ag-NPs were inside some cells, and a small fraction of cells with Ag-NPs started to die. Shrinkage and detachment of the plasma membrane from the outer membrane can be seen in Figure 4-1E, which potentially indicates apoptosis (Pandian et al., 2010). Ag-NPs has been reported to cause an apoptosis-like response in bacteria (Lee et al., 2014). However, in over 50% of biofilm areas examined after 24 hours of Ag-NP treatment, there were no Ag-NPs observed in the cells, as illustrated in Figure 4-1F. There were no significant differences observed between areas near the surface of the biofilm in contact with the bulk liquid and those close to the substratum.

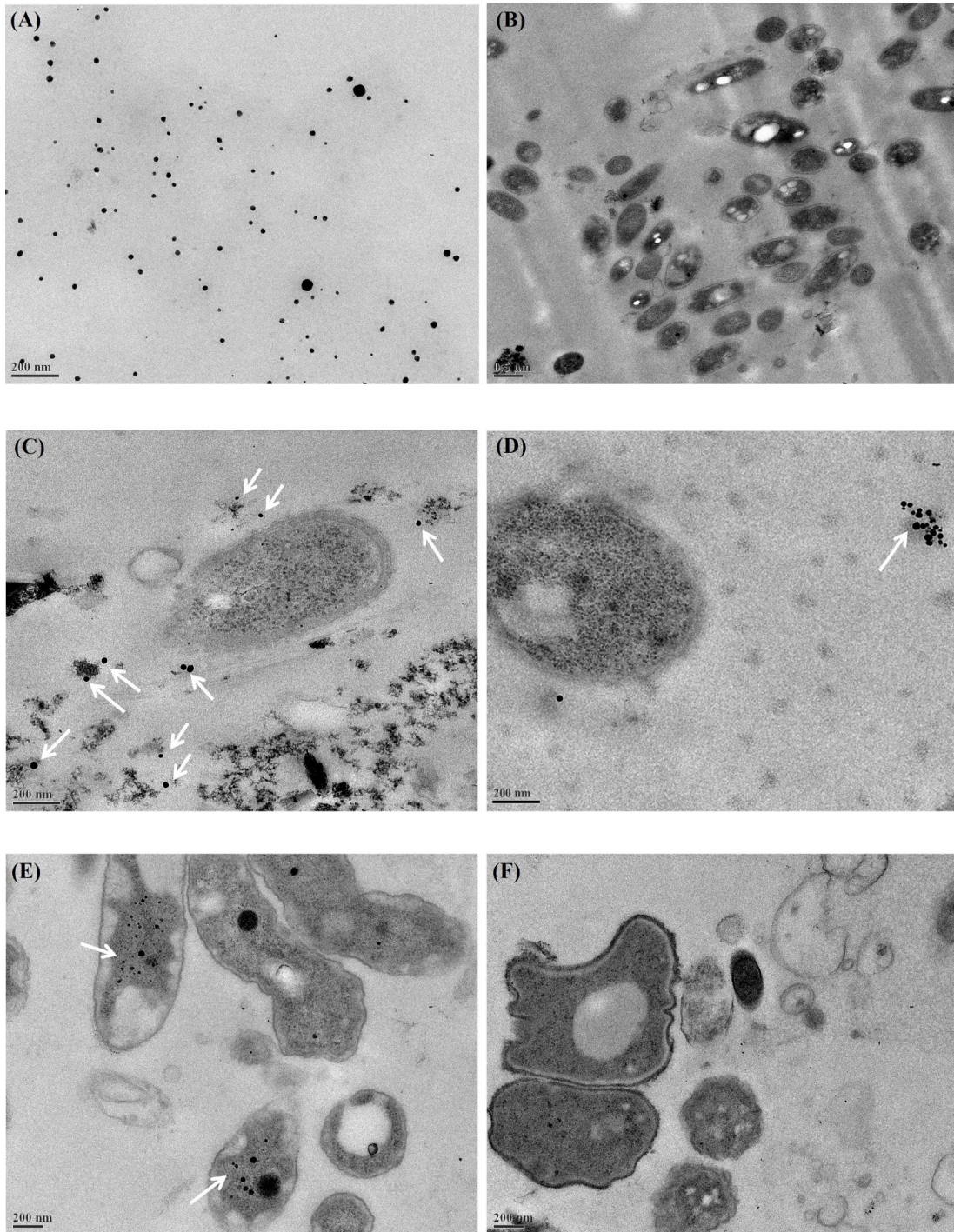


**Figure 4-1** Transmission electron microscopy (TEM) images. (A) Ag-NPs in wastewater, (B) Original wastewater biofilms, (C), (D) Wastewater biofilms incubated with Ag-NPs for 45 min, (E), (F) Wastewater biofilms incubated with Ag-NPs for 24 h. Ag-NPs are indicated by white arrows.

### 4.3.2 Overview of the effects of Ag-NP treatment on the biofilm microbial community

After 24 h, the HPC in the wastewater biofilm without Ag-NP treatment was  $3.07 \times 10^8$  CFU/cm<sup>2</sup> and the HPC in the wastewater biofilm with Ag-NP treatment was  $2.43 \times 10^8$  CFU/cm<sup>2</sup> (Table 4-2). There was no significant change in the viability of heterotrophic bacteria ( $p > 0.05$ ) although the concentration of Ag-NPs applied was as high as 200 mg Ag/L. The GeoChip results indicated that the relative abundance of genes in each functional category was almost identical with and without Ag-NP treatment as shown in Figure 4-2A, indicating no significant change in evenness (how equal the community is) of the microbial community. Some changes were detected by GeoChip analysis after the 24 h treatment with Ag-NPs. Figure 4-2B shows the number of genes detected (i.e., positive gene number) in each category. A ~40% decrease in positive gene number was observed with no significant decrease in total signal intensity for each category, indicating that enrichment occurred during the treatment. The GeoChip analysis indicated that there was a decrease in richness in the biofilm microbial community after the Ag-NP treatment.

Table 4-2 Viability of heterotrophic bacteria in intact wastewater biofilms under Ag-NP treatment.

Sample	HPC after 24 h (CFU/cm <sup>2</sup> )	<i>p</i> -value
No treatment (0 mg Ag/L)	$(3.07 \pm 0.45) \times 10^8$	0.11
With Ag-NPs (200 mg Ag/L)	$(2.43 \pm 0.27) \times 10^8$	

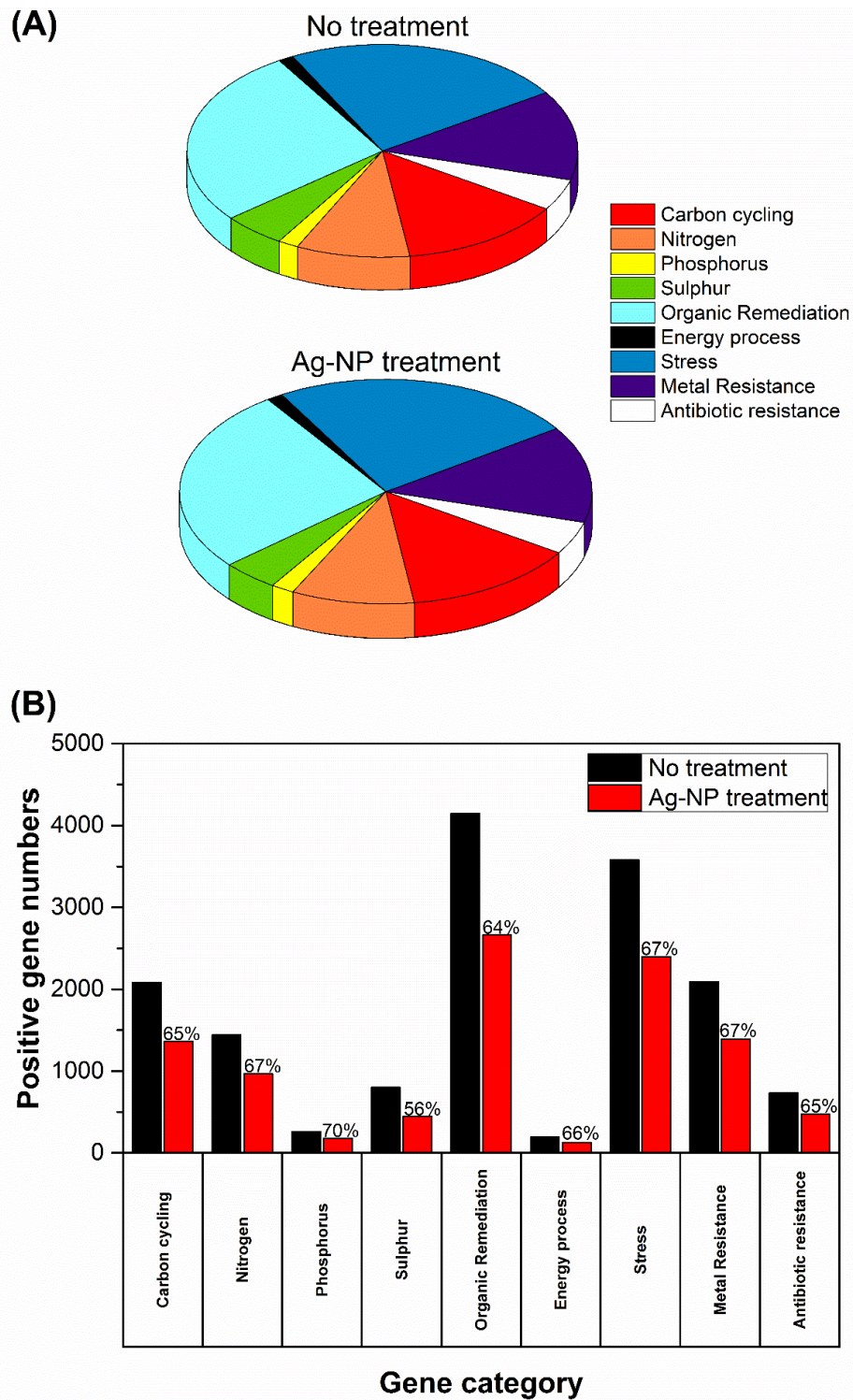


**Figure 4-2** Effects of Ag-NP treatment on gene abundance. (A) Relative abundance of genes in each category, (B) The number of genes detected; the fraction of positive genes detected after Ag-NP treatment is labeled on top of the bar.

### **4.3.3 Effects of Ag-NP treatment on nutrient and pollutant removal genes**

Gene profiles associated with carbon cycling, the nitrogen cycle, phosphorus utilization, and organic remediation are illustrated in Figure 4-3. There was a slight decrease (< 15%) in total signal intensity for these genes. However, in terms of relative abundance of genes in each subcategory (or for specific genes for phosphorus utilization), there was no significant change after Ag-NP treatment. The Pearson correlation coefficients ( $r$ ) between no treatment and Ag-NP treated samples for these four categories were all above 0.99. This indicated that in terms of function, the effects of Ag-NPs were not selective; that is, bacteria are equally sensitive to Ag-NPs if they are considered as functional groups. There was a small proportion of bacteria killed by Ag-NPs in each functional group. However, since the majority of bacteria survived in each functional group, the wastewater biofilm was still capable of degrading numerous types of nutrients and pollutants.

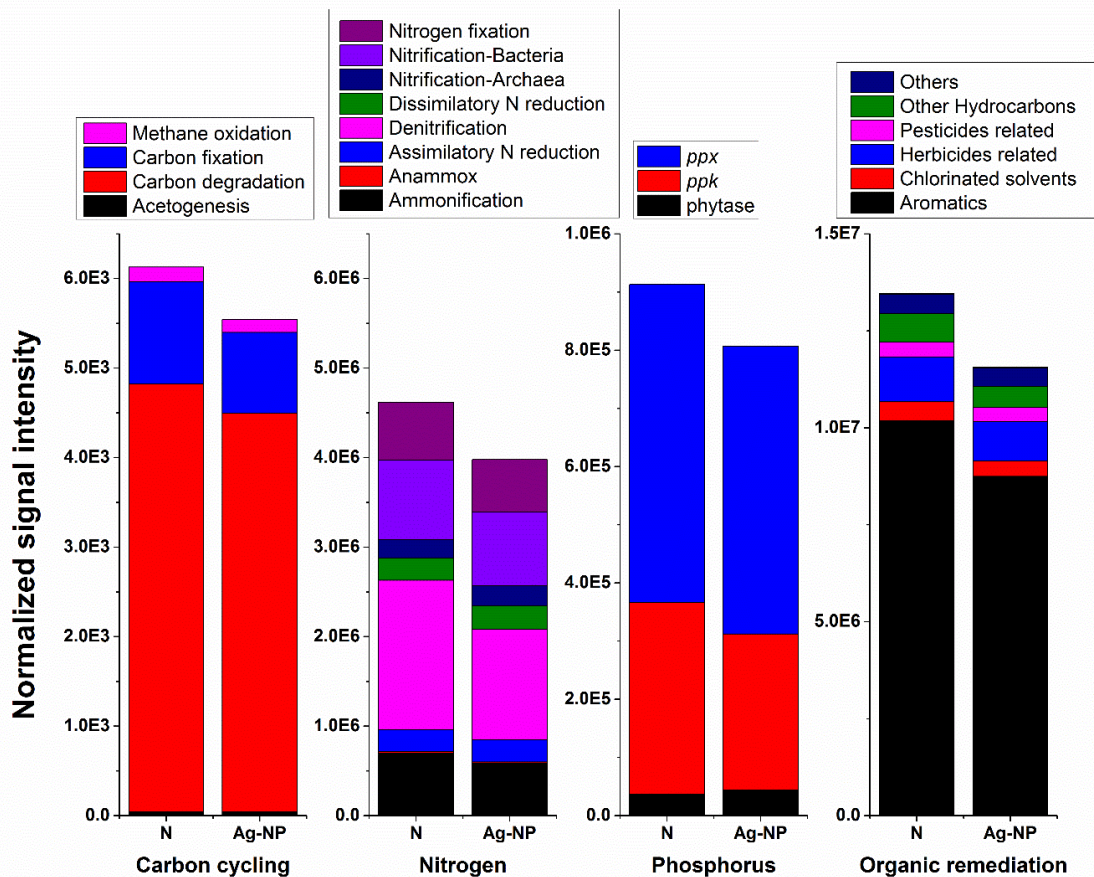


**Figure 4-3** Effects of Ag-NP treatment on genes associated with nutrient and pollutant removals. N indicates samples with no treatment and Ag-NP indicates samples with Ag-NP treatment.

#### 4.3.4 Response of the biofilm microbial community to stress caused by Ag-NPs

At the gene level, the trend was similar to the trends discussed above. There was a slight decrease in signal intensity in each gene but the relative abundance of each gene did not change significantly. However, when the lineage of each gene was examined, differences were observed as discussed below.

#### 4.3.4.1 Response of the microbial community to silver species

Overall, the total number of silver resistance gene (*silA*, *silC*, *silP*) variants decreased by 34% after Ag-NP treatment while the total signal intensity didn't decrease as much (only 17%). This trend is similar to genes in other categories: Ag-NP reduced gene diversity, but the effect on the corresponding overall function is not as significant. Some gene variants were missing after Ag-NP treatment (listed in supplementary Table B-1). However, this reduction has been compensated by the increase of some other variants. If only genes that were detected after Ag-NP treatment are considered, there was a higher abundance of these genes in the Ag-NP exposed samples (Figure 4-4 with the lineage color coded). For *silA* and *silP*, the signal intensity for most of the gene variants (four out of six strains and seven out of eight strains, respectively) increased in the Ag-NP treated sample. For *silC*, a similar increase in abundance was observed as well as some additional gene variants not detected in the control biofilm and indicated by black arrows in Figure 4-4. They are derived from *Rhodospirillum rubrum* ATCC 11170, *Pseudomonas syringae* pv. *syringae* B728a, *Burkholderia* sp. H160, and *Ralstonia pickettii* 12J. *Ralstonia pickettii* 12J is a heavy-metal resistant bacterium (NCBI-BioProject, 2008), and the other three all belong to the phylum *Proteobacteria*, which is very common in wastewater treatment systems. While the presence of these four specific strains cannot be absolutely confirmed based on such a short probe, the functional gene derived from or similar to these strains is present. In addition, these results do indicate that some strains are enriched in the Ag-NP treated sample.

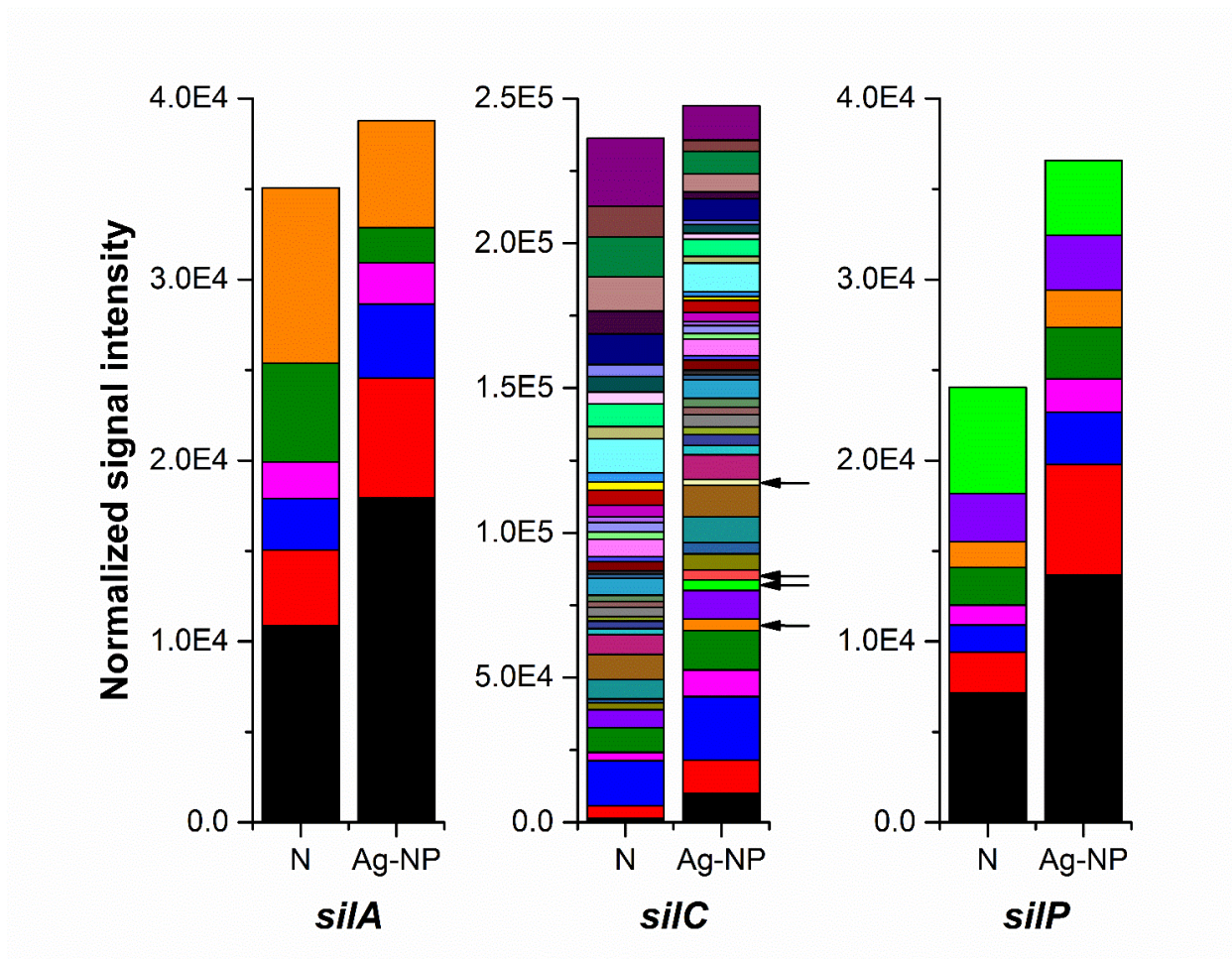


**Figure 4-4** Effects of Ag-NP treatment on genes associated with silver resistance. N indicates samples with no treatment and Ag-NP indicates samples with Ag-NP treatment. Colors are coded according to the lineage; genes from gene variants present only in Ag-NP treated samples are indicated with black arrows.

#### 4.3.4.2 Response of the microbial community to oxidative stress

It is well accepted that one important mechanism for the toxicity of Ag-NPs is oxidative stress caused by producing reactive oxygen species (ROS) (Choi and Hu, 2008, Kim and Ryu,

2013, Lee et al., 2014). Five genes associated with oxidative stress were examined: *ahpC*, *ahpF*, *katA*, *katE*, *oxyR*. Genes *ahpC* and *ahpF* encode the two components of the alkyl hydroperoxide reductase. This enzyme detoxifies hydroperoxides produced under oxidative stress (Smillie et al., 1992). Genes *katA* and *katE* encode two kinds of catalases. Gene *katA* is specifically induced by hydrogen peroxide while *katE* encodes a general sigma-factor dependent stress protein (Smillie et al., 1992). Both alkyl hydroperoxide reductase and the catalases require the positive regulator, *oxyR* gene, for hydrogen peroxide induction, and the *oxyR* gene functions as a positive regulator (Christman et al., 1989, Smillie et al., 1992, Dalla Costa et al., 2009). The response of these genes was very similar to the response of the silver resistance genes. The number of gene variants detected decreased by 36%, 34%, 42%, 36% and 39% for *ahpC*, *ahpF*, *katA*, *katE*, *oxyR*, respectively. Again, the reduction in total signal intensity remained below 20% for most of these genes, indicating more significant reduction of gene diversity instead of overall function. The only exception is the *oxyR* gene, where the total signal intensity decreased by 32%. This unique decrease in the regulator gene *oxyR* may indicate that cells didn't have much chance to adapt to Ag-NPs before they were inhibited when high concentration of Ag-NP was used. If only strains detected in the Ag-NP treated samples are considered, the majority of these strains increased in abundance in the Ag-NP treated sample (44 out of 66 strains, 20 out of 29 strains, 11 out of 14 strains, 68 out of 101 strains and 41 out of 63 strains for *ahpC*, *ahpF*, *katA*, *katE*, *oxyR*, respectively). Gene variants that were detected only in the Ag-NP treated sample (Figure 4-5, black arrows) indicated that genes associated with oxidative stress were also enriched in the

presence of Ag-NPs. Specifics of gene variants reduced and enriched has been included in the supplementary Tables B-1 and B-2.

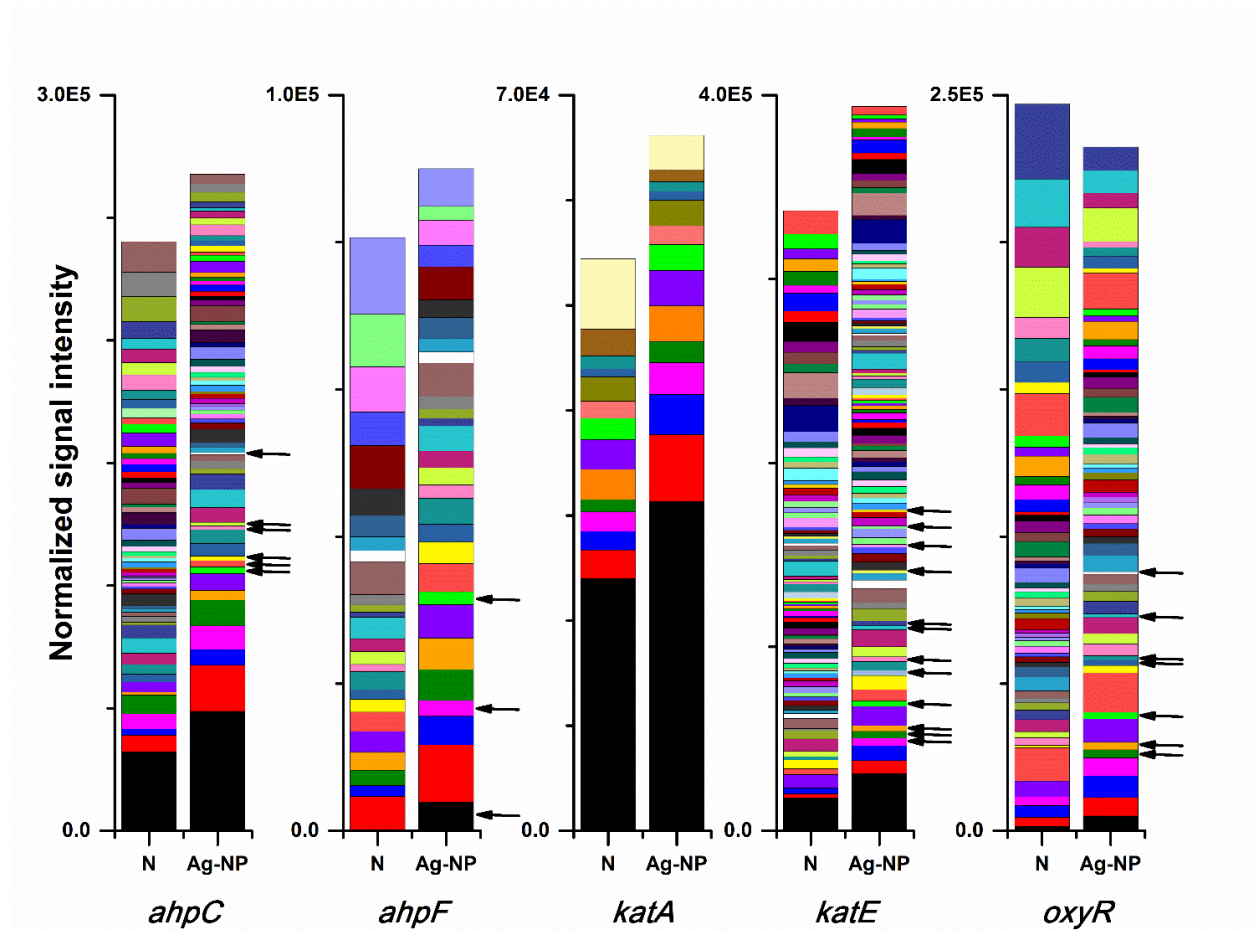


**Figure 4-5** Effects of Ag-NP treatment on genes associated with oxidative stress. N indicates samples with no treatment and Ag-NP indicates samples with Ag-NP treatment. Colors are coded according to the lineage; genes from gene variants present only in Ag-NP treated samples are indicated with black arrows.

### 4.3.5 Confirmation by qPCR

The total bacteria was quantified with qPCR to confirm the HPC results, and the number of two major functional groups (nitrification and denitrification) of bacteria was also quantified by qPCR to confirm the GeoChip results. As shown in Figure 4-6, there was no significant

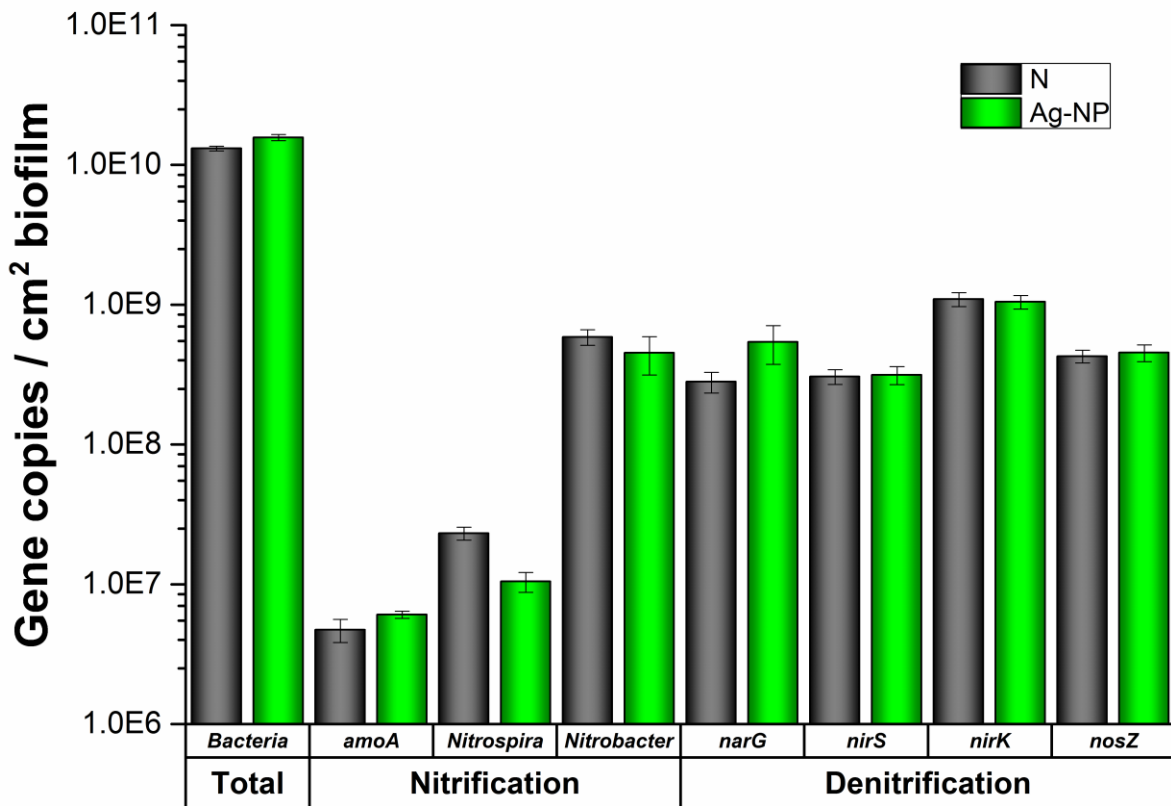


**Figure 4-6** qPCR results. N indicates samples with no treatment and Ag-NP indicates samples with Ag-NP treatment. Error bar indicates standard deviation.

difference between the Ag-NP treated biofilm and the control biofilm in terms of total bacteria density. Slightly larger amount of bacteria was detected in the Ag-NP treated biofilm. However,

the difference is smaller than one log unit and is not statistically significant. Although cultivable heterotrophic bacteria account for only a small proportion of the total microbial community, this result suggests that qPCR and HPC results are consistent with each other. Wastewater biofilms are highly tolerant to Ag-NPs. For nitrification and denitrification bacteria, there was no significant difference in majority of the genes examined. There was a minor decrease in *Nitrospira* spp. and a minor increase in *narG* gene. However, if the nitrification and denitrification bacteria are considered as two groups, no significant difference was observed. Especially when the ratio of nitrification and denitrification bacteria to the total bacteria was calculated, there was no statistically significant difference. The ratio of nitrification to total bacteria for control and Ag-NP treated biofilms were 5% and 3%, respectively. The ratio of denitrification to total bacteria for control and Ag-NP treated samples were 16% and 15%, respectively. All the *p*-values are larger than 0.05, indicating a good agreement with GeoChip results showing no significant difference in relative abundance.

## **4.4 Discussion**

### **4.4.1 Functional stability and functional redundancy**

GeoChip functional gene analysis indicated that wastewater biofilm functions are fairly robust in the presence of Ag-NPs. Our results showed no significant changes in the relative abundance of functional genes in wastewater biofilms after 24 hours of Ag-NP treatment at 200 mg Ag/L. This is consistent with previous research (Christman et al., 1989, Smillie et al., 1992, Dalla Costa et al., 2009). There was no significant change at the category, subcategory, and gene

levels ( $r > 0.99$ ). For each gene, there was loss of signal from certain gene variants, which resulted in a loss of positive gene numbers. However, this loss was always compensated for by either an increased abundance of residual strains or an enrichment of non-dominant strains. It is clear that each functional gene has redundancies from many different strains carrying the same gene and that the loss of a single or even several strains is compensated for by an increase in abundance of other strains. It has long been believed that, in an ecosystem, multiple species can perform similar functions. That is to say that these species are functionally redundant and thus are substitutable with minimal impact on the overall function of the ecosystem (Lawton and Brown, 1993, Rosenfeld, 2002). This functional redundancy has been found in both natural and engineered ecosystems (Lawton and Brown, 1993, Rosenfeld, 2002). The results in this study provide direct evidence for the functional redundancy of microbial communities in engineered ecosystems. However, it should be noted that necessary redundancy is required to ensure the stability of an ecosystem under disturbance (Walker, 1995). The enrichment under Ag-NP treatment led to reduced redundancy in the biofilm microbial community and therefore could lead to a decreased stability under future perturbation, a possibility that needs to be further explored.

#### **4.4.2 Compositional and structural stability**

Composition was not as stable as function in the wastewater biofilm microbial community. The decrease in gene number after exposure to Ag-NPs indicated that some bacteria were killed by Ag-NPs, consistent with the TEM observations. The loss and enrichment of genes from different lineages indicated that Ag-NPs triggered changes in the composition of the microbial

community. This is consistent with previous research showing that microbial community composition is often sensitive to disturbance (Shade et al., 2012). However, it should be noted that the concentration of Ag-NPs used in this study (200 mg Ag/L) was much higher than what is expected in real wastewater treatment plants (O'Brien and Cummins, 2010, Gottschalk et al., 2010, Tugulea et al., 2014), which is at the microgram per liter range. 200 mg Ag/L was chosen according to previous study to make sure detectable changes could be seen (Sheng and Liu, 2011, Sun et al., 2013). However, under such a high concentration of Ag-NPs, the effects of Ag-NPs are still minimal. In addition, the effects of Ag-NPs are dose-dependent (Sheng and Liu, 2011, Sun et al., 2013). Therefore, it is probable that biofilms in wastewater treatment plants will not be significantly affected under current Ag-NP release conditions. A considerable fraction of the Ag-NPs go through aggregation and sulfidation in the EPS matrix and therefore cannot reach microbial cells (Holbrook et al., 2006, Fabrega et al., 2009a, Hedberg et al., 2014, Kent et al., 2014). In addition, no significant change in biofilm structure was observed in the TEM study, indicating that the wastewater biofilms were structurally stable. This structural stability likely contributed to the Ag-NP tolerance of the wastewater biofilm as well. However, it should be noted that the decrease of compositional diversity may make the biofilm more vulnerable to future disturbance and potentially reduce the stability of the system.

#### **4.5 Conclusions**

- Intact wastewater biofilms appeared highly resistant to Ag-NPs based on heterotrophic plate counts which detects only cultivable bacteria.

- A clear decrease in gene diversity was evident based on GeoChip analysis, although the complete loss of any specific gene was rare.
- Ag-NP treatment decreased microbial community diversity but did not significantly affect the microbial community function.
- This provides direct evidence for the functional redundancy of microbial community in engineered ecosystems such as wastewater biofilms.

## **Chapter 5 Contradictory effects of silver nanoparticles on activated sludge wastewater treatment**

### **5.1 Introduction**

It is inevitable that nano-silver will be released into domestic and industrial waste streams, as it is the most commonly used nanomaterial in consumer products (Project-on-Emerging-Nanotechnologies, 2014). Considerable attention has been paid to the potential adverse effects on biological wastewater treatment system (BWTS) due to the antimicrobial properties of silver nanoparticles (Ag-NPs). A general conclusion can be made from previous research that the effects of Ag-NPs depend on the dose and time period applied as well as the property of Ag-NPs and the system to which the Ag-NPs are applied. However, great controversy still exists on how each of these parameters affects the impacts of Ag-NPs, and a sophisticated toxicology model has not been built at all. Previous research covers only a tip of the iceberg of all possible combination of these parameters. Not to mention that the mechanisms behind the phenomena are poorly understood.

Higher concentrations of Ag-NPs often results in more significant adverse effects (Kim et al., 2007). Hormetic effects under sublethal concentration have been reported occasionally but stayed as a marginalized concept (Fabrega et al., 2009b, Sheng and Liu, 2011, Xiu et al., 2012, Yang et al., 2013). Properties of Ag-NPs that affect its toxicity include nanoparticle size, shape and coating. Smaller Ag-NPs tend to be more toxic (Morones et al., 2005, Choi and Hu, 2008, Zhang et al., 2008b). Spherical Ag-NPs and polyvinylpyrrolidone (PVP) coating tend to have

weaker bactericidal action (Pal et al., 2007, Arnaout and Gunsch, 2012). However, the effects of shape and coating are not yet well-studied.

The properties of the BWTS are even more complicated. The microbial community compositions, ordered from the most resistant to Ag-NPs to the least, include biofilm/activated sludge, planktonic mixed culture and pure culture of single strains (Kim et al., 2007, Sheng and Liu, 2011, Sun et al., 2013, Kumar et al., 2014). Potential ligands that can bind with Ag-NPs or released Ag<sup>+</sup> ions from influent and in the system can lower the dissolution of Ag-NPs and their bactericidal effects (Lok et al., 2006, Fabrega et al., 2009a, Anderson et al., 2014). These ligands range from organic matter, such as dissolved organic carbon and natural organic matter, to inorganic ions, such as chloride and sulfide. More recent studies tend to focus on long-term effects of Ag-NPs under conditions mimicking the real-world conditions in BWTS. Acute inhibition is often observed at the beginning of Ag-NP addition, but the system usually recovers in the long term (Chen et al., 2013, Alito and Gunsch, 2014). The adverse effects of Ag-NPs are minimal especially when sulfidation plays an important role in most of the BWTSs (Kim et al., 2010, Levard et al., 2012, Doolette et al., 2013, Kaegi et al., 2013, Hedberg et al., 2014, Ma et al., 2014). A toxicological model to estimate the effects of Ag-NPs is beginning to take shape. This raises the question: should the hormesis model be considered here?

This study examines the response of the microbial community to a potentially “least-toxic” combination, which is the case in most of our current BWTSs in practical operation: low dose, long-term, spherical Ag-NPs with PVP coating in activated sludge bioreactors fed with synthetic municipal wastewater. No significant effects were seen on pollutants removal. However,

interestingly, Ag-NPs helped to maintain the microbial community diversity in the activated sludge. 16s rRNA gene based pyrosequencing was used to monitor the bacterial community and GeoChip was used to directly examine the functional diversity of the microbial community. Properties of the sludge, accumulation of silver species inside the sludge and characteristics of the Ag-NPs were examined to explain this phenomenon.

## **5.2 Material and Methods**

### **5.2.1 Reactor setup**

Four sequencing batch reactors were operated for over three months. The total volume of the reactors was 1L and the effective volume was 700 mL. The reactors were run on a 12 cycle (5 min of influent filling, 11 h of aeration, 30 min settling, 5 min effluent withdraw and 20 min idle). Hydraulic retention time was 24 h. Solids retention time was monitored but not controlled. The reactor feed was prepared according to Alito and Gunsch (2014) and contains an average COD of 450 mg/L and ammonia of 40 mg/L with pH adjusted to  $7.3 \pm 0.5$ .

Self-dispersing silver nanopowder was purchased from SkySpring Nanomaterials, Inc. (Houston, USA). According to the Ag-NP product description, the particle size is less than 15 nm, and the particle composition is 25% silver (99.99% purity) and 75% polyvinylpyrrolidone (PVP), similar to Ag-NPs commonly used in commercial products. PVP and silver species addition started after the reactor reached steady state for over two weeks (27 days after start-up). Ag-NPs were added as Aged Ag-NPs and fresh Ag-NPs at a concentration of 1 mg Ag/L in influent. Aged Ag-NPs stock suspension was prepared when reactors were started up and kept at

4°C in dark and was added into the influent tank and kept under room temperature in dark for one week. Fresh Ag-NPs suspension (3.5 g Ag/L) was prepared everyday and 0.1 mL suspension was spiked into the reactor during influent filling in each cycle, producing a concentration equalled to 1 mg Ag/L in influent. 0.1 mL of this freshly prepared Ag-NP suspension was also added into a dialysis unit (Slide-A-Lyzer™ MINI Dialysis Device, 2K MWCO, 0.1 mL, Thermo Scientific, USA) and the dialysis unit was put into the reactor during influent filling in each cycle and float in the activated sludge for 12 h before changing to a new one. Equal amount of PVP (3 mg PVP/L) was added into the control reactor. The tests of Ag-NP and PVP addition have been performed for over two months. Similar operation of reactors and Ag-NP addition were repeated for several times.

### **5.2.2 Reactor performance monitoring**

Effluent quality was monitored in terms of COD and ammonium removal using Hach methods 8000 and 10205. SVI and MLSS were measured according to the standard methods. Reaction kinetics of COD and ammonium removal and nitrate production was also performed using the substrate depletion method (Bassin et al., 2012). Mixed liquor samples were collected at 15, 30, 35, 60, 90, 120, 150, 180, 210, 240, 300, 480 and 660 min, centrifuged at 3000 g for 10 min at 4°C, filtered (0.45 µm) and analyzed for COD, ammonium and nitrate. Nitrate was measured using ion chromatography (IC).

### **5.2.3 Microbial community analysis**

Activated sludge samples were collected in duplicates and genomic DNA was extracted using a Powersoil® DNA Isolation Kit from MO BIO Laboratories, Inc. (Carlsbad, USA). DNA

was analyzed with pyrosequencing and GeoChip.

Paired-end sequencing based on the 16S rRNA gene was performed at the Research and Testing Laboratory (Lubbock, TX, USA), using the Illumina MiSeq platform (Zodrow et al., 2014). Primers 28F (5'-GAGTTTGATCNTGGCTCAG-3') and 519R (5'-GTNTTACNGCGGCKGCTG-3') were used, which covered V1–V3 hypervariable regions (Campbell and Kirchman, 2013). Chimeras and poor quality sequences were removed from the denoised sequence reads. The remaining sequences were clustered into operational taxonomic units (OTUs) with 0% divergence using USEARCH. Taxonomic information was assigned to OTUs based on a database of high quality sequences derived from the NCBI using a distributed .NET algorithm that utilizes BLASTN+ (Kraken BLAST, [www.krakenblast.com](http://www.krakenblast.com)). A principal coordinates analysis (PCoA) of microbial community diversity was performed using the QIIME pipeline (<http://qiime.org/>) with the beta diversity metrics of weighted unifrac (Crawford et al., 2009).

DNA (1 µg) was labeled with Cy3 and hybridized to the GeoChip 5 microarray synthesized by NimbleGen (Madison, WI, USA) and processed as previously described by Lu et al. (Lu et al., 2012). The signal-to-noise ratio threshold for a spot to be considered positive was  $\geq 2$  as described previously (He et al., 2010). Detrended correspondence analysis (DCA) was performed based on sample scores. Hierarchical clustering analysis based on the Bray-Curtis dissimilarity indices was performed and a corresponding heatmap was built with the top 30 abundant functional genes in each sample.

#### **5.2.4 Silver accumulation and release and nanoparticle characterization**

Silver species accumulation and release was measured with inductively coupled plasma mass spectrometry (ICP-MS) using the ELAN 9000 ICP mass spectrometer (PerKinElmer, Canada). Microwave digestion was performed as described by Wu *et al.* (1997) and briefly summarized here. 10 mL concentrated nitric acid and 2 mL ultra-pure water were added to 1g biofilm (wet weight) or 1 mL suspension and kept at room temperature overnight for pre-digestion. Microwave digestion was then carried out using ETHOS EZ Microwave Solvent Extraction Labstation (Milestone Inc., USA) with the following heating program: heat to 190 °C within 15 min and then hold at 190 °C for 10 min. The particle size and zeta potential of Ag-NPs was characterized using a Malvern Zetasizer Nano-ZS (Model: ZEN3600, Malvern Instruments Ltd, Worcestershire, UK). Since PVP dissolves in water completely, parameters of silver were adopted for the analysis: the refractive index was 2.0 and the absorption coefficient was 0.320 (Sur *et al.*, 2010)<sup>43</sup>.

## **5.3 Results**

### **5.3.1 Ag-NPs helped to maintain reactor performance**

No significant change in pollutant removal was observed after Ag-NP addition in any of the four reactors (Figure 5-1 A and B). The COD removal rate was maintained at above 90%, and ammonium removal was above 99% in each reactor at all times. Figure 5-1 C, D and E show the COD, ammonium and nitrate concentration change against time in four reactors on day 64. Only a slight difference in reaction kinetics was observed. The majority of the COD was removed from each reactor within the first 30 min, and ammonium removal was completed within 4 h.

The reaction rate constant for COD removal remained almost the same in all reactors ( $p$ -value  $> 0.05$ ) after two months of Ag-NP addition. Nevertheless, minor differences can be seen in the ammonium removal kinetics. The rate constant for ammonium removal decreased to  $0.35 \text{ h}^{-1}$  in the PVP control and  $0.34 \text{ h}^{-1}$  in the reactor with aged Ag-NP addition ( $p$ -value =  $0.03$ ), compared to the initial value of  $0.55 \text{ h}^{-1}$  before Ag-NP addition. However, this rate constant increased to  $0.66 \text{ h}^{-1}$  in the reactor fed with fresh Ag-NPs ( $p$ -value =  $0.11$ ). The rate constant decreased slightly to  $0.48 \text{ h}^{-1}$  in reactor fed with  $\text{Ag}^+$  ion released from fresh Ag-NPs ( $p$ -value =  $0.18$ ).

Fresh Ag-NP helped to maintain the ammonium oxidizing reaction rate in the reactors. However, it should be noted that if the biomass concentration is taken into account, the ammonium uptake rate decreased in all reactors, compared with the initial values ( $p$ -value  $< 0.05$ ). The initial ammonium uptake rate was  $3.0 \text{ mg N g}^{-1} \text{ VSS h}^{-1}$ ; the ammonium uptake rate decreased to 2.2, 2.0, 1.3,  $2.3 \text{ mg N g}^{-1} \text{ VSS h}^{-1}$  in reactor fed with PVP, Aged Ag-NPs, fresh Ag-NPs and  $\text{Ag}^+$  ion, respectively. Similarly, the reactor fed with fresh Ag-NPs also had the lowest COD uptake rate. This indicates that when averaged to each gram of biomass, the metabolic activity of microbes in the reactor fed with fresh Ag-NPs didn't increase with the biomass concentration. As a matter of fact, the ammonium oxidizing reaction rate constant in the reactor fed with fresh Ag-NPs stayed the highest (above  $0.6 \text{ h}^{-1}$ ) among all the reactors during the three-month period. The ammonium uptake rate in the reactor fed with fresh Ag-NPs was also the highest ( $2.5 \text{ mg N g}^{-1} \text{ VSS h}^{-1}$ ) in all four reactors on day 22, before the significant biomass increase occurred. It appeared that nutrient uptake rates in the reactor fed with fresh Ag-NPs hit a bottleneck when the biomass increased significantly.

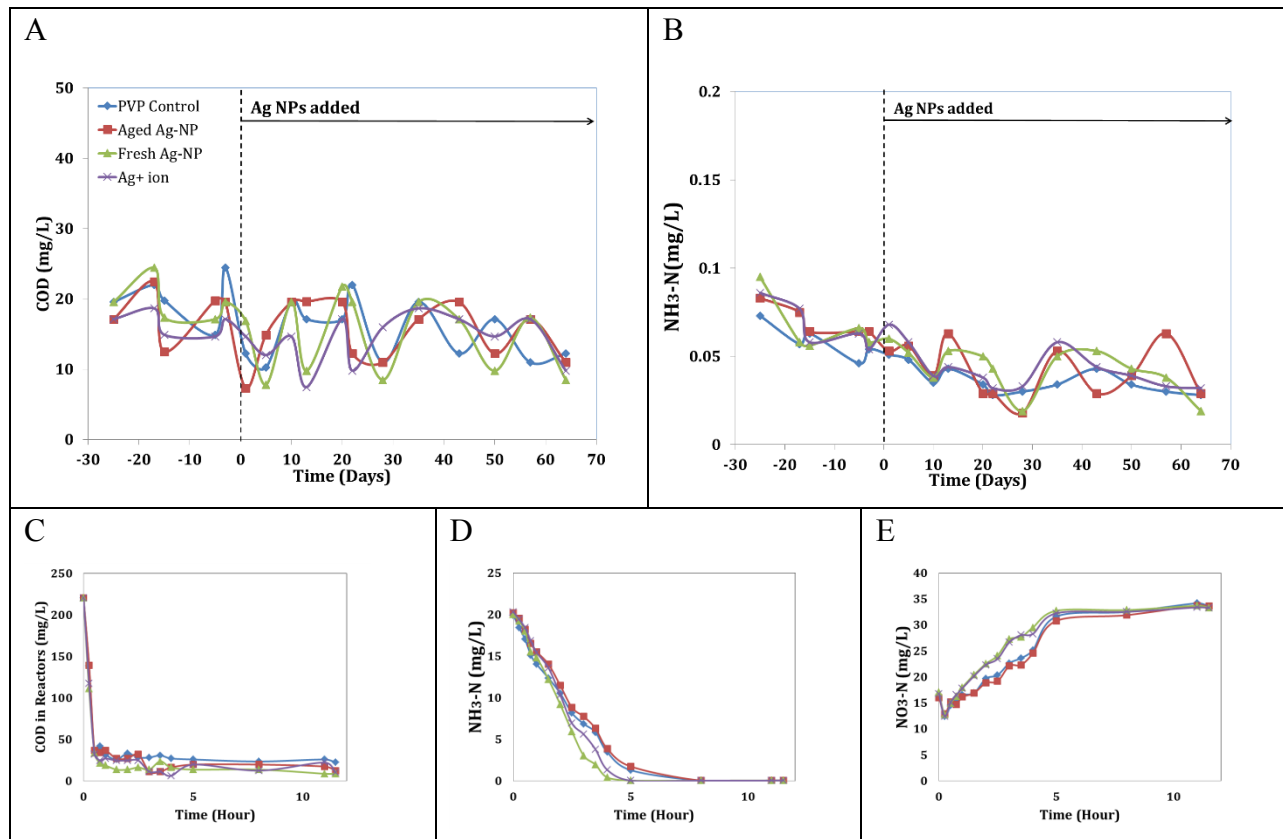


**Figure 5-1** Performance of each reactor. (A) Efluent COD concentration; (B) Effluent ammonia concentration; (C) COD removal kinetics; (D) Ammonia removal kinetics; (E) Nitrate production kinetics.

### 5.3.2 Ag-NPs improved sludge settleability and increased biomass concentration

The biomass concentration in the reactor with fresh Ag-NPs increased significantly after two months of operation, as indicated by mixed liquor suspended solids (MLSS) concentration in Figure 5-2A. The MLSS concentration reached the peak of 4866 mg/L on day 56 in the reactor with fresh Ag-NPs, while it stabilized at about 2400 mg/L in the others. Meanwhile, the sludge volume index (SVI) in this reactor is much lower than the others as well (Figure 5-2B). SVI

stabilized at about 100 mL/g in the reactor with fresh Ag-NPs and stayed below 220 mL/g in reactors fed with aged Ag-NPs and Ag<sup>+</sup> released from fresh Ag-NPs. However, SVI increased to 295.6 mL/g in PVP control and remained above 240 mL/g until the end of the test. Big chunks of sludge could be seen by naked eye in the PVP control (irregular shape with the longest side over 2 cm). Sludge flocs may be physically bridged by of the PVP polymer and therefore they form chunks that are very light and fluffy, which makes them difficult to settle down. This is not hard to explain since PVP can help Ag-NPs to disperse in water using the same mechanism.

Sludge flocs are bigger in the reactor with fresh Ag-NPs. All the reactors have one peak with chord length below 5  $\mu\text{m}$ , while the reactor with fresh Ag-NPs has another major peak at about 20  $\mu\text{m}$  (Figure 5-2C). The density of sludge flocs in this reactor is also slightly larger than those in the other reactors. More extracellular polymeric substances (EPS) were produced by the PVP control, especially protein (Figure 5-2D). This also contributes to the poor settleability of the sludge in the PVP control, since excess EPS will result in sludge bulking (van den Akker et al., 2010).

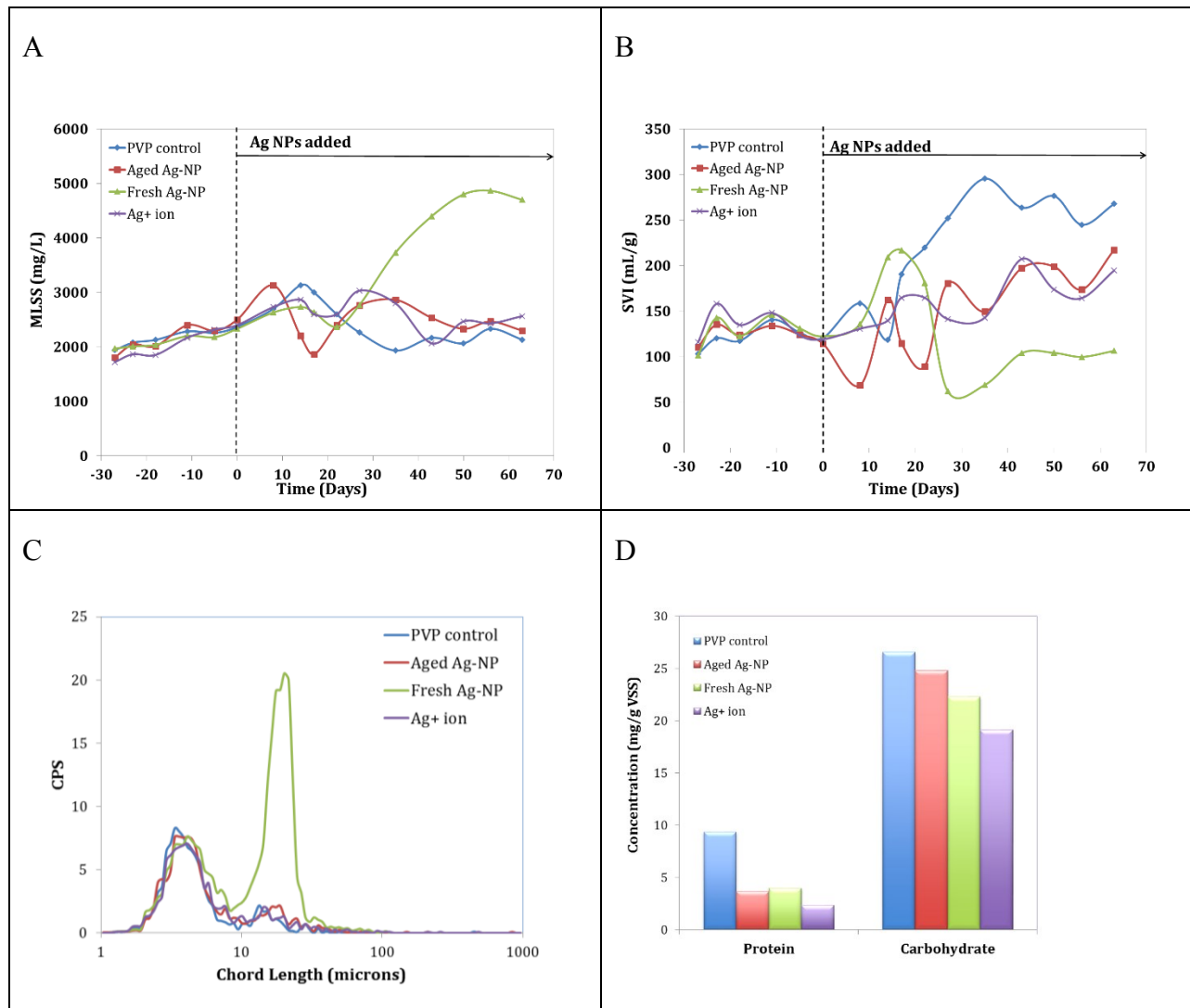


**Figure 5-2** Sludge property in each reactor. (A) MLSS concentration; (B) SVI; (C) Floc size on day 64; (D) Sludge EPS concentration on day 64.

### 5.3.3 Ag-NPs helped to maintain compositional diversity of the microbial community.

Bacterial families vary in each sample as shown in Figure 5-3A. After the thirty-day startup stage (sample S1), the microbial community composition changed slightly from the initial inoculum (sample S0). More significant shifts in community structure can be seen in the samples at the end of the test (S4-S7). Based on the principal coordinate analysis (PCoA) with weighted

unifrac (Figure 5-3B), along the axis accounts for 72% of variance samples S0 and S1 are close to each other while samples S4-S7 are clustered together. This divergence from the initial inoculum is very likely caused by operation time period in the lab since laboratory condition is different from that in the full-scale wastewater treatment plant.

However, what worth noticing is that difference along the next two most significant axes PC2 and PC3 appeared to be closely related to Ag-NP addition. If looking closer into axes PC2 and PC3 (Figure 5-3C), it can be seen that sample S6 (reactor with fresh Ag-NPs, day 64) locates the closest to the initial inoculum S0. S6 is also close to sample S1, which is the initial state before Ag-NP addition for all reactors. Sample S5 (reactor with aged Ag-NPs, day 64) is also close to S6 along both axes PC2 and PC3, indicating that the community structure change caused by aged Ag-NPs is relatively similar to that caused by fresh Ag-NPs. Sample S7 (reactor with Ag<sup>+</sup> released from fresh Ag-NPs, day 64) is closer to sample S1 along axis PC2 than S6 but further from it along axis PC3 than S6, indicating that some of the community composition change is solely caused by the nanoparticle form and that the nanoparticle form helped to reduce certain changes at the mean time.

In terms of diversity indices (richness and evenness, Table 5-1), both richness and evenness were lost at the beginning of the Ag-NP addition (S2, reactor with aged Ag-NPs, day 8; S3, reactor with fresh Ag-NPs, day 14). However, the loss of evenness recovered with time. After two months of Ag-NP addition, fresh Ag-NP (S6) maintained the highest evenness without relatively less loss in richness compared with the initial inoculum (S0).

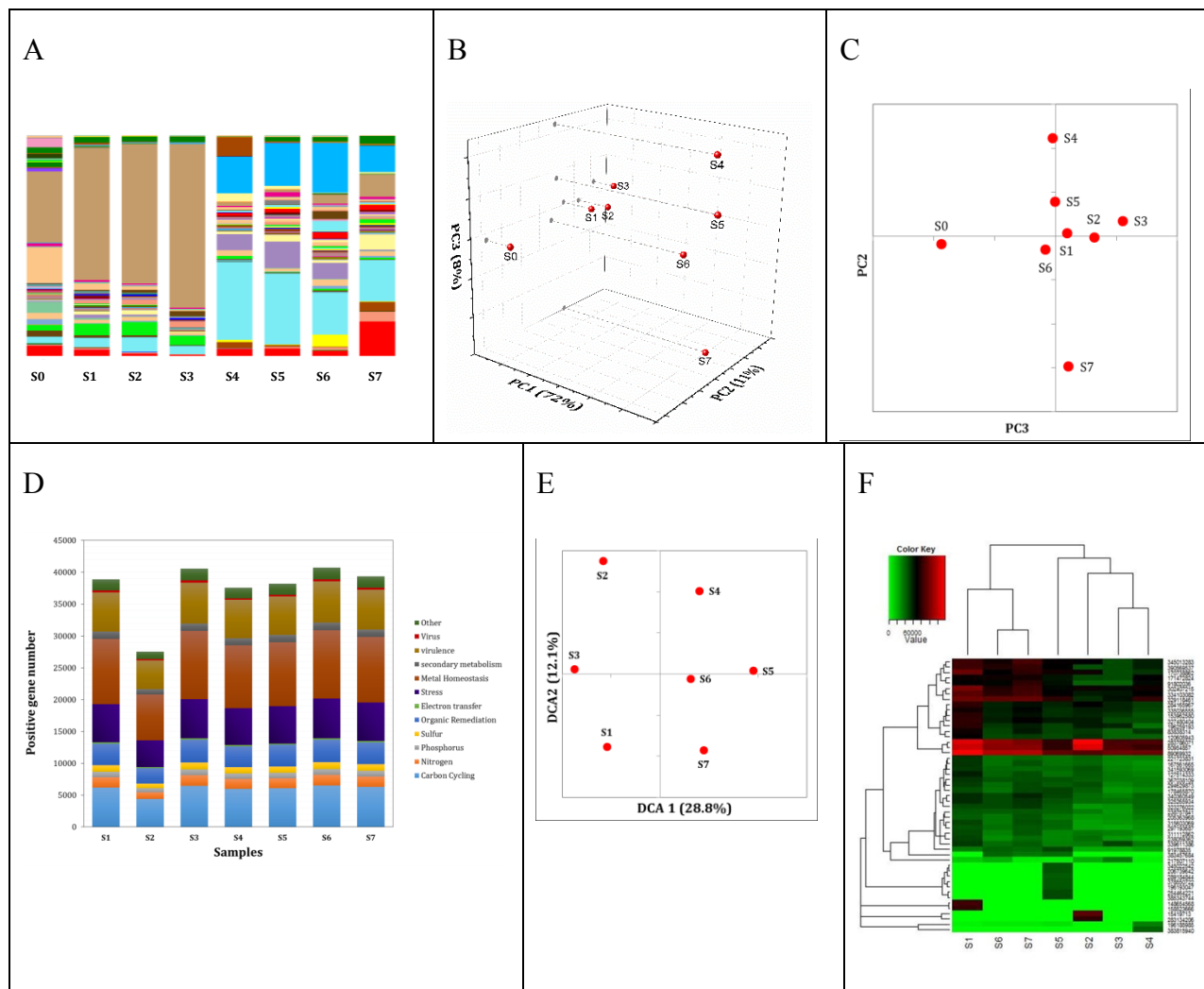


**Figure 5-3** Microbial diversity analysis. (A) Relative abundance of bacteria families; (B) PCoA analysis of microbial community diversity; (C) 2D projection of PCoA analysis on axis PC2 and PC3; (D) The number of genes detected in each functional category; (E) Detrended correspondence analysis of functional gene diversity; (F) Heatmap of the top 30 abundant functional genes; Sample S0: The initial activated sludge inoculum; S1: Sludge after the thirty-day startup stage; S2: Sludge in reactor with aged Ag-NPs, day 8; S3: Sludge in reactor with fresh Ag-NPs, day 14; S4: Sludge in reactor with only PVP as control, day 64; S5: Sludge in reactor with aged Ag-NPs, day 64; S6: Sludge in reactor with fresh Ag-NPs, day 64; S7: Sludge in reactor with Ag<sup>+</sup> released from fresh Ag-NPs, day 64.

Table 5-1 Diversity index of microbial community and functional genes.

Sample	Microbial community (bacteria families)		Functional genes	
	Richness	Evenness	Richness	Evenness
S0	126	0.554	--	--
S1	122	0.407	904	0.796
S2	104	0.381	813	0.802
S3	93	0.296	906	0.797
S4	88	0.538	888	0.796
S5	86	0.558	891	0.796
S6	97	0.626	918	0.796
S7	110	0.552	915	0.795

#### 5.3.4 Ag-NPs helped to maintain functional diversity of the microbial community.

In terms of functional diversity, reactor with fresh Ag-NPs (S6) has the highest number of genes detected (Figure 5-3D) and the highest richness (Table 5-1). Evenness is almost identical for all samples for functional genes, which is consistent with the fact that there is no significant change in gene distribution in each function category. Detrended correspondence analysis (DCA) showed that (Figure 5-3E) samples are clustered by time period along DCA1 and samples with Ag-NP addition (S5-7) are closer to the initial state (S1) compared to the PVP control (S4). This indicates that Ag-NP addition helped to maintain the functional diversity of the microbial community in the reactors. Fresh Ag-NP even increased functional diversity in terms of richness. Heatmap of the top 30 abundant functional genes also indicated that S6 and S7 are clustered with the initial state S1 (Figure 5-3F). Some antioxidant enzyme and metal and stress resistant genes

has been elevated by fresh Ag-NPs (S6). More significant increase in these genes was seen in sample S5 with aged Ag-NPs, which makes sense since aged Ag-NPs release more Ag<sup>+</sup> ions and Ag<sup>+</sup> ion plays an important role in the toxicity of Ag-NPs (Bradford et al., 2009, Kittler et al., 2010, Colman et al., 2012, Priester et al., 2014). Particle size and zeta potential of aged and fresh Ag-NPs are at the same scale as shown in Table 5-2. The data also confirmed that much more Ag<sup>+</sup> ion was released from Aged Ag-NPs.

Table 5-2 Particle characterization and silver dissolution.

	<b>Particle size (nm)</b>	<b>Zeta potential in synthetic wastewater (mV)</b>	<b>Released silver ion concentration in reactor (mg/L)</b>
<b>Aged Ag-NP</b>	74.2 ± 5.1	-9.4 ± 1.5	0.35 ± 0.05
<b>Fresh Ag-NP</b>	67.9 ± 1.0	-4.2 ± 1.0	0.05 ± 0.01

### 5.3.5 Silver species accumulation and release

The silver concentration in effluent and sludge was monitored. The dissolved Ag<sup>+</sup> ion concentration in the effluent in all reactors with Ag-NP addition remained below 0.01 mg/L at all times (Figure 5-4A). The total silver release with the effluent was the highest (0.017 mg/L) on the first day of Ag-NP addition in the reactor with Ag<sup>+</sup> ion released from fresh Ag-NPs. The reactor adapted to the silver addition within two weeks and the total silver release thereafter never exceeded 0.01 mg/L. The total silver release increased with time in the reactors fed with fresh and aged Ag-NP and reached 0.76 and 0.89 mg/L respectively at the end of the test. The only difference is the release increased in steps in the reactor with fresh Ag-NPs, indicating that

this reactor has more capacity to maintain Ag-NPs in the sludge, which is consistent with the total silver accumulation in the sludge (Figure 5-4B). Silver accumulation in the sludge appeared to be periodical to some extent which is coupled with biomass concentration changes. When the accumulation reached a threshold and the cells started to die, more silver is released through the effluent, and after the concentration in the sludge decreased after the release, cell growth recovered and a new round of accumulation started. More biomass was maintained in the reactor with fresh Ag-NPs and more silver was accumulated in the sludge in that reactor.

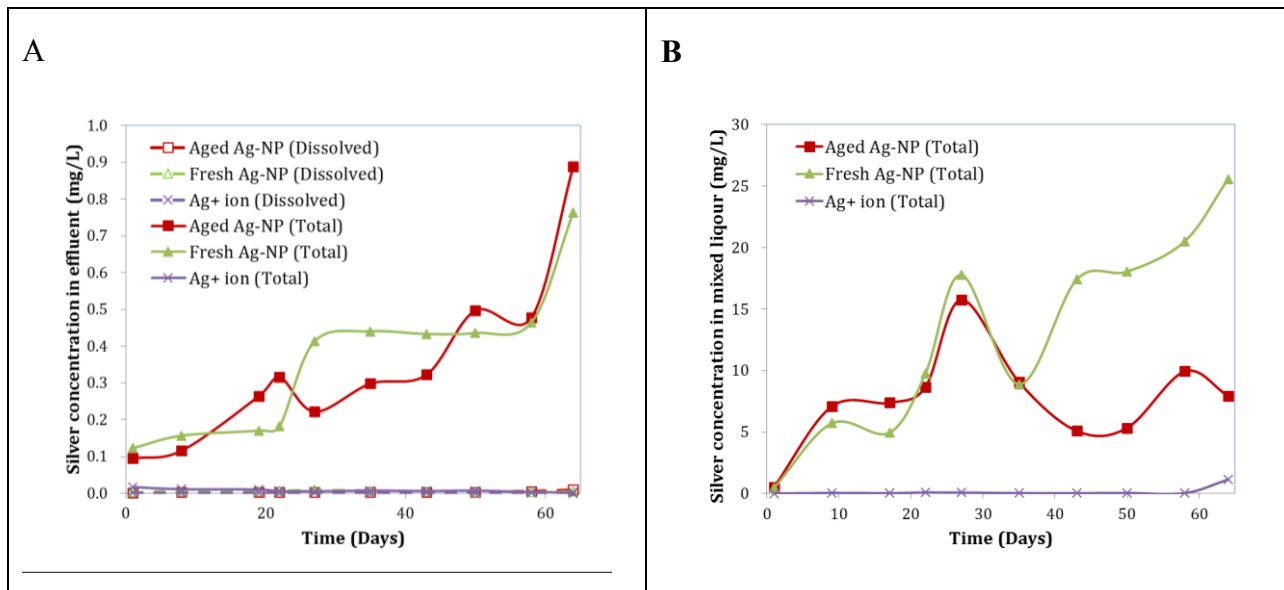


**Figure 5-4** Silver species accumulation and release. (A) Silver release via effluent; (B) Silver accumulation in activated sludge. Silver concentrations in effluent and sludge from the PVP control reactor were both below the detection limit.

## 5.4 Discussion

### 5.4.1 Hormesis model

There is ample evidence that bacterial growth can be stimulated when sublethal concentrations of antimicrobial agents are applied (Davies et al., 2006, Calabrese, 2014). An inverted U-shaped dose-response relationships, the so called hormesis model, have been reported for many antibiotics (Calabrese and Baldwin, 2001). Most of these research studies were carried out with pure-cultured bacteria. Similar dose response behaviour has also been seen in studies with Ag-NPs (Fabrega et al., 2009b, Sheng and Liu, 2011, Xiu et al., 2012, Yang et al., 2013). However, controversy exists and these findings did not attract significant attention. The majority of the literature reports non-significant to adverse effects of Ag-NP when tested at the mg/L scale. In this study, an increase in biomass concentration was clearly observed in reactors with fresh Ag-NPs, and it was stably repeated in several batch of tests under similar Ag-NP concentrations. Results in this study and in the literature indicate that the effect of Ag-NP may conform to the hormesis model as well. When tested with pure-cultured bacteria, the hormetic effects were less significant and difficult to replicate. However, when tested with a sophisticated bacterial community, such as the activated sludge used in this study, the positive effects appeared to be evident and stable. The maintenance of community diversity played a very important role in the hormetic effect observed here. The increased microbial community diversity by fresh Ag-NP is the most significant phenomenon observed besides the increase in biomass concentration. Acute effects at the beginning of addition come from loss of both richness and evenness. This is also

consistent with the hormesis model where the initial decrease in growth was followed by the adaptive rebound response (Calabrese and Baldwin, 2001). More experiments with systematically designed dosages and treatment time need to be carried out to confirm the hormesis model in Ag-NP toxicology.

#### **5.4.2 The positive effects may come from better maintenance instead of stimulation**

In this study, better maintenance of sludge in the reactor may play a more important role other than stimulation of growth. In the reactor with fresh Ag-NPs, increased floc size and density led to better settleability and therefore less sludge was lost through effluent withdrawal, and more biomass was accumulated in the reactor. In addition, higher diversity of the microbial community makes the microbes more resistant to stress, which contributes to the higher biomass concentration as well. It has been reported that nano zero-valent iron can be used to control sludge bulking (Xu et al., 2014a), and Ag-NPs can be another option. This is also supported by the fact that nutrient uptake rates didn't increase with biomass concentration in the reactor fed with fresh Ag-NPs. More cells were maintained in the reactor but not all of them are metabolically active or they may not be in their most active state. However, it should be noted that the lack of sufficient nutrients in the reactor might also contribute to the bottleneck in nutrient uptake rate increase. It should also be noted that the increased biomass concentration and resistance to stress can potentially trigger the appearance of "superbugs" that would pose a significant danger to the health of the public and environment.

### **5.4.3 The positive effects of Ag-NPs come from both the nanoparticle form and the released Ag<sup>+</sup> ions**

Without considering time, the microbial community structure in samples with fresh and aged Ag-NPs resembled more closely the initial inoculum, compared to the sample with only Ag<sup>+</sup> ion released from fresh Ag-NPs. This indicated that the nanoparticle form may play a more important role in the maintenance of microbial community diversity. In addition, Ag<sup>+</sup> ions don't improve sludge settling nor increase biomass concentration in the reactor. However, in terms of reactor performance, especially ammonium removal kinetics, the reactor with Ag<sup>+</sup> ions performed in a more similar manner to the reactor with fresh Ag-NPs instead of aged Ag-NPs. This indicates, to some extent, that the released Ag<sup>+</sup> ions play an important role in maintaining the pollutant removal capacity. To better understand the mechanism behind the positive effects of Ag-NPs, tests with equal Ag<sup>+</sup> ion concentration but different nanoparticle concentration can be run in the future, along with additional control with no treatment to verify the effects of operation time period. A longer startup stage can also be considered. High influent ammonium concentrations may help to test if Ag-NPs can improve high-ammonium concentration removal.

### **5.4.4 Comparison between Ag-NP and other agents that can potentially cause hormetic effects**

Hormetic effects can be triggered by many kinds of toxic substances, such as radiation and chemical reagents including antibiotics. The term "hormesis" was initially used to describe effects caused by low dose radiation and is now generally used to describe the inverted U-shape biological dose-response to stress (Calabrese and Baldwin, 2002, Davies et al., 2006). Reports on

the hormetic dose-response to antibiotics date back to the 1950s, and various antibiotics were found to be able to cause hormetic effects (Calabrese and Baldwin, 2002, Davies et al., 2006). Low-intensity pulsed ultrasound (LIPUS) was also found to stimulate cell growth and antibody production, although high dose of ultrasound can kill cells (Zhao et al., 2014).

Agents that can cause hormetic effects can be classified into two types: 1) chemical toxins that can leave residuals and accumulate in cells, such as Ag-NP and other antibiotics; 2) agents that can physically change cells and leave no residuals, such as LIPUS. Radiation is more complicated and can cause both physical and chemical effects. Ag-NPs are chemically toxic to cells and can be accumulated in or near cells, therefore, the positive effects caused by Ag-NPs can be limited. This is consistent with the result that the biomass concentration started to decrease in the reactor fed with fresh Ag-NPs at the end of the test, which may result from the high concentration of silver species accumulated in the sludge. Longer term of operation will help to verify the effects of silver accumulation. This is also consistent with the result that nutrient uptake didn't increase with biomass concentration in the reactor fed with fresh Ag-NPs. The toxicity of Ag-NPs may induce a dormancy state of the cells; therefore no enhanced metabolic activity was observed although more cells were maintained in the reactor. LIPUS work with a different mechanism as it increases cell permeability which leads to better circulation, faster cell metabolism and enhanced antibody secretion. Because no residual is left by LIPUS, repeated stimulation with LIPUS can cause more significant beneficial effects than Ag-NP.

Substances that can cause hormetic effects can also be classified as non-selective and selective. LIPUS can work on many kinds of cells and is non-selective. Ag-NP, which can be

taken as a broad-spectrum antibiotic, is also relatively non-selective. Therefore, agents such as Ag-NP and LIPUS tend to work equally on various kinds of cells. This explains why Ag-NP increase the diversity of microbial community in activated sludge without significant changes in the distribution of genes in each functional group. On the contrary, selective agents such as narrow-spectrum antibiotics, are more inclined to cause selective effects, such as changes in dominant species in microbial community. As reported in literature, changes in gene expression caused by subinhibitory concentration of broad-spectrum antibiotics are often termed with “enhance”, “increase” or “stimulation”; effects caused by subinhibitory concentration of narrow-spectrum antibiotics are often described by the word “inhibited” or “reduced” (Davies et al., 2006).

In regard to a complicated ecosystem, such as activated sludge in wastewater treatment, it is easier for non-selective agents with no residuals (such as LIPUS) to cause significant beneficial effects; non-selective agents with residuals (such as Ag-NP) ranks the second, but there are limitations caused by the toxicity and accumulation; it is relatively difficult for selective agents with residuals (such as narrow-spectrum antibiotics) to cause significant beneficial effects on such a complicated microbial community.

## **5.5 Conclusions**

- Ag-NPs, especially freshly prepared Ag-NPs, can have stimulatory effects even in long-term treatment.

- Ag-NP helped to maintain or even increased the diversity of microbial community in activated sludge.
- Improved sludge settleability also played a very important role in the positive effects observed.
- The hormesis model may need to be considered for the toxicology of Ag-NPs.
- The stimulatory effects caused by Ag-NPs does not correspond with better reactor performance, which may indicate that Ag-NPs improved the microbial community's resistance to stress but not its activity.
- Ag-NPs under stimulatory concentration can potentially trigger the burst of “superbugs”.

## **Chapter 6 Investigation on the stability of full-scale wastewater biological treatments for potential disturbance**

### **6.1 Introduction**

Biological wastewater treatment has now become the largest (by volume) biotechnology industry in the world (Mielczarek et al., 2012). It seeks to protect human health and the environment by removing organic compounds, nutrients (nitrogen and phosphorus) and other pollutants using microbes. The performance of a biological wastewater treatment process is determined by the activity of the microbial community present, and many critical process failures can be attributed to the disruption of the microbial community (Graham and Smith, 2004). Therefore, the stability of the microbial community under disturbances is essential for biological wastewater treatment. However, critical questions remain unanswered, especially in full-scale operation: How robust is the microbial community under disturbance? Are the outcomes after disturbance predictable, reproducible, and controllable? Understanding the relationship between the microbial community and disrupting conditions should greatly facilitate the maintenance of stable performance under disturbance (Rittmann et al., 2006).

The stability of a microbial community under disturbance is comprised of resistance (no change after disturbance) and resilience (quick recovery after disturbance) (Shade et al., 2012). Stability can be examined in terms of composition and function. In most cases, the microbial community is sensitive to disturbance (i.e., the community has low resistance) (Allison and Martiny, 2008). Community function was observed to be more resilient than community

composition after a pulse (short-term, instant) disturbance, whereas the recovery of function and composition were almost the same after a press (long-term, continuous) disturbance (Shade et al., 2012). However, most previous evaluations of stability have been based on soil microbial communities and experiments under laboratory conditions. In addition, a majority of the studies reported resistance and few studies explicitly measured resilience. Direct observations of microbial community stability in engineered systems, such as full-scale wastewater treatment plants (WWTPs), are rare, although it is well known that microbiology in full-scale WWTPs is much more complicated (albeit more robust) than in lab-scale reactors run under artificial conditions (Shade et al., 2012). With the development of molecular techniques, especially next generation sequencing technology, it has become feasible to monitor the microbial community in full-scale WWTPs (Wang et al., 2012, Hu et al., 2012, Ye and Zhang, 2013). However, the response of a microbial community to disturbance in a full-scale WWTP has not been studied to the authors' knowledge.

Activated sludge, the most widely used form of secondary wastewater treatment, is a collection of suspended biological flocs that consist of microorganisms, extracellular biopolymers, and organic and inorganic compounds (Wang et al., 2012, Hu et al., 2012, Ye and Zhang, 2013). While activated sludge direct microscopy is routinely used to aid WWTP operations it poorly describes actual taxonomic members (McIlroy et al., 2010). Furthermore, studies focused on the stability of microbial communities in activated sludge are rare, yet variations in microbial communities are thought to be influenced by both deterministic and stochastic properties (Curtis and Sloan, 2006). Deterministic properties include reactor design,

environmental and operational conditions (Curtis and Sloan, 2006), and are easier to control and monitor than stochastic properties. Operational parameters affecting microbial community dynamics include influent nutrient loading, dissolved oxygen, pH, temperature, solid retention time (SRT), hydraulic retention time (HRT), etc. (Kim et al., 2005, Hong-Yan et al., 2006, Huang et al., 2008, Li et al., 2013, Cydzik-Kwiatkowska et al., 2014, Xu et al., 2014b). The impact on the microbial community of an increased influent flow rate is a combination of changes in nutrient loading, SRT, and HRT. It has been reported that with a fixed SRT and influent concentration, an increased flow rate (i.e., increase in organic loading and decrease in HRT) results in elevated biomass concentration and improved nitrogen removal in a membrane coupled sequencing batch reactor (MSBR) (Xu et al., 2014b). With a relative stable nutrient loading rate and uncontrolled SRT, an increased flow rate (i.e., decreased HRT) leads to improved nitrogen removal kinetics (Li et al., 2013). However, the flow rate increase affects various microbial groups differently (Hong-Yan et al., 2006, Li et al., 2013). The fraction of nitrite-oxidizing bacteria (NOB) increases significantly and the increase in nitrite oxidation is also more significant than ammonium oxidation (Li et al., 2013). The effect of increased flow rate on the removal of slow degradable pollutants, such as antibiotics or other complex chemicals, is less significant than on ammonium removal (Kim et al., 2005, Huang et al., 2008). With a fixed SRT, the effect of a decreased HRT is insignificant, while a decreased SRT significantly reduces pollutant removal. The effect of increased flow rate has rarely been evaluated in full-scale WWTPs because a significantly increased flow rate in a full-scale WWTP cannot be easily maintained during routine operation.

This study examined the response of the microbial community to a significantly increased influent flow rate in a full-scale WWTP. Both reactor performance and microbial community profile were monitored. Dissolved chemical oxygen demand (COD), ammonium, nitrate, and orthophosphate phosphorus, were monitored in a series of locations in the bioreactor. Biomass concentration and sludge settleability were also examined. Also, 16S rRNA gene-based 454 pyrosequencing was undertaken to track variations in the microbial communities in each zone during the flow rate change. A BioWin model was constructed to simulate the performance and biomass dynamics of the full-scale WWTP under increased flow rate. Modeled results were compared with the experimental data.

## **6.2 Materials and Methods**

### **6.2.1 Sampling**

Samples were taken from Bioreactor #1 in a local Waste Water Treatment Plant (Edmonton, AB, Canada). A single bioreactor has an average designed capacity of 31 ML/d and a peak treatment capacity for a short duration (2 to 4 h) of 42 ML/d; this is defined as the normal flow condition. A storm event provided the opportunity to maintain the flow rate to Bioreactor #1 at 42 ML/d for five days (24 h/d). Samples were collected at 1:00 p.m. every day during the high-flow test. For tests on seasonal variations, samples were collected on three days in each season. Samples (1 L) were collected from nine locations in Bioreactor #1, as shown in Figure 6-1. A depth sampler was used to obtain samples at a depth of one meter underwater.

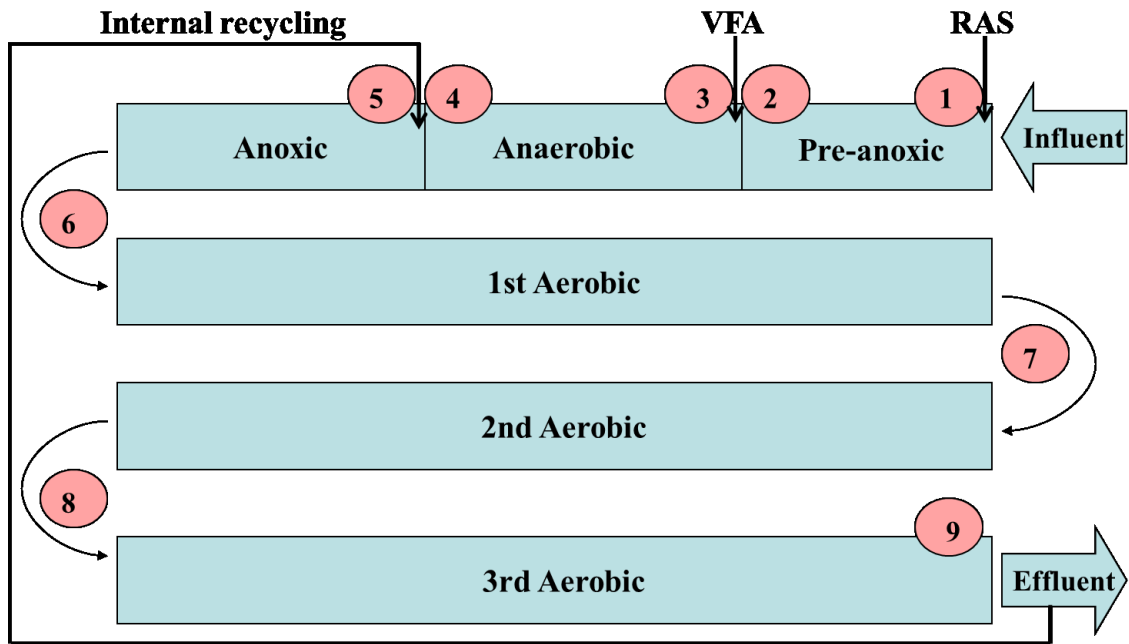


**Figure 6-1** Configuration of Bioreactor #1 and sampling locations numbered in the order from inlet to outlet.

### 6.2.2 Reactor performance analysis

After 30 min settling, the sample supernatant was filtered with a syringe filter (0.45  $\mu\text{m}$  pore size) before measurement of dissolved COD, ammonium, nitrate, and orthophosphate phosphorus. The concentrations of COD, ammonium, nitrate, and orthophosphate phosphorus were measured using Hach methods 8000, 10205, 10020, and 10209, respectively. The sludge volume index (SVI), mixed liquor suspended solids (MLSS), and mixed liquor volatile suspended solids (MLVSS) were measured according to standard methods.

### 6.2.3 Microbial community analysis

Activated sludge samples were collected in duplicates from each zone in the bioreactor and genomic DNA was extracted using a Powersoil<sup>®</sup> DNA Isolation Kit from MO BIO Laboratories,

Inc. (Carlsbad, USA).

Bacterial tag-encoded FLX amplicon pyrosequencing (bTEFAP) based on the 16S rRNA gene was performed at the Research and Testing Laboratory (Lubbock, TX, USA), using the Roche Titanium sequencing platform. Primers 28F (5'-GAGTTTGATCNTGGCTCAG-3') and 519R (5'-GTNTTACNGCGGCKGCTG-3') were used, which covered V1–V3 hypervariable regions (Kim et al., 2005, Huang et al., 2008). Chimeras and poor quality sequences were removed from the denoised sequence reads. The remaining sequences were clustered into operational taxonomic units (OTUs) with 0% divergence using USEARCH. Taxonomic information was assigned to OTUs based on a database of high quality sequences derived from the NCBI using a distributed .NET algorithm that utilizes BLASTN+ (Kraken BLAST, [www.krakenblast.com](http://www.krakenblast.com)). Identity cut-off for classification at the family level was 90–95%. A principal coordinates analysis (PCoA) of microbial community diversity was performed using the QIIME pipeline (<http://qiime.org/>) with the beta diversity metrics of weighted unifracs (Crawford et al., 2009).

qPCR was used to quantify ammonia oxidizing bacteria (AOB) and NOB. A CFX 96 real-time PCR system with a C1000 Thermal cycler (Bio-Rad Laboratories, Inc.) was used to run the reactions; using 10  $\mu$ L of SsoFast EvaGreen Supermix (Bio-Rad Laboratories, Inc.), 6  $\mu$ L of sterile water, 10 pmol of each primer, and 2  $\mu$ L of DNA template added to each 20  $\mu$ L reaction system. The primers used and reaction programs are shown in Table 6-1. Calibration was performed with serial dilutions of a known quantity of the target fragments. Triplicate reactions were run for all samples analysed. Melting curves were examined to eliminate primer dimer

formation or nonspecific amplification.

Table 6-1 qPCR primers and conditions.

Primers and references		Program
<b>Ammonia oxidizing bacteria</b>	amoA-1F5'-GGG GTT TCT ACT GGT GGT-3' amoA-2R-TC5'-CCC CTC TGC AAA GCC TTC TTC-3' (Risgaard-Petersen et al., 2004)	Initial denaturation for 1 min at 95 °C; 40 cycles of 95 °C for 5 s, and 57 °C annealing for 20 s and 72 °C for 45 s a; and a final melting curve analysis from 65 to 95 °C, measuring fluorescence every 0.5 °C.
<b>Nitrite oxidizing bacteria</b>	Nitro 1198f5'-ACC CCT AGC AAA TCT CAA AAA ACC G-3' Nitro 1423r5'-CTT CAC CCC AGT CGC TGA CC-3' (Kim et al., 2011)	Initial denaturation for 3 min at 95 °C; 50 cycles of 94 °C for 20 s, and 58°C annealing for 60 s and 72 °C for 40 s a; and a final melting curve analysis from 65 to 95 °C, measuring fluorescence every 0.5 °C.
<b>Nitrite oxidizing bacteria</b>	NSR 1113f5'-CCT GCT TTC AGT TGC TAC CG -3' NSR 1264r5'-GTT TGC AGC GCT TTG TAC CG -3' (Kim et al., 2011)	Initial denaturation for 3 min at 95 °C; 50 cycles of 95 °C for 30 s, and 60°C annealing for 60 s; and a final melting curve analysis from 65 to 95 °C, measuring fluorescence every 0.5 °C.
<b>Total bacteria</b>	rpoB 1698f 5'-AAC ATC GGT TTG ATC AAC-3' rpoB 2041r 5'-CGT TGC ATG TTG GTA CCC AT-3' (Dahllof et al., 2000)	Initial denaturation for 3 min at 95 °C; 35 cycles of 95 °C for 30 s, and 47 °C annealing for 90 s; and a final melting curve analysis from 65 to 95 °C, measuring fluorescence every 0.5 °C.

#### 6.2.4 BioWin simulation

A model with the same configuration as the full-scale WWTP Bioreactor #1 was constructed using the process simulator software BioWin (EnviroSim Associates Ltd., Hamilton, ON). First, a steady state was reached under the normal flow condition with a controlled SRT of 6.4 d. The model was calibrated so that it agreed with experimental data. In the second step, a series of dynamic simulations were run for 30 days with conditions (influent loading, SRT, and sludge

blanket level) changed additively, one by one. Influent loading was changed to mimic the high flow test in the first dynamic run without changing the SRT, then the SRT was changed to 5.5 d as observed during the high flow test besides the influent loading change. In the third run, the change of sludge blanket level was added, raising to the value observed during the high flow test. All the dynamic simulations started from the same initial steady state.

## **6.3 Results**

### **6.3.1 Bioreactor performance (functional stability)**

The effluent water quality was satisfactory under normal flow conditions (average of 31 ML/d). As indicated with 'N' in Figure 6-2A, the average effluent COD concentration under normal flow condition was approximately 20 mg/L with an influent loading rate of 0.56 kg COD/m<sup>3</sup>·d. During high flow conditions (42 ML/d), the influent COD concentration was lower than that under normal conditions. As a result, the influent COD loading rate was only slightly increased to an average of 0.63kgCOD/m<sup>3</sup>·d, although there was a significant increase in the flow rate. With the increase influent COD loading, the effluent COD concentration was maintained at about 20 mg/L, without significant change throughout the high flow test.

Under normal flow conditions, the effluent ammonium concentration was below the detection limit. With a significant increase in the ammonium loading rate from 0.051 kgNH<sub>3</sub>-N/m<sup>3</sup>·d under normal conditions to 0.067 kgNH<sub>3</sub>-N/m<sup>3</sup>·d during the high flow test, a slight increase in effluent ammonium concentration was observed, especially on Day 4 when the influent ammonium loading rate reached its peak value of 0.082 kgNH<sub>3</sub>-N/m<sup>3</sup>·d (Figure 6-2B).

However, the ammonium removal was still satisfactory according to the local standard (3 mg/L, 30 day average).

There was no significant change in phosphorus removal during the high flow test, although an increase in influent phosphorus loading from 0.028 kgPO<sub>4</sub>-P/m<sup>3</sup>·d to 0.044 kgPO<sub>4</sub>-P/m<sup>3</sup>·d was observed (Figure 6-2C). The effluent nitrate concentration increased significantly during the high flow test as shown in Figure 6-2D. This could be attributed to the increased influent ammonium loading without a significant increase in COD loading, which resulted in a lack of sufficient carbon source for denitrification.

The wastewater quality at different locations of the bioreactor was examined under normal and high flow conditions. In general, the pollutant concentration in each tank was similar under both conditions, as shown in Figure 6-2E-G. This indicated that in terms of function, the microbial community was not sensitive to the applied, significant flow rate increase in the full-scale WWTP, which is consistent with previous research concerning functional redundancy in ecosystems (Lawton and Brown, 1993, Rosenfeld, 2002). In particular, there was no significant change in the COD removal profile throughout the bioreactor. Ammonium was exhausted in the third aerobic zone (location #9) during the high flow test, compared to the second aerobic zone (location #8) under the normal flow conditions (Figure 6-2F). This finding implies that ammonium removal was slightly affected by the increased flow rate, which is consistent with previous research (Hong-Yan et al., 2006). Sufficient phosphorus removal was achieved during the high flow test as well. The phosphorus removal in the first aerobic zone on day 4 was higher than that under normal conditions; this might be a result of the active growth of

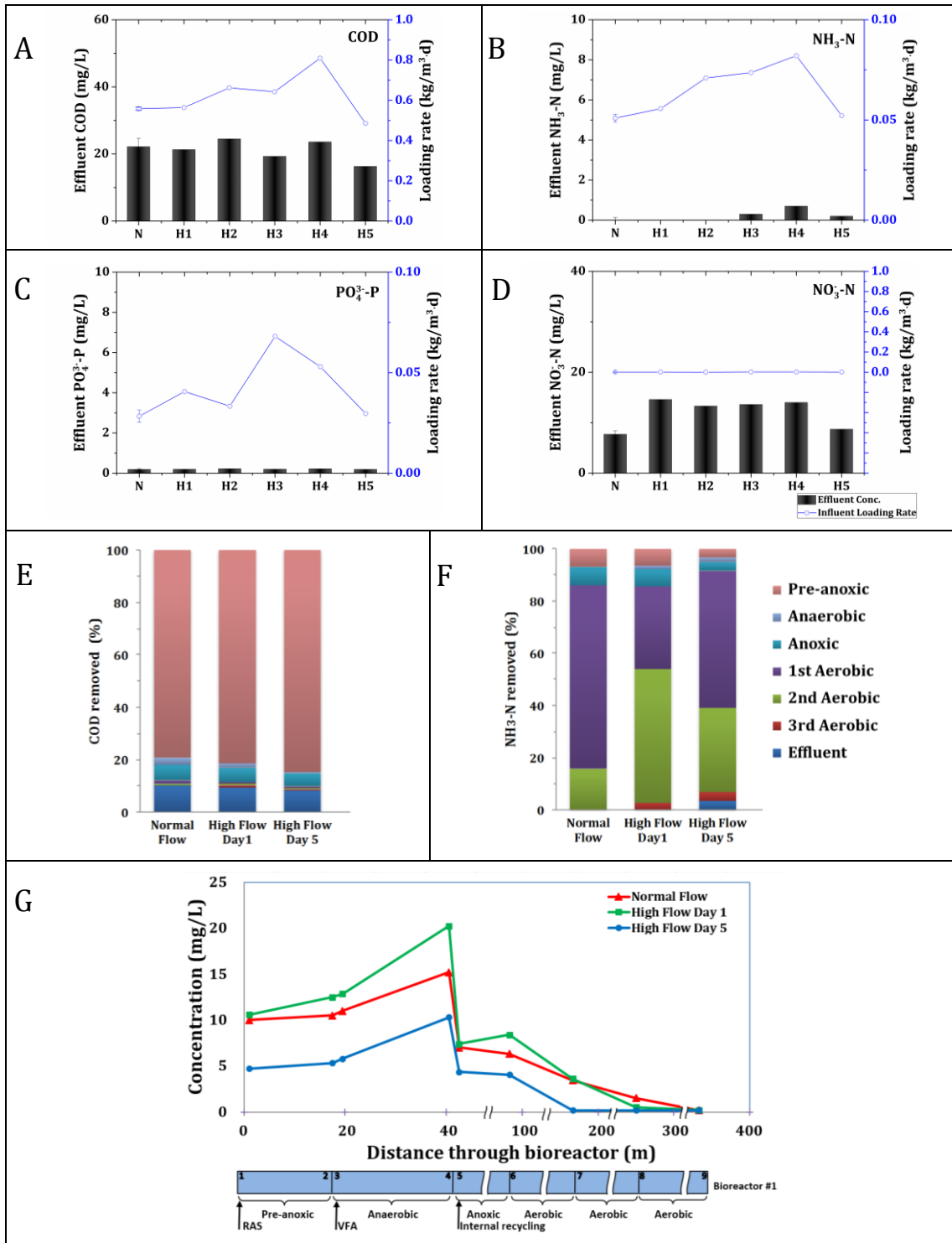


**Figure 6-2** Bioreactor performance during high-flow test. (A)(B)(C)(D), COD, ammonia, orthophosphate, and nitrate in influent and effluent; (E)(F), COD and ammonia removal in each zone; (G) Phosphorous release and removal in the bioreactor (N: Normal flow; H1-5: High flow Day 1-5; Ammonia, nitrate, and orthophosphate were presented as ammonia nitrogen (NH<sub>3</sub>-N), nitrate nitrogen (NO<sub>3</sub><sup>-</sup>-N) and phosphorus (PO<sub>4</sub><sup>3-</sup>-P), respectively; error bars represent one standard deviation).

polyphosphate accumulating bacteria, as discussed below.

## **6.3.2 Microbial community resilience**

### **6.3.2.1 Changes in activated sludge properties**

One day after the start of the high flow test, the MLSS decreased from about 4000 to approximately 2700 mg/L (Table 6-2). This is consistent with previous research indicating that a decreased HRT led to the washout of biomass arising from the increased hydraulic pressure (Pan et al., 2004). The SVI increased from below 100 to over 220 mL/g at the same time indicating a poor sludge settling capacity. The height of the sludge blanket level in the secondary clarifier also increased as a result of the decreased sludge settleability (data not shown). Clearly the increased flow rate had adverse effects on the activated sludge. With an increased flow rate and increased influent nutrient loading, and a decreased biomass concentration, a higher food to microorganism ratio (F/M) was reached. The SRT decreased from 6.4 days to 5.5 days during the high flow test, and microorganisms that grow relatively faster were selectively retained in the bioreactor. As a result, the sludge age became younger and the SVI became higher (Federation, 2008). However, four days after the beginning of the high flow test, a recovery of the biomass was observed with a decrease in the SVI. A similar biomass increase in activated sludge has been observed in a bench-scale MSBR under increased flow rate (Xu et al., 2014b).

Table 6-2 Biomass change during high-flow test.

Zone Operation	SVI (mL/g)			MLSS (mg/L)			MLVSS (mg/L)		
	N*	H1*	H4*	N*	H1*	H4*	N*	H1*	H4*
<b>Pre-anoxic</b>	82.5	<b>228.1</b>	202.8	3940	<b>2630</b>	3240	2850	<b>2180</b>	2790
<b>Anaerobic</b>	99.0	<b>228.1</b>	197.4	3890	<b>2630</b>	3040	2780	<b>2210</b>	2610
<b>Anoxic</b>	83.1	<b>225.8</b>	128.2	3850	<b>2790</b>	3120	2810	<b>2230</b>	2640
<b>Aerobic</b>	65.5	<b>258.1</b>	155.8	4000	<b>2770</b>	3210	2840	<b>2200</b>	2520

\*Note: N: Normal flow; H1: High flow Day 1; H4: High flow Day 4

### 6.3.2.2 Changes in microbial community structure

Under normal flow conditions, the top five dominant microbial families in the full-scale WWTP were *Rhodocyclaceae*, *Comamonadaceae*, *Saprospiraceae*, *Burkholderiales*, and *Flavobacteriaceae*. These families belong to the phylum *Proteobacteria* or *Bacteroidetes*, which is typical of the dominant phyla reported for activated sludge (Hu et al., 2012). In sludge samples from North America, the families *Comamonadaceae* and *Flavobacteriaceae* have been reported to be more abundant (Wang et al., 2012). The family *Rhodocyclaceae* includes genera such as *Dechloromonas* and *Thauera*, which can degrade aromatic compounds under anoxic conditions (Coates et al., 2001, Liu et al., 2013). The family *Saprospiraceae* includes filamentous bacteria such as *Haliscomenobacter* and bacteria that attach to filamentous bacteria (Seviour et al., 1994, Xia et al., 2008). The family *Comamonadaceae* includes denitrifiers such as *Curvibacter* and bacteria with diverse metabolic capacities such as *Variovorax* (Ding and Yokota, 2004, Han et al., 2011).

Within 24 h of the beginning of the high flow test, the microbial community shifted significantly (Figure 6-3A), with remarkable changes in three families. The family *Rhodocyclaceae* decreased significantly, while the families *Saprospiraceae* and *Comamonadaceae* increased notably, compensating for this reduction. The genera reduced in the family *Rhodocyclaceae* were all involved to some extent in denitrification (Garrity et al., 2005). The family *Comamonadaceae* also includes denitrifiers (Ding and Yokota, 2004, Han et al., 2011), and the increase in this family might have contributed to the functional stability of the bioreactor under the high-flow conditions. As the family *Saprospiraceae* includes filamentous bacteria and bacteria that attach to filamentous bacteria, the increase in this family supports the hypothesis that filamentous bacteria and bacteria firmly attached to them are more resistant to washout effects under decreased HRT than free floating bacteria. However, the increased proportion of filamentous bacteria could lead to sludge bulking; as an increased SVI had already been observed, this factor warrants closer attention.

The microbial community structure in each zone was restored to its initial state within five days, as shown in Figure 6-3A. The family *Rhodocyclaceae* increased to its initial level, while the families *Saprospiraceae* and *Comamonadaceae* decreased correspondingly. The genus *Rhodocyclus*, which functions in polyphosphate accumulation, was responsible for the recovery of the family *Rhodocyclaceae* (Zilles et al., 2002). *Rhodocyclus* decreased slightly at the beginning of the experiment, then increased by about 6% during the next four days. This explains why increased phosphorus loading did not significantly affect phosphorous removal. Comparing with Figure 6-3B, the changes in bacteria families during the high-flow test was much more

significant than the seasonal variations throughout the year. This indicates that the shifts and recovery of microbial community during the high-flow test cannot be simply attributed to routine fluctuation.

The PCoA result (Figure 6-3C) clearly illustrated the surprisingly high resilience of the microbial community structure in the full-scale WWTP. Relative abundance was used as the weights when calculating the weighted unifrac diversity metrics, and therefore Figure 6-3C illustrates changes in the microbial community composition. Along the most significant axis, which accounts for 63% of the variance, samples on Day 4 were closely clustered with samples under normal flow conditions whereas samples on Day 1 of the high flow test were far from this cluster. This indicates that the community structure changed significantly on Day 1 but was restored to its initial state by Day 4. Samples with the same date but from various locations are clustered together, indicating that the bacterial populations throughout the bioreactor were fairly uniform through a well-mixed condition because of the nitrified liquor and sludge recycle streams.

It should be noted that organisms such as nitrifiers in the family of *Nitrosomonadaceae* decreased and did not recover within five days. It takes time for autotrophs to recover because they grow slowly (Watson et al., 1989). Thus factors such as growth rate may help to explain why samples from different dates are not clustered together along PC2 and PC3 in Figure 3C. However, as shown in Figure 6-3D, the copy number of the functional gene *amoA* recovered on day 4. No significant changes in nitrite oxidizing genes were detected (Figure 6-3E). These results confirmed the functional redundancy of microbial communities in this engineered system.

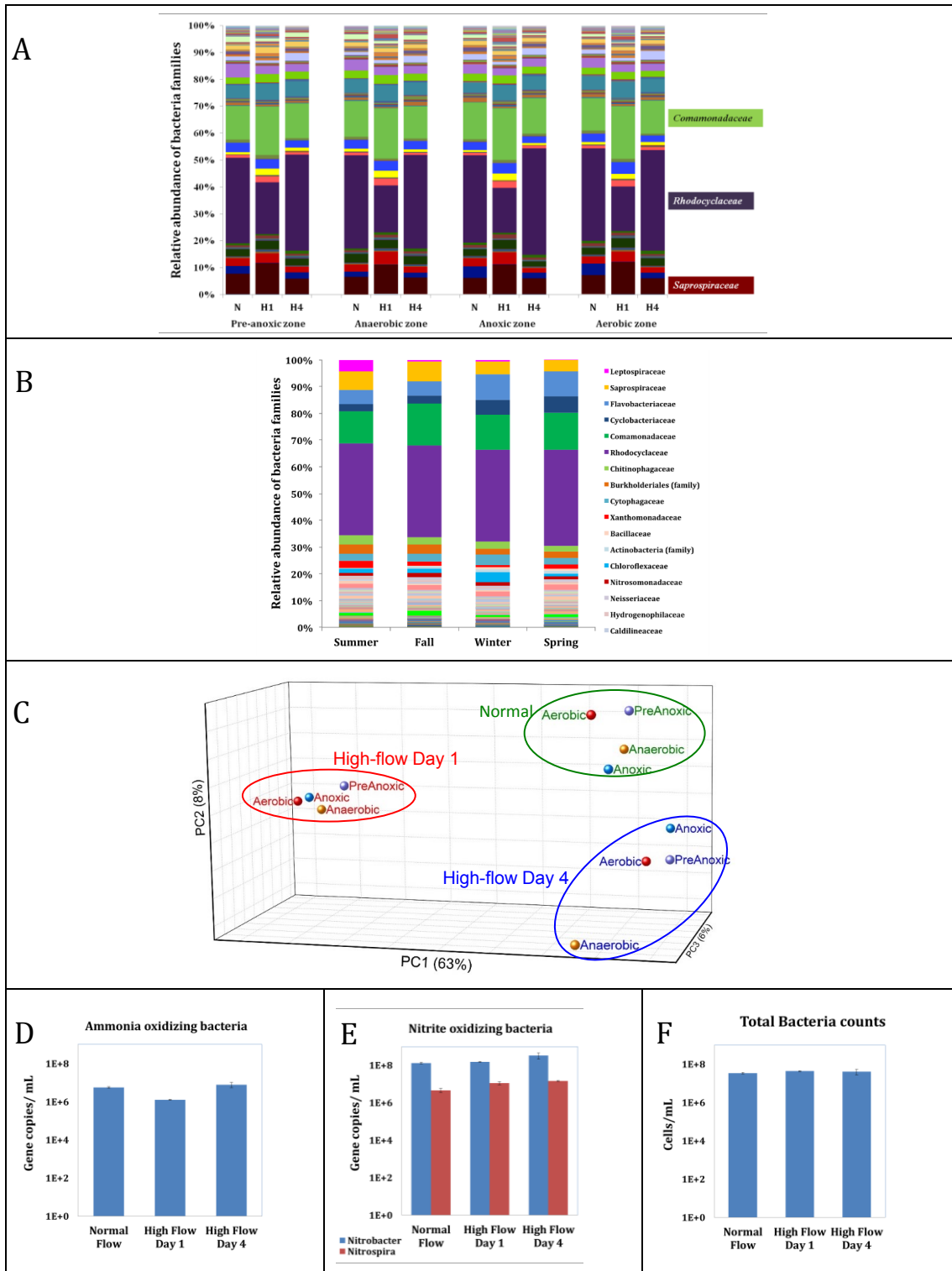


**Figure 6-3** Microbial community changes in the bioreactor. (A) Changes in relative abundance of bacteria at family level during high-flow test; (B) Seasonal variations in relative abundance of bacteria at family level; (C) PCoA analysis of microbial community diversity; (D) Abundance of ammonia-oxidizing bacteria; (E) Abundance of nitrite-oxidizing bacteria; (F) Total bacteria number (N: Normal flow; H1: High flow Day 1; H4: High flow Day 4).

No significant changes were detected in total bacteria number based on qPCR results ( $p > 0.05$ , Figure 6-3F), indicating that the changes in absolute bacteria number are clearly within one log unit. This makes sense since the majority of biomass was successfully maintained in the reactor during the high-flow test. Part of the biomass loss may also come from non-dominant bacteria and non-cell material such as loosely bound extracellular polymeric substances. Cell numbers detected by the *rpoB* gene may be underestimated and qPCR results can also be biased by PCR inhibitors in the sample and DNA extraction efficiency.

### **6.3.3 Microbial stability prediction/validation using the BioWin model**

The increased flow rate in this study led to three major changes in conditions: an increased influent nutrient loading rate, a decreased SRT, and an elevated sludge blanket level in the clarifier. The additive inclusions of these three conditions fit the BioWin model with experimental data, as shown in Figure 6-4A. (1) With only the increased influent loading included in the model, the model predicted that the MLSS would keep increasing in the first five days and reach about 120% of the initial value after 30 days, indicating a considerable increase in biomass concentration. A slight washout was observed within 24 h of the flow rate increase. (2) When both the influent loading increase and the decreased SRT were included in the model, the model predicted a slower increase in MLSS than the increase predicted in (1) and the modeled value was closer to the initial MLSS when the curve flattened after 15 days. (3) When the sludge blanket level increase was included with the influent loading increase and the decreased SRT in the model, the model predicted MLSS stabilization after about five days and the final MLSS concentration was similar to the initial value. An MLSS washout was predicted on

the first day was more significant than that predicted in (1) and (2). With influent loading, SRT, and sludge settleability changed in the final model (3), the trend of the MLSS change was consistent with the experimental data; the recovery of MLSS suggests the recovery of biomass and the microbial community.

In Figure 6-4B the experimental effluent quality was compared with data from the final model (3). The simulated effluent COD and phosphorus concentrations were fairly consistent with those measured in the experiment. The slight decrease in ammonium removal measured in the experiment was also observed in the simulation. However, the most significant increase in effluent ammonium concentration appeared at the beginning of the simulated test whereas the peak in effluent ammonium concentration occurred on Day 4 during the experiment. The most important cause for the increased experimental effluent ammonium concentration on Day 4 is the elevated influent ammonium loading, which was not taken into account during simulation. Meanwhile, in the ideal model, only growth rate parameters are specified for slow-growers such as AOB while changes in functional gene expression under disturbance was not taken into account.

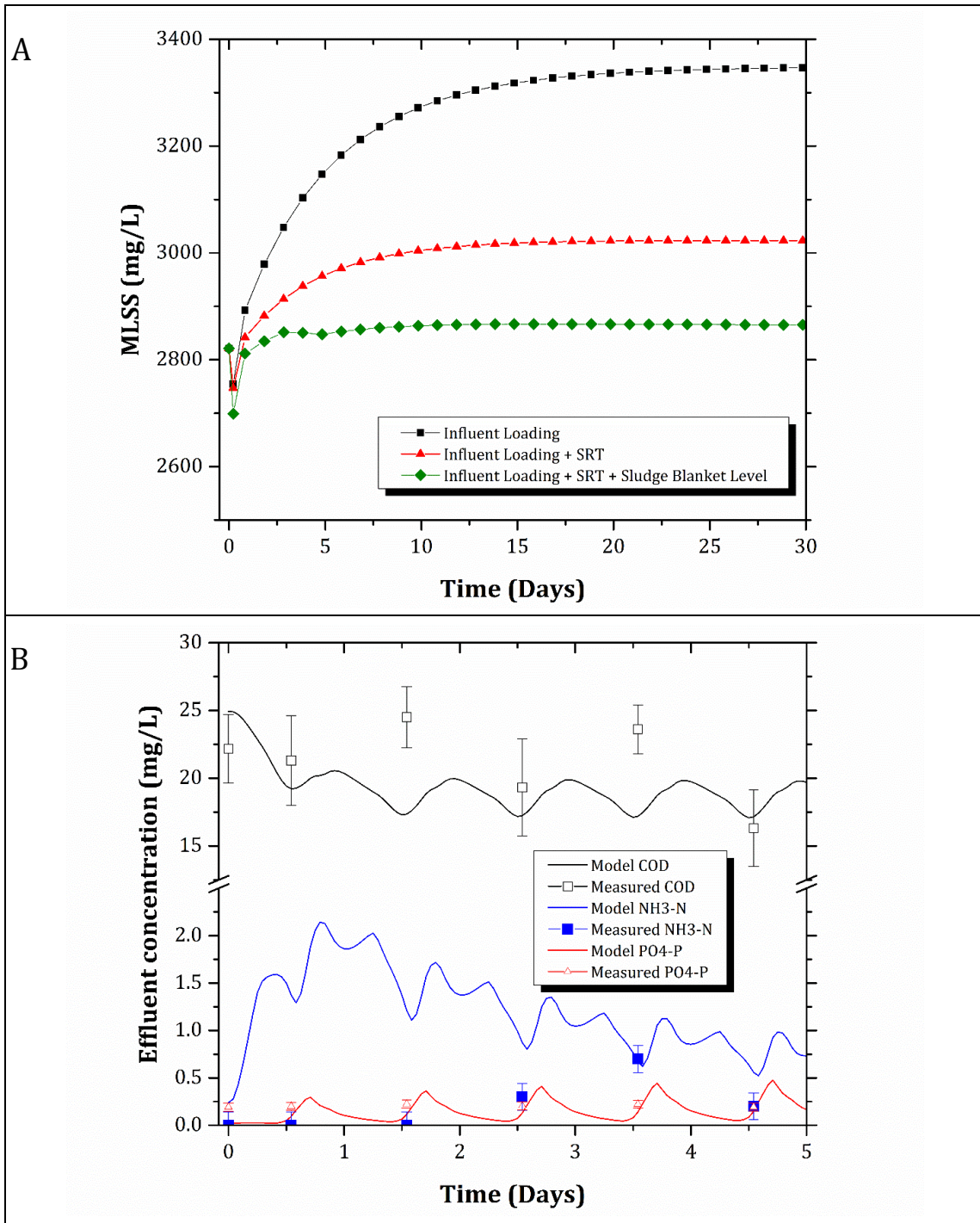


**Figure 6-4** BioWin model results. (A) Simulated MLSS variation with conditions changed in series; (B) Effluent quality simulation based on the final model (Day 0 indicates normal flow condition).

## **6.4 Discussion**

### **6.4.1 Potential mechanisms of microbial community stability**

A flow rate increase that is maintained for five days can be considered to be a press (long-term) disturbance. The reactor performance was stable, which was consistent with previous research showing that microbial community function is more resistant to press than community composition (Watson et al., 1989). The microbial community composition in the full-scale WWTP was sensitive to this disturbance, which is also consistent with previous research (Shade et al., 2012). However, the microbial community structure recovered surprisingly quickly from such a significant press disturbance. This high resilience and functional stability can be explained by the microbial growth rate and functional redundancy, as discussed below.

#### **6.4.1.1 Growth rate and composition resilience**

According to the r- and K-selection framework proposed by Andrews and Harris, the bacterial population quickly recovered from the flow rate disturbance belongs to r-strategists (or opportunistic populations) which typically grow fast (Andrews and Harris, 1986, Weinbauer and Höfle, 1998). The increased flow rate increased the nutrient loading, providing fast-growing bacteria an advantage over slow-growing bacteria because the former are more efficient in resource use than the latter. Meanwhile, there are also bacteria that stayed with stable density under the flow rate change and these are K-strategists (or equilibrium populations). K-strategists often do not grow as fast as r-strategists. The balance between r- and K-strategists helped to maintain the microbial community functional stability under disturbance. This is consistent with previous

research showing that fast-growing microbes are more resilient while slow-growing microbes are more resistant (de Vries et al., 2012, Xu et al., 2014b).

#### **6.4.1.2 Functional redundancy and functional stability**

In the complex microbial community present in activated sludge in a full scale WWTP, various microbes with the same function coexist, and some remain dormant under normal conditions (Lawton and Brown, 1993). When the flow rate in a WWTP is increased, some members of the microbial community may be washed away, diminishing the nutrient degradation activity in the reactor. However, the microbes retained in the reactor might carry the same functional genes and dormant microbes may be activated at the higher flow rate. Bacteria can also express multiple genes for a range of degradation capacities (Meyer et al., 2004, Swingley et al., 2007). Therefore, the overall degradation function may not be significantly affected at the higher flow rate. The fact that the family *Nitrosomonadaceae* did not recover but the number of *amoA* genes did recover within five days is consistent with the characteristics described above.

#### **6.4.2 Correlation between flow rate change and microbial community**

The increased flow rate in Bioreactor #1 led to a decrease in the HRT, an increase in nutrient loading, and a decrease in the SRT. Under this condition, the biomass concentration (density of microbial community) decreased. Both fast-growing and slow-growing bacteria were reduced significantly, but the fast-growing bacteria recovered quickly, while some slow-growing bacteria were slower to recover. The microbial community composition was sensitive to the condition change but very resilient, while the microbial function was actually fairly resistant. The BioWin model proved that the outcomes under this flow rate increase can be predicted to some extent. It

is possible that the responses to similar conditional changes can be reproduced and might be to some extent controlled.

### **6.4.3 Future work**

Direct monitoring of the microbial community changes in a full-scale WWTP will shed some light on the rational design and future control of biological wastewater treatment.

Emerging genomic and metagenomic tools have been used to describe individual members to aid in development of wastewater treatment models (McIlroy et al., 2013); here we evolve this approach to whole community analyses on a daily bases. It is true that this is a case study and may not be simply generalized. However, it shows the possibility that full-scale systems can be much more resilient than expected and a finer monitoring on a daily basis may be necessary in future studies. Nondominant but functionally important bacterial species and the effects of other environmental and operational conditions should be investigated, including seasonal variation, addition of carbon sources, and changes in aeration conditions. A reactor upgrade to integrated fixed-film activated sludge (IFAS) might also improve microbial community stability.

## **6.5 Conclusions**

- Full-scale WWTPs are robust under disturbance.
- Microbial community in full-scale WWTP is highly resilient to flow rate increase.
- The function of full-scale WWTP is stable under flow rate increase.
- Daily monitoring by next generation sequencing enables detection of this resilience.

## Chapter 7 Conclusions and recommendations

### 7.1 Conclusions

In this dissertation, the effects of Ag-NPs were examined under different conditions in various systems. Results in each kind of system are summarized below.

Biofilm bacteria treated as isolated pure culture are highly sensitive to Ag-NPs and 100% mortality occurred for most strains after 24 h under an Ag-NP treatment dose of 1 mg Ag/L. However, mixed bacterial cultures can survive better. Five out of eight strains survived after 24 h treatment with an Ag-NP treatment dose of 1 mg Ag/L in artificially mixed cultures. Mixed cultures inoculated from biofilms were even more tolerant, and six out of eight strains survived with one of them growing even better than in the no treatment control.

Original wastewater biofilms are highly tolerant to Ag-NPs. Biofilm bacteria with loosely bound EPS removed are more sensitive to Ag-NPs, indicating that biofilms can provide physical protection for bacteria under Ag-NP treatment, and EPS may play an important role in this protection. Susceptibility to Ag-NPs is different for each microorganism in the biofilm microbial community. For example, *Thiothrichales* is more sensitive than other biofilm bacteria. With closer monitoring with TEM and GeoChip on intact biofilms, it was seen that Ag-NPs entered biofilm EPS within forty-five min and entered a small portion of cells after 24 h. A decrease in gene diversity (34.6% decrease in gene number) was detected in the GeoChip analysis. However, there was no significant changes in gene distribution in different functional categories. Signal intensity decreased in certain variants in each family while other variants increased to

compensate the effects of Ag-NPs. The results indicate that Ag-NP treatment decreased microbial community diversity in biofilm when the concentration is high (200 mg Ag/L) but did not significantly affect the microbial community function. This provides direct evidence for the functional redundancy of microbial community in engineered ecosystems such as wastewater biofilms.

Ag-NPs, especially freshly prepared Ag-NPs, had positive effects in the three-month study with low dose (1 mg Ag/L in the influent), spherical Ag-NPs with PVP coating in activated sludge bioreactors fed with synthetic municipal wastewater. Based on taxonomy and functional gene analysis, Ag-NP helped to maintain or even increased the diversity of microbial community in activated sludge. Improved sludge settleability also played a very important role in the positive effects observed. Adverse effects started to be seen when the accumulated silver concentration in the mixed liquor reached 20 mg Ag/L. This result indicates that the hormesis model needs to be considered for the toxicology of Ag-NPs.

Since the same kind of Ag-NPs were used in all experiments, these systems were compared with each other and the tolerance from the lowest to the highest followed the order: single strain < laboratory mixed culture < activated sludge in laboratory reactor < biofilm without loosely bound EPS < original biofilm. Higher tolerance corresponds with higher community diversity and more compact EPS structure. It was also observed that the stimulatory effects were easier to repeat when the system diversity was higher and the system itself was more robust. No significant difference was detected between PBS buffer and wastewater, and this lack of difference can be attributed to the presence of EPS in these systems.

Full-scale biological wastewater treatment processes are observed to be very stable under disturbance. Considering the high robustness of full-scale biological wastewater treatment processes, they may be able to stand a relatively high concentration of Ag-NPs and a potentially wider stimulatory dose range can even be observed compared with laboratory systems.

## **7.2 Recommendations and future research**

To better understand the implications of Ag-NPs on biological wastewater treatment processes, the effects of Ag-NPs need to be systematically tested with multiple doses carefully chosen from low to high ranges and on systems from pure cultured model bacteria to complex microbial community in biological wastewater treatment. Longer treatment times are also required to better understand the implications of Ag-NPs on biological wastewater treatment, especially under lower dose. The accumulation and fate of silver species need to be closely monitored and correlated with the observed phenomenon. Meanwhile, Ag-NPs with various size, shape, and coating should also be considered when building the theoretical hormetic model. These factors can change the position and width of the stimulatory zone.

After a theoretical model is built, tests can be carried out in pilot and full-scale systems. In those systems, the potential breakthrough of silver species and release through the effluent should be monitored as well, considering the effects of silver species on human and environmental health, although the effects of Ag-NPs on the microbial community and treatment performance may be negligible under low concentration.

In addition, the stimulatory effects of Ag-NPs on pathogens need to be investigated carefully as well. The pathogenic population in biological wastewater systems need to be carefully monitored with the presence of Ag-NPs under systematically selected concentrations, and the stimulatory range of Ag-NPs that can potentially cause “superbug” bursts should be reported.

## Bibliography

- Alito, C.L. and Gunsch, C.K. (2014) Assessing the effects of silver nanoparticles on biological nutrient removal in bench-scale activated sludge sequencing batch reactors. *Environ Sci Technol* 48(2), 970-976.
- Allison, D.G. (2000) *Community structure and co-operation in biofilms*, Cambridge University Press: New York.
- Allison, S.D. and Martiny, J.B.H. (2008) Resistance, resilience, and redundancy in microbial communities. *P Natl Acad Sci USA* 105(Suppl 1), 11512-11519.
- Amarneh, B. and Vik, S.B. (2005) Direct transfer of NADH from malate dehydrogenase to complex I in *Escherichia coli*. *Cell Biochem Biophys* 42(3), 251-261.
- Anderson, J.W.; Semprini, L. and Radniecki, T.S. (2014) Influence of water hardness on silver ion and silver nanoparticle fate and toxicity toward *Nitrosomonas europaea*. *Environ Eng Sci* 31(7SI), 403-409.
- Andrews, J. and Harris, R. (1986) r- and K-selection and microbial ecology. *Adv Microb Ecol* 9:99-147.
- Arnaout, C.L. and Gunsch, C.K. (2012) Impacts of silver nanoparticle coating on the nitrification potential of *Nitrosomonas Europaea*. *Environ Sci Technol* 46(10), 5387-5395.
- Baba, T.; Ara, T.; Hasegawa, M.; Takai, Y.; Okumura, Y.; Baba, M.; Datsenko, K.A.; Tomita, M.; Wanner, B.L. and Mori, H. (2006) Construction of *Escherichia coli* K-12 in-frame, single-gene knockout mutants: the Keio collection." *Mol Syst Biol* 2, 2006-2008.

- Bassin, J. P.; Kleerebezem, R.; Rosado, A. S.; van Loosdrecht, M. C. and Dezotti, M. (2012) Effect of different operational conditions on biofilm development, nitrification, and nitrifying microbial population in moving-bed biofilm reactors. *Environ Sci Technol* 46 1546-1555.
- Beer, M.; Stratton, H.M.; Griffiths, P.C. and Seviour, R.J. (2006) Which are the polyphosphate accumulating organisms in full-scale activated sludge enhanced biological phosphate removal systems in Australia? *J Appl Microbiol* 100(2), 233-243.
- Benn, T.M. and Westerhoff, P. (2008) Nanoparticle silver released into water from commercially available sock fabrics. *Environ Sci Technol* 42(11), 4133-4139.
- Besinis, A.; De Peralta, T. and Handy, R.D. (2014) Inhibition of biofilm formation and antibacterial properties of a silver nano-coating on human dentine. *Nanotoxicology* 8(7), 745-754.
- Blaser, S.A.; Scheringer, M.; Macleod, M. and Hungerbuhler, K. (2008) Estimation of cumulative aquatic exposure and risk due to silver: contribution of nano-functionalized plastics and textiles. *Sci Total Environ* 390(2-3), 396-409.
- Bradford, A.; Handy, R.D.; Readman, J.W.; Atfield, A. and Mühlhng, M. (2009) Impact of silver nanoparticle contamination on the genetic diversity of natural bacterial assemblages in estuarine sediments. *Environ Sci Technol* 43(12), 4530-4536.
- Briones, A. and Raskin, L. (2003) Diversity and dynamics of microbial communities in engineered environments and their implications for process stability. *Curr Opin Biotech* 14(3), 270-276.

- Brown, M.; Allison, D.G. and Gilbert, P. (1988) Resistance of bacterial biofilms to antibiotics - a growth-rate related effect. *J Antimicrob Chemoth* 22(6), 777-780.
- Calabrese, E.J. (2001) Overcompensation stimulation: a mechanism for hormetic effects. *Crit Rev Toxicol* 31(4-5), 425-470.
- Calabrese, E.J. (2002) Hormesis: Changing view of the dose-response, a personal account of the history and current status. *Mutat Res* 511(3), 181-189.
- Calabrese, E.J. (2014) Hormesis: a fundamental concept in biology. *Microbial Cell* 1(5), 145-149.
- Calabrese, E.J. and Baldwin, L.A. (2001) Hormesis: U-shaped dose responses and their centrality in toxicology. *Trends Pharmacol Sci* 22(6), 285-291.
- Calabrese, E.J. and Baldwin, L.A. (2002) Defining hormesis. *Hum Exp Toxicol* 21(2), 91-97.
- Campbell, B.J. and Kirchman, D.L. (2013) Bacterial diversity, community structure and potential growth rates along an estuarine salinity gradient. *ISME J* 7(1), 210-220.
- Cao, H.; Liu, X.; Meng, F. and Chu, P.K. (2011) Biological actions of silver nanoparticles embedded in titanium controlled by micro-galvanic effects. *Biomaterials* 32(3), 693-705.
- Chen, C.Y.; Kao, C.M. and Chen, S.C. (2008) Application of *Klebsiella oxytoca* immobilized cells on the treatment of cyanide wastewater. *Chemosphere* 71(1), 133-139.
- Chen, H.; Zheng, X.; Chen, Y. and Mu, H. (2013) Long-term performance of enhanced biological phosphorus removal with increasing concentrations of silver nanoparticles and ions. *R Soc Chem Adv* 3(25), 9835-9842.

- Chen, Y.; Chen, H.; Zheng, X. and Mu, H. (2012) The impacts of silver nanoparticles and silver ions on wastewater biological phosphorous removal and the mechanisms. *J Hazard Mater* 239, 88-94.
- Choi, O. and Hu, Z. (2008) Size dependent and reactive oxygen species related nanosilver toxicity to nitrifying bacteria. *Environ Sci Technol* 42(12), 4583-4588.
- Choi, O.; Cleuenger, T.E.; Deng, B.L.; Surampalli, R.Y.; Ross, L. and Hu, Z.Q. (2009) Role of sulfide and ligand strength in controlling nanosilver toxicity. *Water Res* 43(7), 1879-1886.
- Choi, O.; Deng, K.K.; Kim, N.J.; Jr Ross, L.; Surampalli, R.Y. and Hu, Z. (2008) The inhibitory effects of silver nanoparticles, silver ions, and silver chloride colloids on microbial growth. *Water Res* 42(12), 3066-3074.
- Choi, O.K. and Hu, Z.Q. (2009) Nitrification inhibition by silver nanoparticles. *Water Sci Technol* 59(9), 1699-1702.
- Chopra, I. (2007) The Increasing Use of silver-based products as antimicrobial agents: a useful development or a cause for concern?. *J Antimicrob Chemoth* 60(2), 447-448.
- Christman, M.F.; Storz, G. and Ames, B.N. (1989) OxyR, a positive regulator of hydrogen peroxide-inducible genes in *Escherichia coli* and *Salmonella typhimurium*, is homologous to a family of bacterial regulatory proteins. *P Natl Acad Sci USA* 86(10), 3484-3488.
- Coates, J.D.; Chakraborty, R.; Lack, J.G.; O'Connor, S.M.; Cole, K.A.; Bender, K.S. and Achenbach, L.A. (2001) Anaerobic benzene oxidation coupled to nitrate reduction in pure culture by two strains of *Dechloromonas*. *Nature* 411(6841), 1039-1043.

- Colman, B.P.; Wang, S.Y.; Auffan, M.; Wiesner, M.R. and Bernhardt, E.S. (2012) Antimicrobial effects of commercial silver nanoparticles are attenuated in natural streamwater and sediment. *Ecotoxicology* 21(7), 1867-1877.
- Cortez, S.; Teixeira, P.; Oliveira, R. and Mota, M. (2008) Rotating biological contactors: a review on main factors affecting performance. *Rev Environ Sci Bio* 7(2), 155-172.
- Crawford, P.A.; Crowley, J.R.; Sambandam, N.; Muegge, B.D.; Costello, E.K.; Hamady, M.; Knight, R. and Gordon, J.I. (2009) Regulation of myocardial ketone body metabolism by the gut microbiota during nutrient deprivation. *Proc Natl Acad Sci USA* 106(27), 11276-11281.
- Cumberland, S.A. and Lead, J.R. (2009) Particle size distributions of silver nanoparticles at environmentally relevant conditions. *J Chromatogr A* 1216(52), 9099-9105.
- Curtis, T.P. and Sloan, W.T. (2006) Towards the design of diversity: stochastic models for community assembly in wastewater treatment plants. *Water Sci Technol* 54(1), 227-236.
- Cydzik-Kwiatkowska, A.; Rusanowska, P.; Zielinska, M.; Bernat, K. and Wojnowska-Baryla, I. (2014) Structure of nitrogen-converting communities induced by hydraulic retention time and COD/N ratio in constantly aerated granular sludge reactors treating digester supernatant. *Bioresource Technol* 154, 162-170.
- Dalla Costa, E.; Ribeiro, M.; Silva, M.; Arnold, L.; Rostirolla, D.; Cafrune, P.; Espinoza, R.; Palaci, M.; Telles, M.; Ritacco, V.; Suffys, P.; Lopes, M.; Campelo, C.; Miranda, S.; Kremer, K.; Da Silva, P.; Fonseca, L.; Ho, J.; Kritski, A. and Rossetti, M. (2009) Correlations of mutations in *katG*, *oxyR-ahpC* and *inhA* genes and in vitro susceptibility in *Mycobacterium*

*tuberculosis* clinical strains segregated by spoligotype families from tuberculosis prevalent countries in South America. BMC Microbiology 9(1), 39.

Das, P.; Williams, C.J.; Fulthorpe, R.R.; Hoque, M.E.; Metcalfe, C.D. and Xenopoulos, M.A. (2012) Changes in bacterial community structure after exposure to silver nanoparticles in natural waters. Environ Sci Technol 46(16), 9120-9128.

Das, S.K.; Khan, M.M.R.; Parandhaman, T.; Laffir, F.; Guha, A.K.; Sekarana, G. and Mandal, A.B. (2013) Nano-silica fabricated with silver nanoparticles: antifouling adsorbent for efficient dye removal, effective water disinfection and biofouling control. Nanoscale 5(12), 5549-5560.

Davies, D. (2003) Understanding biofilm resistance to antibacterial agents. Nat Rev Drug Discov 2(2), 114-122.

Davies, J.; Spiegelman, G.B. and Yim, G. (2006) The world of subinhibitory antibiotic concentrations. Curr Opin Microbiol 9(5), 445-453.

Deguchi, S.; Alargova, R.G. and Tsujii, K. (2001) Stable dispersions of fullerenes, C<sub>60</sub> and C<sub>70</sub>, in water. Preparation and characterization. Langmuir 17(19), 6013-6017.

de Vries, F.T.; Liiri, M.E.; Bjornlund, L.; Bowker, M.A.; Christensen, S.; Setälä, H.M. and Bardgett, R.D. (2012) Land use alters the resistance and resilience of soil food webs to drought. 2(4), 276-280.

Dhas, S.P.; Shiny, P.J.; Khan, S.; Mukherjee, A. and Chandrasekaran, N. (2014) Toxic behavior of silver and zinc oxide nanoparticles on environmental microorganisms. J Basic Microb 54(9), 916-927.

- Ding, L. and Yokota, A. (2004) Proposals of *Curvibacter gracilis* gen. nov., sp. nov. and *Herbaspirillum putei* sp. nov. for bacterial strains isolated from well water and reclassification of [*Pseudomonas*] *huttiensis*, [*Pseudomonas*] *lanceolata*, [*Aquaspirillum*] *delicatum* and [*Aquaspirillum*] *autotrophicum* as *Herbaspirillum huttiense* comb. nov., *Curvibacter lanceolatus* comb. nov., *Curvibacter delicatus* comb. nov. and *Herbaspirillum autotrophicum* comb. nov. Int J Syst Evol Microbiol 54(Pt 6), 2223-2230.
- Doolette, C.L.; McLaughlin, M.J.; Kirby, J.K.; Batstone, D.J.; Harris, H.H.; Ge, H. and Cornelis, G. (2013) Transformation of PVP coated silver nanoparticles in a simulated wastewater treatment process and the effect on microbial communities. Chem Cent J 7(46).
- Engelke, M.; Koeser, J.; Hackmann, S.; Zhang, H.; Maedler, L. and Filser, J. (2014) A miniaturized solid contact test with *Arthrobacter globiformis* for the assessment of the environmental impact of silver nanoparticles. Environ Toxicol Chem 33(5), 1142-1147.
- Engelmann, S. and Hecker, M. (1996) Impaired oxidative stress resistance of *Bacillus subtilis* sigB mutants and the role of katA and katE. Fems Microbiol Lett 145(1), 63-69.
- Fabrega, J.; Fawcett, S.R.; Renshaw, J.C. and Lead, J.R. (2009a) Silver nanoparticle impact on bacterial growth: effect of pH, concentration, and organic matter. Environ Sci Technol 43(19), 7285-7290.
- Fabrega, J.; Renshaw, J.C. and Lead, J.R. (2009b) Interactions of silver nanoparticles with *Pseudomonas putida* biofilms. Environ Sci Technol 43(23), 9004-9009.
- Fabrega, J.; Zhang, R.; Renshaw, J.C.; Liu, W.T. and Lead, J.R. (2011) Impact of silver nanoparticles on natural marine biofilm bacteria. Chemosphere 85(6), 961-966.

- Federation, W.E. (2008) Operation of municipal wastewater treatment plants. Volume 2 – Liquid processes, 6 ed. McGraw Hill Publishers. <http://www.wef.org>.
- Feng, Q.L.; Wu, J.; Chen, G.Q.; Cui, F.Z.; Kim, T.N. and Kim, J.O. (2000) A mechanistic study of the antibacterial effect of silver ions on *Escherichia coli* and *Staphylococcus aureus*. *J Biomed Mater Res* 52(4), 662-668.
- Flemming, H.C.; Wingender, J.; Griegbe, T. and Mayer, C. (2000) Biofilms: recent advances in their study and control. Evans, L.V., p. 19-34, Harwood Academic Publishers: Amsterdam.
- Fortner, J.D.; Lyon, D.Y.; Sayes, C.M.; Boyd, A.M.; Falkner, J.C.; Hotze, E.M.; Alemany, L.B.; Tao, Y.J.; Guo, W.; Ausman, K.D.; Colvin, V.L. and Hughes, J.B. (2005) C<sub>60</sub> in water: nanocrystal formation and microbial response. *Environ Sci Technol* 39(11), 4307-4316.
- Friedrich, T. (1998) The NADH:ubiquinone oxidoreductase (complex I) from *Escherichia coli*. *Biochim Biophys Acta* 1364(2), 134-146.
- Gao, J.; Wang, Y.; Hovsepyan, A. and Bonzongo, J.C.J. (2011) Effects of engineered nanomaterials on microbial catalyzed biogeochemical processes in sediments. *J Hazard Mater* 186(1), 940-945.
- Garrity, G.M.; Brenner, D.J.; Krieg, N.R. and Staley, J.T. (2005) *Bergey's Manual of Systematic Bacteriology, Volume Two: The Proteobacteria, Part C: The Alpha-, Beta-, Delta-, and Epsilonproteobacteria*. Springer: New York, NY.
- Geranio, L.; Heuberger, M. and Nowack, B. (2009) The behavior of silver nanotextiles during washing. *Environ Sci Technol* 43(21), 8113-8118.

- Gong, A.S.; Bolster, C.H.; Benavides, M. and Walker, S.L. (2009) Extraction and analysis of extracellular polymeric substances: comparison of methods and extracellular polymeric substance levels in *Salmonella pullorum* SA 1685. *Environ Eng Sci* 26(10), 1523-1532.
- Gottschalk, F.; Sonderer, T.; Scholz, R.W. and Nowack, B. (2010) Possibilities and limitations of modeling environmental exposure to engineered nanomaterials by probabilistic material flow analysis. *Environ Toxicol Chem* 29(5), 1036-1048.
- Graham, D.W. and Smith, V.H. (2004) Designed ecosystem services: application of ecological principles in wastewater treatment engineering. *Front Ecol Environ* 2(4), 199-206.
- Graves, J.L.; Tajkarimi, M.; Cunningham, Q.; Campbell, A.; Nonga, H.; Harrison, S.H. and Barrick, J.E. (2015) Rapid evolution of silver nanoparticle resistance in *Escherichia coli*. *Front Genet* 6, 42.
- Gupta, A.; Phung, L.T.; Taylor, D.E. and Silver, S. (2001) Diversity of silver resistance genes in IncH incompatibility group plasmids. *Microbiology* 147(Pt 12), 3393-3402.
- Hagendorfer, H.; Lorenz, C.; Kaegi, R.; Sinnet, B.; Gehrig, R.; Goetz, N.V.; Scheringer, M.; Ludwig, C. and Ulrich, A. (2010) Size-fractionated characterization and quantification of nanoparticle release rates from a consumer spray product containing engineered nanoparticles. *J Nanopart Res* 12(7), 2481-2494.
- Hall-Stoodley, L.; Costerton, J.W. and Stoodley, P. (2004) Bacterial biofilms: from the natural environment to infectious diseases. *Nat Rev Microbiol* 2(2), 95-108.
- Han, J.; Choi, H.; Lee, S.; Orwin, P.M.; Kim, J.; LaRoe, S.L.; Kim, T.; O'Neil, J.; Leadbetter, J.R.; Lee, S.Y.; Hur, C.; Spain, J.C.; Ovchinnikova, G.; Goodwin, L. and Han, C. (2011)

Complete genome sequence of the metabolically versatile plant growth-promoting endophyte *Variovorax paradoxus* S110. *J Bacteriol* 193(5), 1183-1190.

Hardman, R.C. (2006) A toxicologic review of quantum dots: toxicity depends on physicochemical and environmental factors. *Environ Health Persp* 114(2), 165-172.

He, Z.; Deng, Y.; Van Nostrand, J.D.; Tu, Q.; Xu, M.; Hemme, C.L.; Li, X.; Wu, L.; Gentry, T.J.; Yin, Y.; Liebich, J.; Hazen, T.C. and Zhou, J. (2010) GeoChip 3.0 as a high-throughput tool for analyzing microbial community composition, structure and functional activity. *ISME J* 4(9), 1167-1179.

Hedberg, J.; Baresel, C. and Wallinder, I.O. (2014) Transport and fate of silver as polymer-stabilised nanoparticles and ions in a pilot wastewater treatment plant, followed by sludge digestion and disposal of sludge/soil mixtures: A case study. *J Environ Sci Heal A* 49(12), 1416-1424.

Holbrook, R.D.; Morrow, J. and Maugel, T. (2006) Fate of nanoparticles in biological systems - quantum dot behavior in bacterial cells and biofilms. *Microsc Microanal* 12(Supplement S02), 618-619.

Hong-Yan, L.; Yu, Z.; Feng, G.; Tao, Y. and Min, Y. (2006) Effects of hydraulic retention time (HRT) on nitrification performance and microbial community of conventional activated sludge (CAS). *Huanjing Kexue* 27(9), 1862-1865.

Howarth, R.; Unz, R.F.; Seviour, E.M.; Seviour, R.J.; Blackall, L.L.; Pickup, R.W.; Jones, J.G.; Yaguchi, J. and Head, I.M. (1999) Phylogenetic relationships of filamentous sulfur bacteria (*Thiothrix* spp. and Eikelboom type 021n bacteria) isolated from wastewater-treatment plants

and description of *Thiothrix eikelboomii* sp. nov., *Thiothrix unzii* sp. nov., *Thiothrix fructosivorans* sp. nov. and *Thiothrix defluvii* sp. nov. Int J Syst Bacteriol 49(Part 4), 1817-1827.

Hu, M.; Wang, X.; Wen, X. and Xia, Y. (2012) Microbial community structures in different wastewater treatment plants as revealed by 454-pyrosequencing analysis. Bioresource Technol 117(0), 72-79.

Hu, Z. (2010) Impact of silver nanoparticles on wastewater treatment, Water Environment Research Foundation, Alexandria.

Huang, M.; Li, Y. and Gu, G. (2008) The effects of hydraulic retention time and sludge retention time on the fate of di-(2-ethylhexyl) phthalate in a laboratory-scale anaerobic-anoxic-aerobic activated sludge system. Bioresource Technol 99(17), 8107-8111.

Hwang, E.T.; Lee, J.H.; Chae, Y.J.; Kim, Y.S.; Kim, B.C.; Sang, B.I. and Gu, M.B. (2008) Analysis of the toxic mode of action of silver nanoparticles using stress-specific bioluminescent bacteria. Small 4(6), 746-750.

Jeong, E.; Im, W.; Kim, D.; Kim, M.; Kang, S.; Shin, H. and Chae, S. (2014) Different susceptibilities of bacterial community to silver nanoparticles in wastewater treatment systems. J Environ Sci Heal A 49(6), 685-693.

Johnston, H.J.; Hutchison, G.R.; Christensen, F.M.; Aschberger, K. and Stone, V. (2010) The biological mechanisms and physicochemical characteristics responsible for driving fullerene toxicity. Toxicol Sci 114(2), 162-182.

- Juan, L.; Zhimin, Z.; Anchun, M.; Lei, L. and Jingchao, Z. (2010) Deposition of silver nanoparticles on titanium surface for antibacterial effect. *Int J Nanomedicine* 5, 261-267.
- Kaegi, R.; Voegelin, A.; Ort, C.; Sinnet, B.; Thalmann, B.; Krismer, J.; Hagendorfer, H.; Elumelu, M. and Mueller, E. (2013) Fate and transformation of silver nanoparticles in urban wastewater systems. *Water Res* 47(12SI), 3866-3877.
- Kaegi, R.; Voegelin, A.; Sinnet, B.; Zuleeg, S.; Hagendorfer, H.; Burkhardt, M. and Siegrist, H. (2011) Behavior of metallic silver nanoparticles in a pilot wastewater treatment plant. *Environ Sci Technol* 45(9), 3902-3908.
- Kalishwaralal, K.; BarathManiKanth, S.; Pandian, S.; Deepak, V. and Gurunathan, S. (2010) Silver nanoparticles impede the biofilm formation by *Pseudomonas aeruginosa* and *Staphylococcus epidermidis*. *Colloids Surf B Biointerfaces* 79(2), 340-344.
- Kent, R.D.; Oser, J.G. and Vikesland, P.J. (2014) Controlled evaluation of silver nanoparticle sulfidation in a full-scale wastewater treatment plant. *Environ Sci Technol* 48(15SI), 8564-8572.
- Khan, S.; Mukherjee, A. and Chandrasekaran, N. (2011) Silver nanoparticles tolerant bacteria from sewage environment. *Journal of Environmental Sciences* 23(2), 346-352.
- Kim, B.; Park, C.; Murayama, M. and Hochella, M.F. (2010) Discovery and characterization of silver sulfide nanoparticles in final sewage sludge products. *Environ Sci Technol* 44(19), 7509-7514.

- Kim, J.S.; Kuk, E.; Yu, K.N.; Kim, J.H.; Park, S.J.; Lee, H.J.; Kim, S.H.; Park, Y.K.; Park, Y.H.; Hwang, C.Y.; Kim, Y.K.; Lee, Y.S.; Jeong, D.H. and Cho, M.H. (2007) Antimicrobial effects of silver nanoparticles. *Nanomedicine* 3(1), 95-101.
- Kim, S. and Ryu, D.Y. (2013) Silver nanoparticle-induced oxidative stress, genotoxicity and apoptosis in cultured cells and animal tissues. *J Appl Toxicol* 33(2), 78-89.
- Kim, S.; Eichhorn, P.; Jensen, J.N.; Weber, A.S. and Aga, D.S. (2005) Removal of antibiotics in wastewater: Effect of hydraulic and solid retention times on the fate of tetracycline in the activated sludge process. *Environ Sci Technol* 39(15), 5816-5823.
- Kim, S.B.; Goodfellow, M.; Kelly, J.; Saddler, G.S. and Ward, A.C. (2002) Application of oligonucleotide probes for the detection of *Thiothrix* spp. in activated sludge plants treating paper and board mill wastes. *Water Sci Technol* 46(1-2), 559-564.
- Kittler, S.; Greulich, C.; Diendorf, J.; Köller, M. and Epple, M. (2010) Toxicity of silver nanoparticles increases during storage because of slow dissolution under release of silver ions. *Chem Mater* 22(16), 4548-4554.
- Klaus, T.; Joerger, R.; Olsson, E. and Granqvist, C. (1999) Silver-based crystalline nanoparticles, microbially fabricated. *P Natl Acad Sci USA* 96(24), 13611-13614.
- Königs, A.M.; Flemming, H. and Wingender, J. (2015) Nanosilver induces a nonculturable but metabolically active state in *Pseudomonas aeruginosa*. *Front Microbiol* 6, 395.
- Konopka, M.; Kowalski, Z. and Wzorek, Z. (2009) Disinfection of meat industry equipment and production rooms with the use of liquids containing silver nano-particles. *Archives of Environmental Protection* 35(1), 107-115.

- Kumar, D.; Kumari, J.; Pakrashi, S.; Dalai, S.; Raichur, A.M.; Sastry, T.P.; Mandal, A.B.; Chandrasekaran, N. and Mukherjee, A. (2014) Qualitative toxicity assessment of silver nanoparticles on the fresh water bacterial isolates and consortium at low level of exposure concentration. *Ecotoxicol Environ Saf* 108, 152-160.
- Kumar, M.A.; Anandapandian, K.T.K. and Parthiban, K. (2011) Production and characterization of exopolysaccharides (EPS) from biofilm forming marine bacterium. *Braz Arch Biol Techn* 54, 259-265.
- Kumar, R.V. and Raza, G. (2009) Photocatalytic disinfection of water with Ag-TiO<sub>2</sub> nanocrystalline composite. *Ionics* 15(5), 579-587.
- Kvítek, L.; Panáček, A.; Soukupová, J.; Kolář, M.; Večeřová, R.; Pucek, R.; Holecová, M. and Zbořil, R. (2008) Effect of surfactants and polymers on stability and antibacterial activity of silver nanoparticles (NPs). *J Phys Chem C* 112(15), 5825-5834.
- Lavakumar, V.; Masilamani, K.; Ravichandiran, V.; Venkateshan, N.; Saigopal, D.V.R.; Ashok Kumar, C.K. and Sowmya, C. (2015) Promising upshot of silver nanoparticles primed from *Gracilaria crassa* against bacterial pathogens. *Chem Cent J* 9, 42.
- Lawton, J.H. and Brown, V.K. (1993) Redundancy in ecosystems, p 255-270. *In* Schulze ED and Mooney HA (ed), *Ecological Studies: Analysis and Synthesis*, vol. 99. Springer-Verlag Berlin: Berlin.
- Lee, W.; Kim, K.J. and Lee, D.G. (2014) A novel mechanism for the antibacterial effect of silver nanoparticles on *Escherichia coli*. *Biometals* 27(6), 1191-1201.

- Levard, C.; Hotze, E.M.; Lowry, G.V. and Jr. Brown, G.E. (2012) Environmental transformations of silver nanoparticles: impact on stability and toxicity. *Environ Sci Technol* 46(13), 6900-6914.
- Li, D.; Lyon, D.Y.; Li Q. and Alvarez, P.J.J. (2008) Effect of soil sorption and aquatic natural organic matter on the antibacterial activity of a fullerene water suspension. *Environ Toxicol Chem* 27(9), 1888-1894.
- Li, H.; Zhang, Y.; Yang, M. and Kamagata, Y. (2013) Effects of hydraulic retention time on nitrification activities and population dynamics of a conventional activated sludge system. *Front Environ Sci Eng* 7(1), 43-48.
- Liang, Z.; Das, A. and Hu, Z. (2010) Bacterial response to a shock load of nanosilver in an activated sludge treatment system. *Water Res* 44(18), 5432-5438.
- Lindqvist, A.; Membrillo-Hernandez, J.; Poole, R.K. and Cook, G.M. (2000) Roles of respiratory oxidases in protecting *Escherichia coli* K12 from oxidative stress. *Antonie Van Leeuwenhoek* 78(1), 23-31.
- Liu, B.; Frostegård, Å. and Shapleigh, J.P. (2013) Draft genome sequences of five strains in the genus *Thauera*. *Genome Announc* 1(1).
- Liu, C.; Yang, J.L.; Wu, G.; Zhang, S.; Li, Z.X. and Guo, J.B. (2010) Estimation of dominant microbial population sizes in the anaerobic granular sludge of a full-scale UASB treating streptomycin wastewater by PCR-DGGE. *World J Microb Biot* 26(2), 375-379.

- Liu, Y.; Li, J.; Qiu, X.F. and Burda, C. (2007) Bactericidal activity of nitrogen-doped metal oxide nanocatalysts and the influence of bacterial extracellular polymeric substances (EPS). *J Photoch Photobio A* 190(1), 94-100.
- Liu, Z.; Yin, H. and Dang, Z. (2014) Comment on "Sulfidation of silver nanoparticles: Natural antidote to their toxicity". *Environ Sci Technol* 48(10), 6050.
- Lok, C.N.; Ho, C.M.; Chen, R.; He, Q.Y.; Yu, W.Y.; Sun, H.; Tam, P.K.; Chiu, J.F. and Che, C.M. (2006) Proteomic analysis of the mode of antibacterial action of silver nanoparticles. *J Proteome Res* 5(4), 916-924.
- Lok, C.N.; Ho, C.M.; Chen, R.; He, Q.Y.; Yu, W.Y.; Sun, H.; Tam, P.K.; Chiu, J.F. and Che, C.M. (2007) Silver nanoparticles: partial oxidation and antibacterial activities. *J Biol Inorg Chem* 12(4), 527-534.
- Lu, C.; Brauer, M.J. and Botstein, D. (2009) Slow growth induces heat-shock resistance in normal and respiratory-deficient yeast. *Mol Biol Cell* 20(3), 891-903.
- Lu, Z.; Deng, Y.; Van Nostrand, J.D.; He, Z.; Voordeckers, J.; Zhou, A.; Lee, Y.J.; Mason, O.U.; Dubinsky, E.A.; Chavarria, K.L.; Tom, L.M.; Fortney, J.L.; Lamendella, R.; Jansson, J.K.; D'Haeseleer, P.; Hazen, T.C. and Zhou, J. (2012) Microbial gene functions enriched in the Deepwater Horizon deep-sea oil plume. *ISME J* 6(2), 451-460.
- Lyon, D.Y.; Fortner, J.D.; Sayes, C.M.; Colvin, V.L. and Hughes J.B. (2005) Bacterial cell association and antimicrobial activity of a C<sub>60</sub> water suspension. *Environ Toxicol Chem* 24(11), 2757-2762.

- Lyon, D.Y.; Adams, L.K.; Falkner, J.C. and Alvarez, P.J.J. (2006) Antibacterial activity of fullerene water suspensions: Effects of preparation method and particle size. *Environ Sci Technol* 40(14), 4360-4366.
- Lyon, D.Y.; Brown, D.A. and Alvarez, P.J.J. (2008) Implications and potential applications of bacteriocidal fullerene water suspensions: effect of nC<sub>60</sub> concentration, exposure conditions and shelf life. *Wat Sci Technol* 57(10), 1533-1538.
- Ma, R.; Levard, C.; Judy, J.D.; Unrine, J.M.; Durenkamp, M.; Martin, B.; Jefferson, B. and Lowry, G.V. (2014) Fate of zinc oxide and silver nanoparticles in a pilot wastewater treatment plant and in processed biosolids. *Environ Sci Technol* 48(1), 104-112.
- Mah, T.C. and O'Toole, G.A. (2001) Mechanisms of biofilm resistance to antimicrobial agents. *Trends Microbiol* 9(1), 34-39.
- Marambio-Jones, C. and Hoek, E. (2010) A review of the antibacterial effects of silver nanomaterials and potential implications for human health and the environment. *J Nanopart Res* 12(5), 1531-1551.
- Markowska, K.; Grudniak, A.M. and Wolska, K.I. (2013) Silver nanoparticles as an alternative strategy against bacterial biofilms. *Acta Biochim Pol* 60(4), 523-530.
- McIlroy, S.J.; Kristiansen, R.; Albertsen, M.; Karst, S.M.; Rossetti, S.; Nielsen, J.L.; Tandoi, V.; Seviour, R.J. and Nielsen, P.H. (2013) Metabolic model for the filamentous '*Candidatus* *Microthrix parvicella*' based on genomic and metagenomic analyses. *ISME J* 7(6), 1161-1172.

- McIlroy, S.J.; Nittami, T.; Seviour, E.M. and Seviour, R.J. (2010) Filamentous members of cluster III *Defluviicoccus* have the *in situ* phenotype expected of a glycogen-accumulating organism in activated sludge. *Fems Microbiol Ecol* 74(1), 248-256.
- McInroy, L.; Gibson, M.; Clark, R. and Cullen, B. (2009) Are silver dressings effective against biofilm formation? *Wound Repair Regen* 17(4), A73.
- Metcalf Eddy, I.; Tchobanoglous, G.; Burton, F.L. and Stensel, H.D. (2003) *Wastewater engineering: treatment and reuse*, 4 ed. McGraw-Hill: New York, NY.
- Meyer, A.F.; Lipson, D.A.; Martin, A.P.; Schadt, C.W. and Schmidt, S.K. (2004) Molecular and metabolic characterization of cold-tolerant alpine soil *Pseudomonas* *Sensu Stricto*. *Appl Environ Microbiol* 70(1), 483-489.
- Mielczarek, A.T.; Saunders, A.M.; Larsen, P.; Albertsen, M.; Stevenson, M.; Nielsen, J.L. and Nielsen, P.H. (2012) The Microbial Database for Danish wastewater treatment plants with nutrient removal (MiDas-DK) - a tool for understanding activated sludge population dynamics and community stability. In IWA World Water Congress, Busan, Korea, Republic of.
- Morones, J.R.; Elechiguerra, J.L.; Camacho, A.; Holt, K.; Kouri, J.B.; Ramirez, J.T. and Yacaman, M.J. (2005) The bactericidal effect of silver nanoparticles. *Nanotechnology* 16(10), 2346-2353.
- Mueller, N.C. and Nowack, B. (2008) Exposure modeling of engineered nanoparticles in the environment. *Environ Sci Technol* 42(12), 4447-4453.

Mumper, C.K.; Ostermeyer, A.; Semprini, L. and Radniecki, T.S. (2013) Influence of ammonia on silver nanoparticle dissolution and toxicity to *Nitrosomonas europaea*. *Chemosphere* 93(10), 2493-2498.

NCBI-BioProject. *Ralstonia pickettii* 12J.

<http://www.ncbi.nlm.nih.gov/Taxonomy/Browser/wwwtax.cgi?id=402626>, (accessed on Dec. 6, 2014)

Nguyen, T.G.; Limpiyakorn, T. and Siripattanakul-Ratpukdi, S. (2012) Inhibition kinetics of ammonia oxidation influenced by silver nanoparticles. *Water Air Soil Poll* 223(8), 5197-5203.

Nielsen, P.H.; de Muro, M.A. and Nielsen, J.L. (2000) Studies on the *in situ* physiology of *Thiothrix* spp. present in activated sludge. *Environ Microbiol* 2(4), 389-398.

O'Brien, N. and Cummins, E. (2010) Nano-scale pollutants: fate in Irish surface and drinking water regulatory systems. *Hum Ecol Risk Assess.* 16(4), 847-872.

Pal, S.; Tak, Y.K. and Song, J.M. (2007) Does the antibacterial activity of silver nanoparticles depend on the shape of the nanoparticle? A study of the gram-negative bacterium *Escherichia coli*. *Appl Environ Microb* 73(6), 1712-1720.

Palestrant, D.; Holzknacht, Z.E.; Collins, B.H.; Parker, W.; Miller, S.E. and Bollinger, R.R. (2004) Microbial biofilms in the gut: visualization by electron microscopy and by acridine orange staining. *Ultrastruct Pathol* 28(1), 23-27.

Pan, S.; Tay, J.H.; He, Y.X. and Tay, S.T. (2004) The effect of hydraulic retention time on the stability of aerobically grown microbial granules. *Lett Appl Microbiol* 38(2), 158-163.

Pandian, S.R.K.; Deepak, V.; Kalishwaralal, K.; Viswanathan, P. and Gurunathan, S. (2010)

Mechanism of bactericidal activity of silver nitrate - a concentration dependent bi-functional molecule. *Braz J Microbiol* 41, 805-809.

Parandhaman, T.; Das, A.; Ramalingam, B.; Samanta, D.; Sastry, T.P.; Mandal, A.B. and Das,

S.K. (2015) Antimicrobial behavior of biosynthesized silica-silver nanocomposite for water disinfection: A mechanistic perspective. *J Hazard Mater* 290, 117-126.

Pearson, K. (1896) Mathematical contributions to the theory of evolution. iii. regression, heredity, and panmixia. *Philos T R Soc Lond* 187, 253-318.

Pérez, S.; Farré, M. and Barceló, D. (2009) Analysis, behaviour and ecotoxicity of carbon-based nanomaterials. *Trac-Trends Anal Chem* 28(6), 820-832.

Petit, C.; Lixon, P. and Pileni, M.P. (1993) *In situ* synthesis of silver nanocluster in AOT reverse micelles. *J Phys Chem* 97(49), 12974-12983.

Priester, J.H.; Singhal, A.; Wu, B.; Stucky, G.D. and Holden, P.A. (2014) Integrated approach to evaluating the toxicity of novel cysteine-capped silver nanoparticles to *Escherichia coli* and *Pseudomonas aeruginosa*. *Analyst* 139(5), 954-963.

Radniecki, T.S.; Stankus, D.P.; Neigh, A.; Nason, J.A. and Semprini, L. (2011) Influence of liberated silver from silver nanoparticles on nitrification inhibition of *Nitrosomonas europaea*. *Chemosphere* 85(1), 43-49.

Raffi, M.; Hussain, F.; Bhatti, T.M.; Akhter, J.I.; A, H. and Hasan, M.M. (2008) Antibacterial characterization of silver nanoparticles against *E. Coli* ATCC-15224. *J Mater Sci Technol* 24(02), 192.

- Rai, M.; Yadav, A. and Gade, A. (2009) Silver nanoparticles as a new generation of antimicrobials. *Biotechnol Adv* 27(1), 76-83.
- Rittmann, B.E. and McCarty, P.L. (2001) *Environmental biotechnology: Principles and applications*, McGraw-Hill: New York.
- Rittmann, B.E.; Hausner, M.; Löffler, F.; Love, N.G.; Muyzer, G.; Okabe, S.; Oerther, D.B.; Peccia, J.; Raskin, L. and Wagner, M. (2006) A vista for microbial ecology and environmental biotechnology. *Environ Sci Technol* 40(4), 1096-1103.
- Rosenfeld, J.S. (2002) Functional redundancy in ecology and conservation. *Oikos* 98(1), 156-162.
- Rossetti, S.; Blackall, L.; Levantesi, C.; Uccelletti, D. and Tandoi, V. (2003) Phylogenetic and physiological characterization of a heterotrophic, chemolithoautotrophic *Thiothrix* strain isolated from activated sludge. *Int J Syst Evol Micr* 53(Part 5), 1271-1276.
- Sayes, C.M.; Gobin, A.M.; Ausman, K.D.; Mendez, J.; West, J.L. and Colvin, V.L. (2005) Nano-C<sub>60</sub> cytotoxicity is due to lipid peroxidation. *Biomaterials* 26(36), 7587-7595.
- Schacht, V.J.; Neumann, L.V.; Sandhi, S.K.; Chen, L.; Henning, T.; Klar, P.J.; Theophel, K.; Schnell, S. and Bunge, M. (2013) Effects of silver nanoparticles on microbial growth dynamics. *J Appl Microbiol* 114(1), 25-35.
- Sedlak, R.H.; Hnilova, M.; Grosh, C.; Fong, H.; Baneyx, F.; Schwartz, D.; Sarikaya, M.; Tamerler, C. and Traxler, B. (2012) Engineered *Escherichia coli* silver-binding periplasmic protein that promotes silver tolerance. *Appl Environ Microbiol* 78(7), 2289-2296.

- Seviour, E.M.; Williams, C.; DeGrey, B.; Soddell, J.A.; Seviour, R.J. and Lindrea, K.C. (1994) Studies on filamentous bacteria from Australian activated sludge plants. *Water Res* 28(11), 2335-2342.
- Sezgin, M.; Jenkins, D. and Parker, D.S. (1978) A unified theory of filamentous activated sludge bulking. *Journal of the Water Pollution Control Federation* 50(2), 362-381.
- Shade, A.; Peter, H.; Allison, S.D.; Baho, D.L.; Berga, M.; Burgmann, H.; Huber, D.H.; Langenheder, S.; Lennon, J.T.; Martiny, J.B.; Matulich, K.L.; Schmidt, T.M. and Handelsman, J. (2012) Fundamentals of microbial community resistance and resilience. *Front Microbiol* 3, 417.
- Sheng, Z. and Liu, Y. (2011) Effects of silver nanoparticles on wastewater biofilms. *Water Res* 45(18), 6039-6050.
- Sheng, Z.; Van Nostrand, J.D.; Zhou, J. and Liu, Y. (2015) The effects of silver nanoparticles on intact wastewater biofilms. *Front Microbiol* 6, 680.
- Sheng, Z.; J. D. Van Nostrand; Zhou J.; Liu Y. (2014) Positive effects of silver nanoparticles on activated sludge wastewater treatment. (submitted)
- Shuttleworth, K.L. and Unz, R.F. (1993) Sorption of heavy-metals to the filamentous bacterium *Thiothrix* strain A1. *Appl Environ Microb* 59(5), 1274-1282.
- Silvestry-Rodriguez, N.; Bright, K.R.; Slack, D.C.; Uhlmann, D.R. and Gerba, C.P. (2008) Silver as a residual disinfectant to prevent biofilm formation in water distribution systems. *Appl Environ Microb* 74(5), 1639-1641.

- Siripong, S. and Rittmann, B.E. (2007) Diversity study of nitrifying bacteria in full-scale municipal wastewater treatment plants. *Water Res* 41(5), 1110-1120.
- Smetana, A.B.; Klabunde, K.J.; Marchin, G.R. and Sorensen, C.M. (2008) Biocidal activity of nanocrystalline silver powders and particles. *Langmuir* 24(14), 7457-7464.
- Smillie, D.A.; Hayward, R.S.; Suzuki, T.; Fujita, N. and Ishihama, A. (1992) Locations of genes encoding alkyl hydroperoxide reductase on the physical map of the *Escherichia coli* K-12 genome. *J Bacteriol* 174(11), 3826-3827.
- Sondi, I. and Salopek-Sondi, B. (2004) Silver nanoparticles as antimicrobial agent: a case study on *E. coli* as a model for Gram-negative bacteria. *J Colloid Interface Sci* 275(1), 177-182.
- Song, H.Y.; Ko, K.K.; Oh, I.H. and Lee, B.T. (2006) Fabrication of silver nanoparticles and their antimicrobial mechanisms. *Eur Cells Mater* 11(Suppl 1), 58.
- Stewart, P.S. (2002) Mechanisms of antibiotic resistance in bacterial biofilms. *Int J Med Microbiol* 292(2), 107-113.
- Sun, X.; Sheng, Z. and Liu, Y. (2013) Effects of silver nanoparticles on microbial community structure in activated sludge. *Sci Total Environ* 443, 828-835.
- Sur, I.; Cam, D.; Kahraman, M.; Baysal, A. and Culha, M. (2010) Interaction of multi-functional silver nanoparticles with living cells. *Nanotechnology* 21(17510417).
- Swingley, W.D.; Sadekar, S.; Mastrian, S.D.; Matthies, H.J.; Hao, J.; Ramos, H.; Acharya, C.R.; Conrad, A.L.; Taylor, H.L.; Dejesa, L.C.; Shah, M.K.; O'Huallachain, M.E.; Lince, M.T.; Blankenship, R.E.; Beatty, J.T. and Touchman, J.W. (2007) The complete genome sequence

- of *Roseobacter denitrificans* reveals a mixotrophic rather than photosynthetic metabolism. *J Bacteriol* 189(3), 683-690.
- Tang, J.; Chen, Q.; Xu, L.; Zhang, S.; Feng, L.; Cheng, L.; Xu, H.; Liu, Z. and Peng, R. (2013) Graphene oxide-silver nanocomposite as a highly effective antibacterial agent with species-specific mechanisms. *ACS Appl Mater Inter* 5(9), 3867-3874.
- The Project on Emerging Nanotechnologies. <http://www.nanotechproject.org/>, (accessed Dec. 6, 2014)
- Tu, Q.; Yu, H.; He, Z.; Deng, Y.; Wu, L.; Van Nostrand, J.D.; Zhou, A.; Voordeckers, J.; Lee, Y.; Qin, Y.; Hemme, C.L.; Shi, Z.; Xue, K.; Yuan, T.; Wang, A. and Zhou, J. (2014) GeoChip 4: a functional gene-array-based high-throughput environmental technology for microbial community analysis. *Mol Ecol Resour* 14(5), 914-928.
- Tugulea, A.M.; Berube, D.; Giddings, M.; Lemieux, F.; Hnatiw, J.; Priem, J. and Avramescu, M.L. (2014) Nano-silver in drinking water and drinking water sources: stability and influences on disinfection by-product formation. *Environ Sci Pollut R* 21(20), 11823-11831.
- Van de Peer, Y. and De Wachter, R. (1994) TREECON for Windows: a software package for the construction and drawing of evolutionary trees for the Microsoft Windows environment. *Comput Appl Biosci* 10(5), 569-570.
- van den Akker, B.; Beard, H.; Kaeding, U.; Giglio, S. and Short, M.D. (2010) Exploring the relationship between viscous bulking and ammonia-oxidiser abundance in activated sludge: A comparison of conventional and IFAS systems. *Water Res* 44(9), 2919-2929.

- Verano-Braga, T.; Miethling-Graff, R.; Wojdyla, K.; Rogowska-Wrzesinska, A.; Brewer, J.R.; Erdmann, H. and Kjeldsen, F. (2014) Insights into the cellular response triggered by silver nanoparticles using quantitative proteomics. *ACS Nano* 8(3), 2161-2175.
- Vertelov, G.K.; Krutyakov, Y.A.; Efremenkova, O.V.; Olenin, A.Y. and Lisichkin, G.V. (2008) A versatile synthesis of highly bactericidal Myramistin<sup>®</sup> stabilized silver nanoparticles. *Nanotechnology* 19(35), 355707.
- Walker, B. (1995) Conserving biological diversity through ecosystem resilience. *Conserv Biol* 9(4), 747-752.
- Wang, X.; Hu, M.; Xia, Y.; Wen, X. and Ding, K. (2012) Pyrosequencing analysis of bacterial diversity in 14 wastewater treatment systems in China. *Appl Environ Microbiol* 78(19), 7042-7047.
- Watson, S.W.; Bock, E.; Harms, H.; Koops, H.P. and Hooper, A.B. (1989) Nitrifying bacteria, p 1808–1834. *In* Staley JT, Bryant MP, Pfenning N, and Holt JG (ed), *Bergey's Manual of Systematic Bacteriology*. Williams & Wilkins: Baltimore, MD.
- Wehling, J.; Koser, J.; Lindner, P.; Luder, C.; Beutel, S.; Kroll, S. and Rezwan, K. (2015) Silver nanoparticle-doped zirconia capillaries for enhanced bacterial filtration. *Mat Sci Eng C-Mater* 48, 179-187.
- Weinbauer, M.G. and Höfle, M.G. (1998) Distribution and life strategies of two bacterial populations in a eutrophic lake. *Appl Environ Microbiol* 64(10), 3776-3783.
- Wigginton, N.S.; de Titta, A.; Piccapietra, F.; Dobias, J.; Nesatyy, V.J.; Suter, M.J. and Bernier-Latmani, R. (2010) Binding of silver nanoparticles to bacterial proteins depends on

- surface modifications and inhibits enzymatic activity. *Environ Sci Technol* 44(6), 2163-2168.
- Wong, M.T.; Mino, T.; Seviour, R.J.; Onuki, M. and Liu, W.T. (2005) *In situ* identification and characterization of the microbial community structure of full-scale enhanced biological phosphorous removal plants in Japan. *Water Res* 39(13), 2901-2914.
- Wu, S.; Feng, X. and Wittmeier, A. (1997) Microwave digestion of plant and grain reference materials in nitric acid or a mixture of nitric acid or a mixture of nitric acid and hydrogen peroxide for the determination of multi-elements by inductively coupled plasma mass spectrometry. *J Anal Atom Spectrom* 12(8), 797-806.
- Xia, Y.; Kong, Y.; Thomsen, T.R. and Halkjær Nielsen, P. (2008) Identification and ecophysiological characterization of epiphytic protein-hydrolyzing *Saprospiraceae* (“*Candidatus* Epiflobacter” spp.) in activated sludge. *Appl Environ Microb* 74(7), 2229-2238.
- Xiu, Z.; Zhang, Q.; Puppala, H.L.; Colvin, V.L. and Alvarez, P.J.J. (2012) Negligible particle-specific antibacterial activity of silver nanoparticles. *Nano Lett* 12(8), 4271-4275.
- Xu, S.; Sun, M.; Zhang, C.; Surampalli, R. and Hu, Z. (2014a) Filamentous sludge bulking control by nano zero-valent iron in activated sludge treatment systems. *Environ Sci Process Impacts* 16(12), 2721-2728.
- Xu, S.; Wu, D. and Hu, Z. (2014b) Impact of hydraulic retention time on organic and nutrient removal in a membrane coupled sequencing batch reactor. *Water Res* 55, 12-20.

- Yang, Y.; Li, M.; Michels, C.; Moreira-Soares, H. and Alvarez, P.J.J. (2014a) Differential sensitivity of nitrifying bacteria to silver nanoparticles in activated sludge. *Environ Toxicol Chem* 33(10), 2234-2239.
- Yang, Y.; Quensen, J.; Mathieu, J.; Wang, Q.; Wang, J.; Li, M.; Tiedje, J.M. and Alvarez, P.J.J. (2014b) Pyrosequencing reveals higher impact of silver nanoparticles than Ag<sup>+</sup> on the microbial community structure of activated sludge. *Water Res* 48, 317-325.
- Yang, Y.; Wang, J.; Xiu, Z. and Alvarez, P.J.J. (2013) Impacts of silver nanoparticles on cellular and transcriptional activity of nitrogen-cycling bacteria. *Environ Toxicol Chem* 32(7), 1488-1494.
- Ye, L. and Zhang, T. (2013) Bacterial communities in different sections of a municipal wastewater treatment plant revealed by 16S rDNA 454 pyrosequencing. *Appl Microbiol Biotechnol* 97(6), 2681-2690.
- Yin, B.; Crowley, D.; Sparovek, G.; De Melo, W.J. and Borneman, J. (2000) Bacterial functional redundancy along a soil reclamation gradient. *Appl Environ Microb* 66(10), 4361-4365.
- Yoon, K.; Byeon, J.H.; Park, J.; Ji, J.H.; Bae, G.N. and Hwang, J. (2008a) Antimicrobial characteristics of silver aerosol nanoparticles against *Bacillus subtilis* bioaerosols. *Environ Eng Sci* 25(2), 289-294.
- Yoon, K.Y.; Byeon, J.H.; Park, C.W. and Hwang, J. (2008b) Antimicrobial effect of silver particles on bacterial contamination of activated carbon fibers. *Environ Sci Technol* 42(4), 1251-1255.

- Yu, Z. and Morrison, M. (2004) Comparisons of different hypervariable regions of rrs genes for use in fingerprinting of microbial communities by PCR-denaturing gradient gel electrophoresis. *Appl Environ Microb* 70(8), 4800-4806.
- Yuan, Z.; Li, J.; Cui, L.; Xu, B.; Zhang, H. and Yu, C. (2013) Interaction of silver nanoparticles with pure nitrifying bacteria. *Chemosphere* 90(4), 1404-1411.
- Zahller, J. and Stewart, P.S. (2002) Transmission electron microscopic study of antibiotic action on *Klebsiella pneumoniae* Biofilm. *Antimicrob Agents Ch* 46(8), 2679-2683.
- Zelver, N.; Hamilton, M.; Pitts, B.; Goeres, D.; Walker, D.; Sturman, P. and Heersink, J. (1999) Measuring antimicrobial effects on biofilm bacteria: from laboratory to field. *Methods Enzymol* 310, 608-628.
- Zhang, B.; Cho, M.; Fortner, J.D.; Lee, J.; Huang, C.H.; Hughes, J.B. and Kim, J.H. (2009) Delineating oxidative processes of aqueous C<sub>60</sub> preparations: Role of THF peroxide. *Environ Sci Technol* 43(1), 108-113
- Zhang, C.; Liang, Z. and Hu, Z. (2014) Bacterial response to a continuous long-term exposure of silver nanoparticles at sub-ppm silver concentrations in a membrane bioreactor activated sludge system. *Water Res* 50, 350-358.
- Zhang, Y.; Peng, H.; Huang, W.; Zhou, Y. and Yan, D. (2008b) Facile preparation and characterization of highly antimicrobial colloid Ag or Au nanoparticles. *J Colloid Interf Sci* 325(2), 371-376.

- Zhang, Y.; Peng, H.; Huang, W.; Zhou, Y.; Zhang, X. and Yan, D. (2008a) Hyperbranched poly (amidoamine) as the stabilizer and reductant to prepare colloid silver nanoparticles *in situ* and their antibacterial activity. *J Phys Chem C* 112(7), 2330-2336.
- Zhao, Y. and Nalwa, H.S. (2007) *Nanotoxicology – Interactions of Nanomaterials with Biological Systems*. American Scientific Publishers, Stevenson Ranch, CA (ISBN: 1-58883-088-8).
- Zhao, Y.; Xing, J.; Xing, J.Z.; Ang, W.T. and Chen, J. (2014) Applications of low-intensity pulsed ultrasound to increase monoclonal antibody production in CHO cells using shake flasks or wavebags. *Ultrasonics* 54(6), 1439-1447.
- Zhao, Y.K.; Sung, W.P.; Tsai, T.T. and Wang, H.J. (2010) Application of nanoscale silver-doped titanium dioxide as photocatalyst for indoor airborne bacteria control: A feasibility study in medical nursing institutions. *J Air Waste Manage* 60(3), 337-345.
- Zilles, J.L.; Peccia, J.; Kim, M.W.; Hung, C.H. and Noguera, D.R. (2002) Involvement of *Rhodocyclus*-related organisms in phosphorus removal in full-scale wastewater treatment plants. *Appl Environ Microbiol* 68(6), 2763-2769.
- Zodrow, K. R.; Bar-Zeev, E.; Giannetto, M. J. and Elimelech, M. (2014) Biofouling and microbial communities in membrane distillation and reverse osmosis. *Environ Sci Technol* 48, 13155-13164.

## Appendix A Supporting information for effects of silver nanoparticles on wastewater biofilms

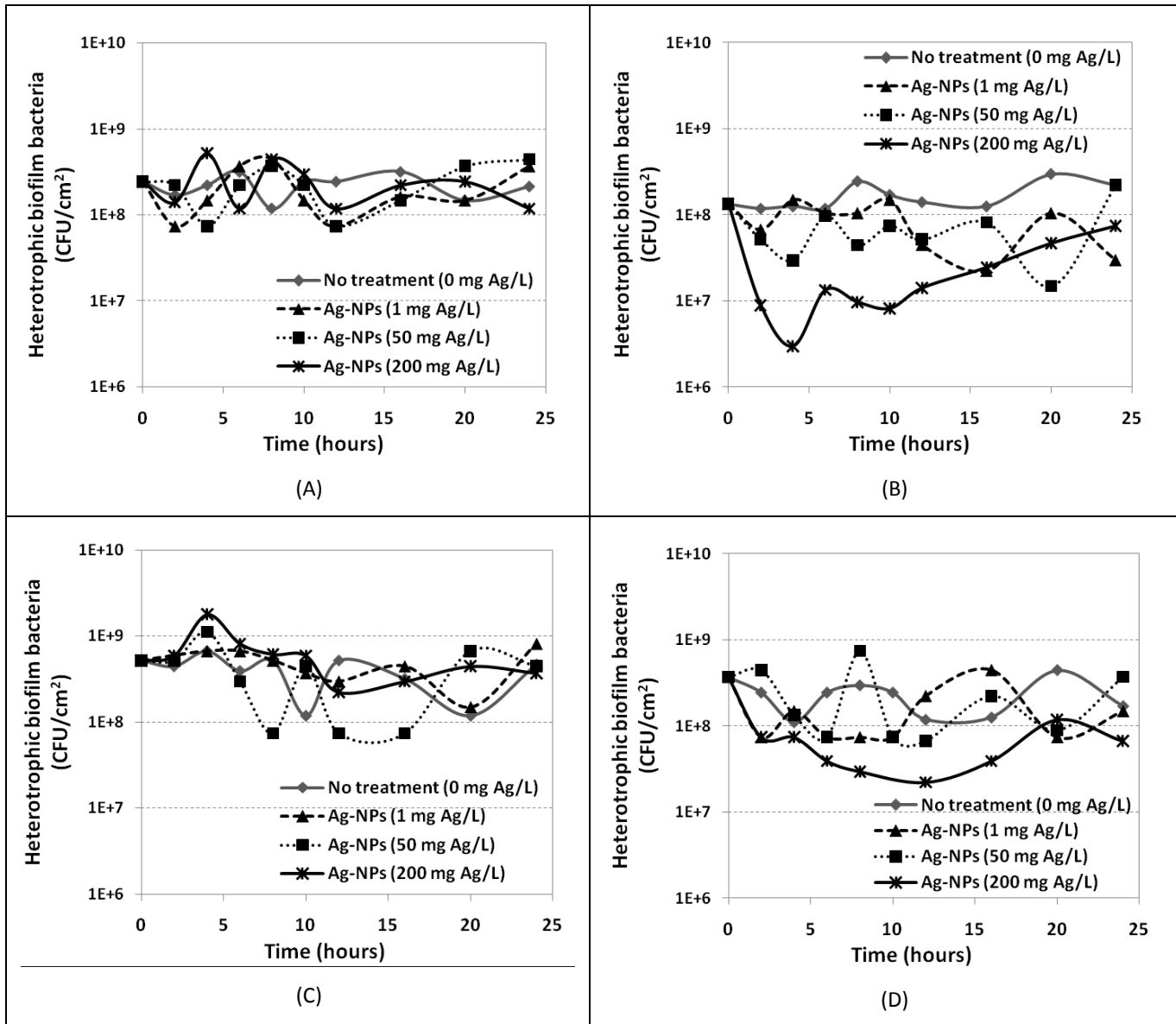


**Figure A-1** Viability of heterotrophic bacteria in wastewater biofilms with (A and C) and without (B and D) loosely bound EPS under Ag-NP treatment at various concentrations: (A) (B) growth of heterotrophic bacteria 24 h after plating; (C) (D) growth of heterotrophic bacteria 4 days after plating. All HPCs shown are average of triplicates, and the standard deviations are around  $1 \times 10^7$  CFU/mL.

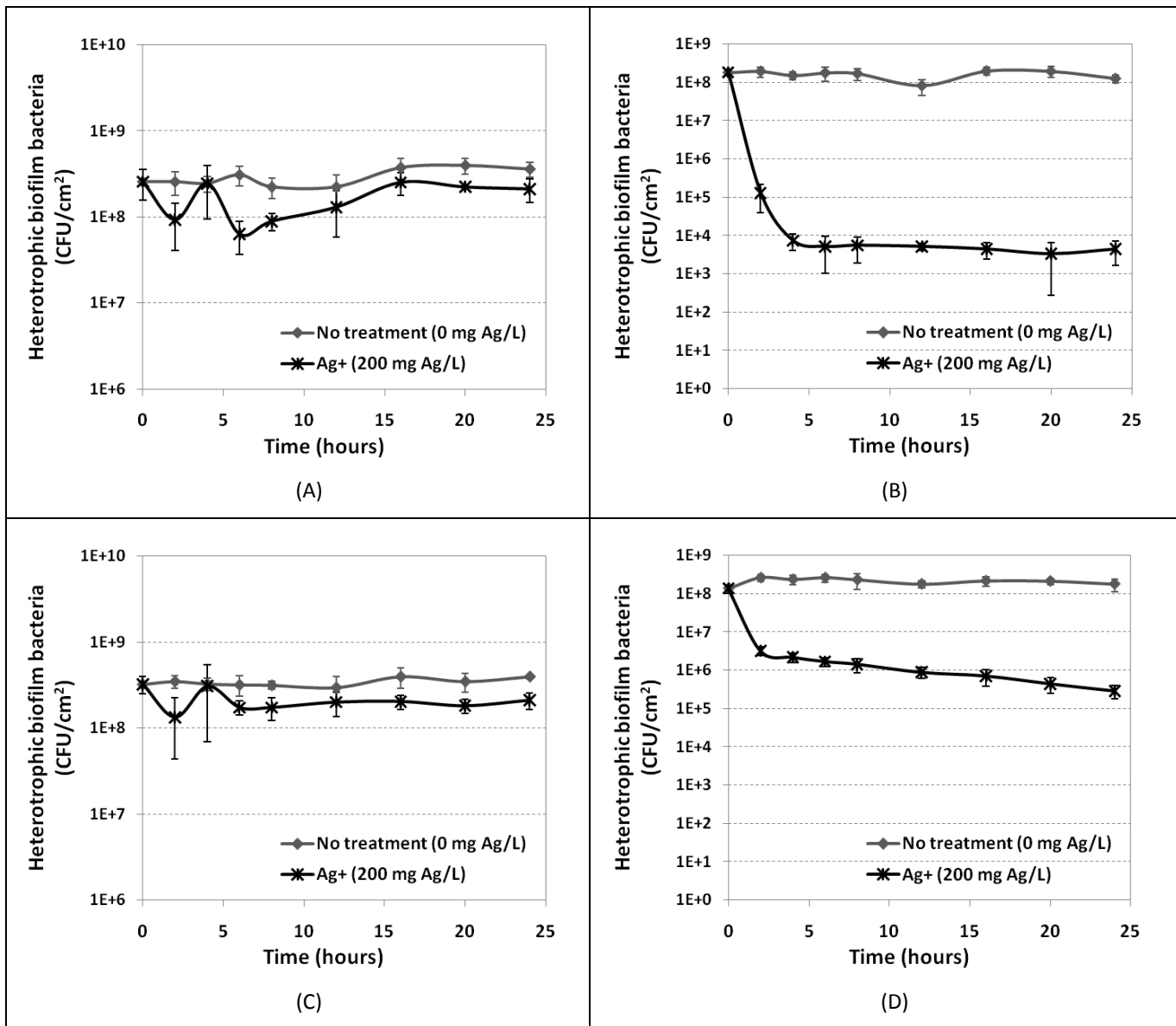


**Figure A-2** Viability of heterotrophic bacteria in wastewater biofilms with (A and C) and without (B and D) loosely bound EPS under Ag<sup>+</sup> treatment (200 mg Ag/L): (A) (B) growth of heterotrophic bacteria 24 h after plating; (C) (D) growth of heterotrophic bacteria 4 days after plating. Error bars represent one standard deviation.

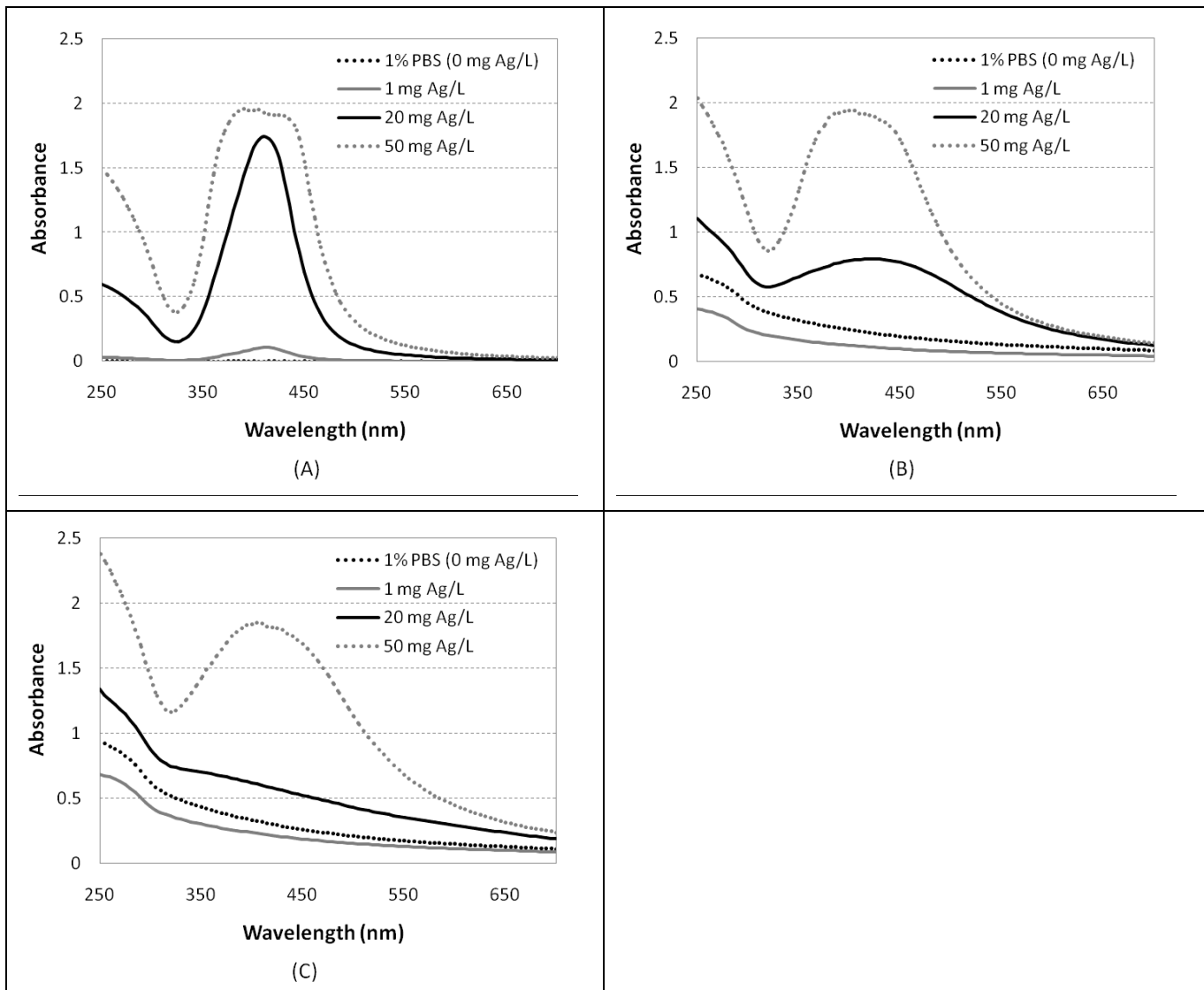


**Figure A-3** UV-vis spectra of remaining Ag-NPs in suspensions with various initial concentrations (0, 1, 20, 50 mg Ag/L) after incubation with wastewater biofilm: (A) initial (0 min of incubation); (B) 45 min of incubation; (C) 140 min of incubation.

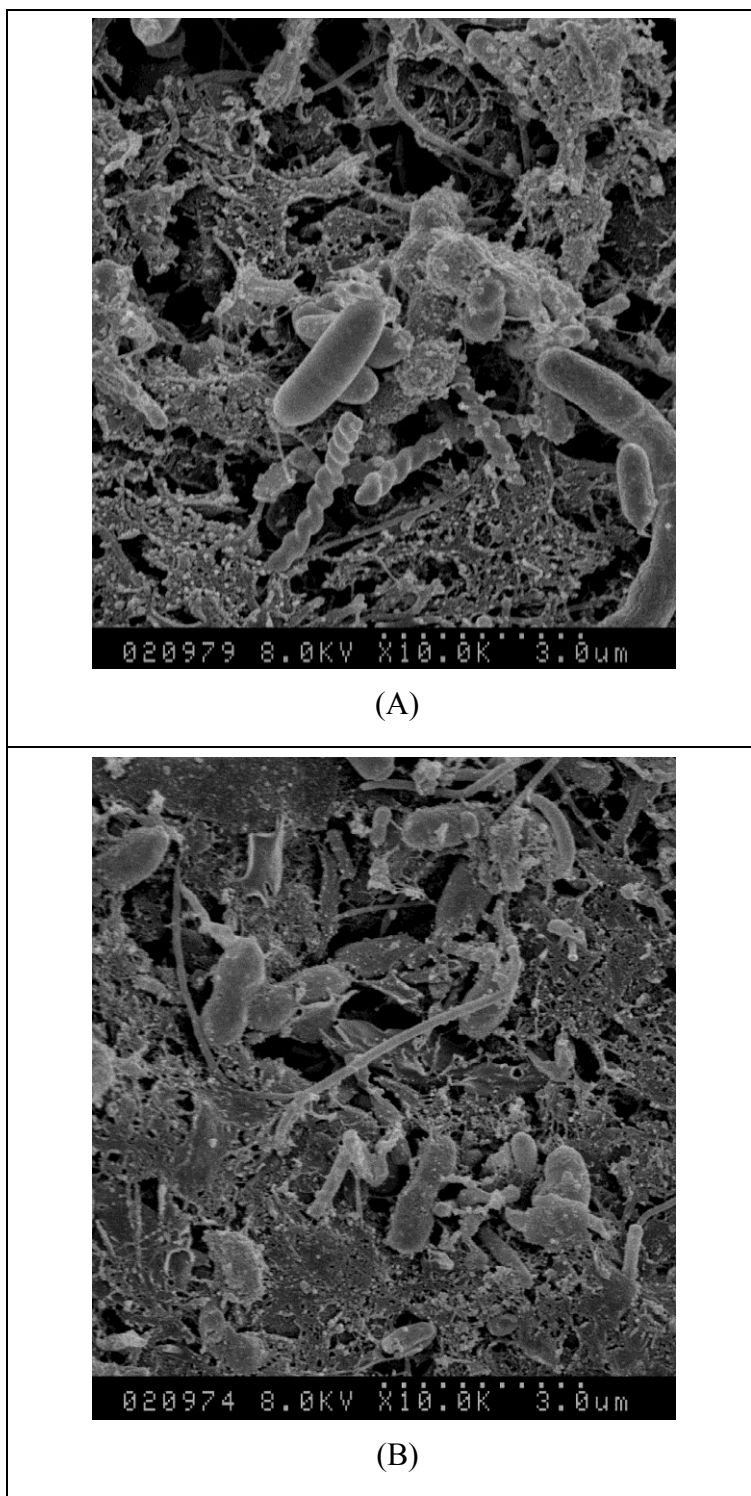


**Figure A-4** SEM images of wastewater biofilms with (A) and without (B) Ag-NPs. Bar size: 3  $\mu\text{m}$ .

Ag-NPs cannot be identified from the images.

Table A-1 Response of intact wastewater biofilms to Ag-NPs.

Sample	HPC after 24 h (CFU/mL)	p-value
No treatment (0 mg Ag/L)	$(3.84 \pm 0.56) \times 10^8$	0.11
With Ag-NPs (200 mg Ag/L)	$(3.04 \pm 0.34) \times 10^8$	

### Material and Methods

**RBC in the Devon Wastewater Treatment Plant and sample processing.** The total surface area of the first stage RBC unit is 9290 m<sup>2</sup>. The average daily influent flow was about 2500 m<sup>3</sup>, with an average influent biochemical oxygen demand (BOD) of 157.5 mg/L. All the RBC units were run indoors under ambient light. The year-round average room temperature is 20°C, and the water temperature varied from 10 to 16°C. Biofilm samples were cut with the plastic substratum just before each experiment, kept in a Petri dish on ice during a 30-min transport. Upon the arrival of the laboratory, biofilms were scraped off the RBC substratum, weighed and divided into 1% PBS or Ag-NP suspension within 30 min. Biofilms were resuspended in 1% PBS and mixed by vortex before dividing into individual tubes to ensure representative and homogenized sampling. Samples in each tube were also mixed by vortex before plating each time.

**SEM imaging.** SEM samples were fixed immediately after treatment with 2.5% glutaraldehyde in phosphate buffer for 30 min and rinsed with the same buffer for three times for a 5 min period each. Samples were then fixed with 1% OsO<sub>4</sub> in phosphate buffer for 30 min and

rinsed briefly with distilled water, followed by dehydration in a serial of ethanol from 50%, 70%, 90% and 100%, 5 min each grade. After two more additional changes in 100%, the samples were subjected to critical point drying at 31 °C for 5 min. Samples were then mounted on the stub and sputter coated (Edwards, Model S150B, England) with gold. The samples were then examined with Hitachi Scanning Electron Microscope S-2500.

**Biofilm community analysis using PCR-DGGE.** The Powersoil<sup>®</sup> DNA Isolation Kit from MO BIO Laboratories, Inc. (Carlsbad, USA) was adopted to extract genomic DNA from each sample. Taq DNA polymerase (Invitrogen Platinum<sup>®</sup>) was used to amplify a ~550 bps fragment of 16s rRNA gene from each DNA sample. The primer pair 357f (5'-CCT ACG GGA GGC AGC AG -3') and 907r (5'-CCG TCA ATT CCT TTG AGT TT -3') was used (Yu and Morrison, 2004). A GC-clamp (5'-CGC CCG CCG CGC GCG GCG GGC GGG GCG GGG GCA CGG GGG G-3') was added to the 5' end of the forward primer. A 50- $\mu$ L system was used in which the final concentration of each component was as follows: PCR buffer, 1 $\times$ ; MgCl<sub>2</sub> 1.5 mM; dNTPs 100  $\mu$ M; Taq, 1.25 U; primer, 0.1  $\mu$ M each; DNA template, ~3 ng. PCR was run with an initial hot start at 94°C for 2 min, followed by 35 cycles of 30 s at 94°C, 30 s at 54°C and 40 s at 72°C, and then a final extension at 72 °C for 10 min. Polyacrylamide (6.5%) gels (16 cm  $\times$  10 cm  $\times$  1 mm) were prepared using a gradient delivery system (Model 475, Bio-Rad Laboratories Ltd., Ontario, Canada). The denaturing gradient of 40–60% was adopted to obtain the best separation. DGGE was run using the D-code system (Bio-Rad Laboratories Ltd., Ontario, Canada) at 150 V, 60°C, for 11 h in 0.5  $\times$  Tris-acetate-EDTA buffer (TAE). 600 ng per lane of PCR products was loaded for each sample. The gels were stained in 0.5 mg/L ethidium bromide

for 20 min, then de-stained in deionized water for 15 min. Selected bands were excised from the DGGE gel, mashed into Tris-HCl buffer (pH 8.5) and kept at 4°C overnight. 2–10  $\mu$ L aliquots of the gel diffusion solution were added as templates into each 50- $\mu$ L PCR system with the composition previously described. PCR was run under the same conditions. PCR products were purified using an ExoSAP-IT<sup>®</sup> PCR Product Clean-Up Kit, and sequenced.

**Ag-NP toxicity to intact biofilms.** For each replicate, two pieces (1.5  $\times$  1.5 cm) of biofilm from the same spot on the RBC unit were cut with the plastic substratum and put into 5 mL of 1% PBS with and without Ag-NPs respectively. After shaking at 100 rpm for 24 h in the dark at room temperature (25.5°C), the biofilms were scraped off the RBC substratum and enumeration was performed.

## Results

**Sorption of Ag-NPs to wastewater biofilms.** Without biofilms, the absorbance of the suspension did not change during the experimental period. As shown in Figure A-3, the UV-vis absorption spectra of all the suspensions with biofilms became more and more similar to 1% PBS over time, which indicates a decrease in free Ag-NPs in the suspension. At higher Ag-NP concentrations, the decline of absorbance was not as significant, but was still detectable. It's noted that the absorbance of the 1% PBS control (0 mg Ag/L) increased over time, which can be explained by the slow release of certain biofilm compounds into the aqueous phase. This made it impossible to detect the amount of free Ag-NPs in the 1 mg Ag/L suspension over time. However, it is clear that after 500 min, the absorbance of the 1 mg Ag/L suspension was the same as that of 1% PBS, which may indicate complete sorption of Ag-NPs.

**Appendix B Supporting information for the effects of silver nanoparticles on intact wastewater biofilms**

Table B-1 Gene variants missing in Ag-NP treated biofilm.

Category	Gene	Organisms of missing gene variants
Silver resistance genes	silA	<i>Rhodopseudomonas palustris</i> CGA009
		<i>Sagittula stellata</i> E-37
		<i>Sphingomonas</i> sp. SKA58
		<i>Sulfitobacter</i> sp. NAS-14.1
	silC	<i>Alcanivorax</i> sp. DG881
		<i>Alteromonadales bacterium</i> TW-7
		<i>Bordetella petrii</i> DSM 12804
		<i>Burkholderia cenocepacia</i> PC184
		<i>Burkholderia pseudomallei</i> 1655
		<i>Burkholderia ubonensis</i> Bu
		<i>Burkholderia vietnamiensis</i> G4
		<i>Candidatus Desulfococcus oleovorans</i> Hxd3
		<i>Caulobacter crescentus</i> CB15
		<i>Comamonas testosteroni</i> KF-1
		<i>Desulfovibrio vulgaris</i> subsp. <i>vulgaris</i> DP4
		<i>Geobacter bemidjiensis</i> Bem
		<i>Geobacter lovleyi</i> SZ
		<i>Gluconacetobacter diazotrophicus</i> PAL5
		<i>Leptothrix cholodnii</i> SP-6
		<i>Methylobacillus flagellatus</i> KT
		<i>Pseudomonas aeruginosa</i> C3719
		<i>Pseudomonas aeruginosa</i> PACS2
		<i>Pseudomonas fluorescens</i>
		<i>Pseudomonas stutzeri</i> A1501
		<i>Ralstonia eutropha</i> H16
		<i>Ralstonia solanacearum</i> UW551
		<i>Rhodoferax ferrireducens</i> DSM 15236
		<i>Salmonella enterica</i> subsp. <i>enterica</i> serovar Choleraesuis str. SC-B67
		<i>Sphingomonas</i> sp. SKA58
		<i>Verrucomicrobiae bacterium</i> DG1235
		<i>Xanthomonas campestris</i> pv. <i>vesicatoria</i> str. 85-10

Table B-1 (continued) Missing gene variants in Ag-NP treated biofilm.

Category	Gene	Organisms of missing gene variants	
Silver resistance genes	<i>silP</i>	<i>Bifidobacterium adolescentis</i> ATCC 15703	
		<i>Ralstonia eutropha</i> H16	
		<i>Herminiimonas arsenicoxydans</i>	
Genes associated with oxidative stress	<i>ahpC</i>	<i>Actinomyces urogenitalis</i> DSM 15434	
		<i>Agrobacterium radiobacter</i> K84	
		<i>Aspergillus clavatus</i> NRRL 1	
		<i>Aspergillus niger</i>	
		<i>Bifidobacterium longum</i> NCC2705	
		<i>Bordetella avium</i> 197N	
		<i>Bordetella parapertussis</i> 12822	
		<i>Capnocytophaga ochracea</i> DSM 7271	
		<i>Chlamydia muridarum</i> Nigg	
		<i>Clavispora lusitaniae</i> ATCC 42720	
		<i>Coprinopsis cinerea</i> okayama7#130	
		<i>Corynebacterium jeikeium</i> ATCC 43734	
		<i>Cyanothece</i> sp. PCC 7425	
		<i>Dechloromonas aromatica</i> RCB	
		<i>Desulfovibrio magneticus</i> RS-1	
		<i>ahpC</i>	<i>Desulfovibrio vulgaris</i> subsp. <i>vulgaris</i> DP4
			<i>Eggerthella lenta</i> DSM 2243
	<i>Gemmata obscuriglobus</i> UQM 2246		
	<i>Geobacter</i> sp. M21		
	<i>Gramella forsetii</i> KT0803		
	<i>Haliangium ochraceum</i> DSM 14365		
	<i>Idiomarina baltica</i> OS145		
	<i>Listeria innocua</i> Clip11262		
	<i>Marinobacter aquaeolei</i> VT8		
	<i>Methylobacillus flagellatus</i> KT		
	<i>Mycobacterium abscessus</i>		
	<i>Nitrobacter hamburgensis</i> X14		
	<i>Nitrobacter winogradskyi</i> Nb-255		
	<i>Prosthecochloris vibrioformis</i> DSM 265		
	<i>Rhodobacteriales bacterium</i> HTCC2654		
<i>Rhodococcus jostii</i> RHA1			
<i>Rhodothermus marinus</i> DSM 4252			
<i>Rothia mucilaginosa</i> ATCC 25296			

Table B-1 (continued) Missing gene variants in Ag-NP treated biofilm.

Category	Gene	Organisms of missing gene variants
Genes associated with oxidative stress	<i>ahpC</i>	<i>Saccharomonospora viridis</i> DSM 43017
		<i>Sphaerobacter thermophilus</i> DSM 20745
		<i>Sphingomonas</i> sp. SKA58
		<i>Stackebrandtia nassauensis</i> DSM 44728
	<i>ahpF</i>	<i>Alcanivorax borkumensis</i> SK2
		<i>Bacillus licheniformis</i> DSM 13
		<i>Bacteroides capillosus</i> ATCC 29799
		<i>Brevibacillus brevis</i> NBRC 100599
		<i>Burkholderia thailandensis</i> E264
		<i>Cardiobacterium hominis</i> ATCC 15826
		<i>Desulfobacterium autotrophicum</i> HRM2
		<i>Desulfomicrobium baculatum</i> DSM 4028
		<i>Leuconostoc mesenteroides</i> subsp. <i>cremoris</i> ATCC 19254
		<i>Marinobacter algicola</i> DG893
		<i>Nectria haematococca</i> mpVI 77-13-4
		<i>Pantoea</i> sp. At-9b
		<i>Paracoccus denitrificans</i> PD1222
		<i>Pseudomonas putida</i> GB-1
		<i>Teredinibacter turnerae</i> T7901
	<i>katA</i>	<i>Alicyclobacillus acidocaldarius</i> LAA1
		<i>Bacillus firmus</i>
		<i>Bacillus subtilis</i>
		<i>Corynebacterium pseudogenitalium</i> ATCC 33035
		<i>Deinococcus radiodurans</i>
		<i>Gluconacetobacter diazotrophicus</i> PAI 5
		<i>Ochrobactrum anthropi</i> ATCC 49188
		<i>Pseudomonas stutzeri</i> A1501
		<i>Pseudomonas syringae</i> pv. <i>phaseolicola</i> 1448A
		<i>Rhodococcus opacus</i> B4
	<i>katE</i>	<i>Acetobacter pasteurianus</i> IFO 3283-26
		<i>Acinetobacter radioresistens</i> SH164
		<i>Arthrobacter aurescens</i> TC1
		<i>Aspergillus oryzae</i>
<i>Aurantimonas manganooxydans</i> SI85-9A1		
<i>Bacillus coagulans</i> 36D1		
<i>Bacillus mycoides</i> DSM 2048		

Table B-1 (continued) Missing gene variants in Ag-NP treated biofilm.

Category	Gene	Organisms of missing gene variants
Genes associated with oxidative stress	<i>katE</i>	<i>Bacillus subtilis</i> subsp. <i>subtilis</i> str. 168
		<i>Bordetella avium</i> 197N
		<i>Clavibacter michiganensis</i> subsp. <i>michiganensis</i> NCPPB 382
		<i>Corynebacterium diphtheriae</i>
		<i>Delftia acidovorans</i> SPH-1
		<i>Desulfovibrio piger</i> ATCC 29098
		<i>Edwardsiella tarda</i>
		endosymbiont of <i>Onchocerca volvulus</i>
		<i>Exiguobacterium</i> sp. CNU020
		<i>Frankia alni</i> ACN14a
		<i>Fulvimarina pelagi</i> HTCC2506
		<i>Geobacillus</i> sp. Y412MC10
		<i>Gibberella moniliformis</i>
		<i>Granulibacter bethesdensis</i> CGDNIH1
		<i>Herpetosiphon aurantiacus</i> ATCC 23779
		<i>Lachancea thermotolerans</i>
		<i>Malassezia globosa</i> CBS 7966
		<i>Methanococcoides burtonii</i> DSM 6242
		<i>Methylobacillus flagellatus</i> KT
		<i>Methylocella silvestris</i> BL2
		<i>Mycobacterium avium</i> subsp. <i>avium</i> ATCC 25291
		<i>Mycobacterium avium</i> subsp. <i>paratuberculosis</i> K-10
		<i>Mycobacterium gilvum</i> PYR-GCK
		<i>Paenibacillus</i> sp. JDR-2
		<i>Paracoccus denitrificans</i> PD1222
		<i>Ralstonia metallidurans</i> CH34
		<i>Rhizobium leguminosarum</i> bv. <i>trifolii</i> WSM1325
		<i>Rhodobacter sphaeroides</i> KD131
		<i>Rhodococcus equi</i>
		<i>Rhodococcus erythropolis</i> PR4
		<i>Rhodococcus erythropolis</i> SK121
		<i>Rhodopseudomonas palustris</i> TIE-1
		<i>Roseovarius</i> sp. TM1035
<i>Schizosaccharomyces japonicus</i> yFS275		
<i>Shewanella putrefaciens</i> 200		
<i>Shewanella</i> sp. ANA-3		

Table B-1 (continued) Missing gene variants in Ag-NP treated biofilm.

Category	Gene	Organisms of missing gene variants
Genes associated with oxidative stress	katE	<i>Sinorhizobium meliloti</i> 1021
		<i>Spirosoma linguale</i> DSM 74
		<i>Sporothrix schenckii</i>
		<i>Streptomyces avermitilis</i> MA-4680
		<i>Streptomyces hygroscopicus</i> ATCC 53653
		<i>Uncinocarpus reesii</i> 1704
		<i>Verticillium albo-atrum</i> VaMs.102
		<i>Xanthomonas axonopodis</i> pv. <i>citri</i> str. 306
		<i>Yarrowia lipolytica</i>
		<i>Yarrowia lipolytica</i>
		<i>Yersinia mollaretii</i> ATCC 43969
		<i>Zygosaccharomyces rouxii</i>
		<i>Zymomonas mobilis</i> subsp. <i>mobilis</i> NCIMB 11163
		oxyR
	<i>Bradyrhizobium</i> sp. BTAi1	
	<i>Congregibacter litoralis</i> KT71	
	<i>Corynebacterium urealyticum</i> DSM 7109	
	<i>Cronobacter turicensis</i>	
	<i>Dinoroseobacter shibae</i> DFL 12	
	<i>Frankia</i> sp. EAN1pec	
	<i>Geobacillus</i> sp. Y412MC10	
	<i>Gluconacetobacter diazotrophicus</i> PAI 5	
	<i>Granulibacter bethesdensis</i> CGDNIH1	
	<i>Kangiella koreensis</i> DSM 16069	
	<i>Legionella drancourtii</i> LLAP12	
	<i>Magnetospirillum gryphiswaldense</i> MSR-1	
	<i>Maricaulis maris</i> MCS10	
	<i>Mycobacterium ulcerans</i> Agy99	
	<i>Nitrococcus mobilis</i> Nb-231	
	<i>Novosphingobium aromaticivorans</i> DSM 12444	
	<i>Ochrobactrum intermedium</i> LMG 3301	
	<i>Parvularcula bermudensis</i> HTCC2503	
	<i>Pasteurella multocida</i> subsp. <i>multocida</i> str. Pm70	
<i>Rhodococcus erythropolis</i> SK121		
<i>Rhodococcus jostii</i> RHA1		
<i>Rhodoferax ferrireducens</i> T118		

Table B-1 (continued) Missing gene variants in Ag-NP treated biofilm.

Category	Gene	Organisms of missing gene variants
<p style="text-align: center;"><b>Genes associated with oxidative stress</b></p>	<i>oxyR</i>	<i>Roseovarius</i> sp. HTCC2601
		<i>Ruegeria pomeroyi</i> DSS-3
		<i>Ruegeria</i> sp. R11
		<i>Salinibacter ruber</i> DSM 13855
		<i>Shewanella benthica</i> KT99
		<i>Sinorhizobium meliloti</i> 1021
		<i>Stappia aggregata</i> IAM 12614
		<i>Streptomyces clavuligerus</i> ATCC 27064
		<i>Streptomyces flavogriseus</i> ATCC 33331
		<i>Thiomonas intermedia</i> K12
		<i>Vibrio alginolyticus</i> 12G01
		<i>Vibrio angustum</i> S14
		<i>Vibrio harveyi</i> HY01
		<i>Vibrio mimicus</i> VM223
		<i>Vibrio orientalis</i> CIP 102891
		<i>Vibrio</i> sp. RC586
		<i>Xanthomonas albilineans</i>
<i>Xanthomonas campestris</i>		

Table B-2 Gene variants detected only in Ag-NP treated biofilm.

Category	Gene	Organisms of missing gene variants
<b>Silver resistance genes</b>	<i>silC</i>	<i>Rhodospirillum rubrum</i> ATCC 11170
		<i>Pseudomonas syringae</i> pv. <i>syringae</i> B728a
		<i>Burkholderia</i> sp. H160
		<i>Ralstonia pickettii</i> 12J
<b>Genes associated with oxidative stress</b>	<i>ahpC</i>	<i>Chlorobium phaeobacteroides</i> DSM 266
		<i>Pseudomonas fluorescens</i> Pf-5
		<i>Dialister invisus</i> DSM 15470
		<i>Actinobacillus succinogenes</i> 130Z
		<i>Lachancea thermotolerans</i>
		<i>Acaryochloris marina</i> MBIC11017
	<i>ahpF</i>	<i>Magnetospirillum gryphiswaldense</i> MSR-1
		<i>Bifidobacterium animalis</i> subsp. <i>lactis</i> DSM 10140
		<i>Asticcacaulis excentricus</i> CB 48
	<i>katE</i>	<i>Stigmatella aurantiaca</i> DW4/3-1
		<i>Bacteroides plebeius</i> DSM 17135
		<i>Streptomyces pristinaespiralis</i> ATCC 25486
		<i>Sphingomonas wittichii</i> RW1
		<i>Methylovorus</i> sp. SIP3-4
		<i>Streptomyces ambofaciens</i> ATCC 23877
		<i>Ajellomyces capsulatus</i>
		<i>Colwellia psychrerythraea</i> 34H
		<i>Roseovarius</i> sp. HTCC2601
		<i>Providencia rettgeri</i> DSM 1131
		<i>Polaromonas naphthalenivorans</i> CJ2
		<i>Parabacteroides johnsonii</i> DSM 18315
	<i>oxyR</i>	<i>Streptomyces</i> sp. Mg1
		<i>Streptomyces</i> sp. C
		<i>Erwinia tasmaniensis</i> Et1/99
		<i>Corynebacterium jeikeium</i> K411
		<i>Aliivibrio salmonicida</i> LFI1238
<i>Capnocytophaga gingivalis</i> ATCC 33624		
<i>Dickeya dadantii</i> Ech703		

\*Variants in Table B-2 are arranged in the same order as indicated by black arrows in Figure 4 and Figure 5 (from bottom to top).

## Appendix C Investigation on other nanoparticles

### — Biochemical investigation on the antibacterial activity of aqueous nano-C<sub>60</sub> against

#### *Escherichia coli*

##### Introduction

Recent developments in nanotechnology enabled the fabrication of highly functional engineered materials with structure of the size  $\leq 100$  nanometers (*i.e.*, nanomaterials) for use in a variety of consumer products and industrial processes. Like any other chemical products, spent engineered nanomaterials find their way to the soils and aquatic environment, as well as to the biosphere. Health and safety implications of environmental nanomaterials have become a huge concern among consumers, industries, academics and regulatory agencies. A number of studies have reported substantial cytotoxicity of various nanomaterials, such as fullerenes, titanium dioxide, and silver, in bacteria, crustaceans, and mammalian cells (Zhao and Nalwa, 2007).

Recent studies showed that an aqueous suspension of nanometer-sized buckyball fullerene aggregates (nano-C<sub>60</sub>) has antibacterial activity toward various bacterial species, such as *Escherichia coli*, *Bacillus subtilis*, and *Pseudomonas aeruginosa* (Fortner *et al.*, 2005; Lyon *et al.*, 2005, 2008). The toxicity of fullerene in other aquatic organisms has also been reported (Pérez *et al.*, 2009). Because of the probable occurrence of nano-C<sub>60</sub> in the aquatic environment (Pérez *et al.*, 2009), it is highly important to understand the toxicity mechanisms of this industrially important nanomaterial.

Several pathways for the nano-C<sub>60</sub> toxicity have been proposed, such as physical penetration, oxidative stress via reactive oxygen species (ROS) generation and photo-sensitization (Johnston *et al.*, 2010). Recently, Lyon and Alvarez (2008) proposed that the antibacterial effect of nano-C<sub>60</sub> could be caused by ROS-independent protein oxidation. However, neither biochemical nor molecular data are currently available to support any of these toxicity mechanisms in bacteria. Additionally, our knowledge on the potential impact of the habitat conditions that are normally found in the soils and aquatic environment, such as the presence of natural organic matter (NOM), on bacterial biochemical response is still lagging. Thus, the major **objective** of this study is to investigate the biochemical mechanisms of the aqueous nano-C<sub>60</sub> antibacterial activity against *E. coli*. We adapted the *E. coli* Keio Knockout Collection to systematically analyze the effect of individual gene knockout on the survival of *E. coli* cells during C<sub>60</sub> treatment.

## **Materials and methods**

Purified C<sub>60</sub> (>99.9%) was purchased from MER Corporation (Tucson, AZ). Suwannee River humic acid (Standard II) and Suwannee River fulvic acid (Standard I) were purchased from the International Humic Substances Society (St. Paul, MN).

Two types of aqueous nano-C<sub>60</sub> suspensions were prepared. The first one was so-called “*THFC*<sub>60</sub>”, which was prepared by a tetrahydrofuran (THF) to water exchange protocol originally described by Deguchi *et al.* (2001). The average particle size of the prepared *THFC*<sub>60</sub> was 105.3 nm, indicating the presence of nanometer-sized aggregates of molecular

fullerene. The second one “*aquC<sub>60</sub>*” was prepared by direct dispersion in purified water by extended stirring for two weeks at ambient temperature. Both C<sub>60</sub> suspensions were filtered through 0.2 µm membrane filters. The concentration of C<sub>60</sub> was determined spectrophotometrically by measuring the absorbance at 330 nm ( $\log \epsilon = 4.71$ ) after destabilization with 4% sodium chloride followed by extraction with toluene (Deguchi *et al.*, 2001).

Two strains of *E. coli*, DH5 $\alpha$  and wild-type K-12 BW25113 (Genotype: *rrnB3*  $\Delta$ *lacZ4787* *hsdR514*  $\Delta$ (*araBAD*)567  $\Delta$ (*rhaBAD*)568 *rph-1*), maintained on Luria-Bertani (LB) agar plates and in LB broth, were used to test the toxicity of nano-C<sub>60</sub>. Modified minimum Davis (MMD) broth [0.7 g/L K<sub>2</sub>HPO<sub>4</sub>, 0.2 g/L KH<sub>2</sub>PO<sub>4</sub>, 1 g/L (NH<sub>4</sub>)<sub>2</sub>SO<sub>4</sub>, 0.1 g/L MgSO<sub>4</sub>·7H<sub>2</sub>O] that contained no carbon source was used as a medium for toxicity tests. An initial cell density of about 10<sup>5</sup> cfu/mL was used. All *E. coli* toxicity tests were conducted in triplicate and under aerobic conditions in the dark at 37°C. The viability of each strain after treatment was measured by heterotrophic plate counting (HPC) on LB agar.

In order to investigate the toxicity mechanisms of C<sub>60</sub> in *E. coli*, 46 strains of the *E. coli* Keio Knockout Collection (Thermo Scientific Open Biosystems) were used in this study, as well as their parent wild-type strain *E. coli* K-12 BW25113 (Baba *et al.*, 2006). The *E. coli* Keio Knockout Collection is a set of precisely defined, single-gene deletions of all non-essential genes in *E. coli* K-12. The complete collection comprises of a total of 7970 strains (Baba *et al.*, 2006). In this study, however, 46 mutant strains which are associated with carbon-source energy metabolism were tested.

The mutant toxicity tests required a replication step. First, a new 96-well plate with 160  $\mu\text{L}$  of LB-Lennox broth (low salt) per well was prepared. Each strain was inoculated from the source plate (frozen at  $-80^{\circ}\text{C}$ ) into a well on the new plate, and incubated without nano- $\text{C}_{60}$  at  $37^{\circ}\text{C}$  without shaking for 19 h. Subsequently, the mutant toxicity tests were performed with an initial cell density of about  $10^5$  cfu/mL. Diluted LB culture of each strain was inoculated into 200  $\mu\text{L}$  media with or without 0.2 mg/L *aquC*<sub>60</sub> and incubated at  $37^{\circ}\text{C}$  without shaking for 19 hours. The media used for the toxicity tests were 10% MMD. The viability of each strain after treatment was measured by comparing with its own control using HPC on LB agar.

## Results and discussion

Figure C-1a shows the dose-effect of nano- $\text{C}_{60}$  (*THFC*<sub>60</sub>) on the survival of *E. coli* DH5 $\alpha$  at  $37^{\circ}\text{C}$ . A  $>2$ -log reduction in cell viability was achieved with 1 mg/L of *THFC*<sub>60</sub> within 24 h. Humic acid and fulvic acid showed little or no impact on the  $\text{C}_{60}$  toxicity (Figure 1b), which is contradictory to the previous study by Li et al. (2008) which showed that as little as 0.05 mg/L of humic acid could eliminate the toxicity of 1 mg/L  $\text{C}_{60}$ .

Since an impact of THF on the antibacterial activity of nano- $\text{C}_{60}$  has been reported (Lyon *et al.*, 2006; Zhang *et al.*, 2009), the toxicity of *aquC*<sub>60</sub> was also tested (Figure C-2). A wild-type *E. coli* K-12 was used here to test the effect of  $\text{C}_{60}$  on an *E. coli* strain closer to natural ones. As shown in Figure 2, although its toxic effect was less pronounced than *THFC*<sub>60</sub>, *aquC*<sub>60</sub> showed clear growth inhibition as compared with untreated controls.

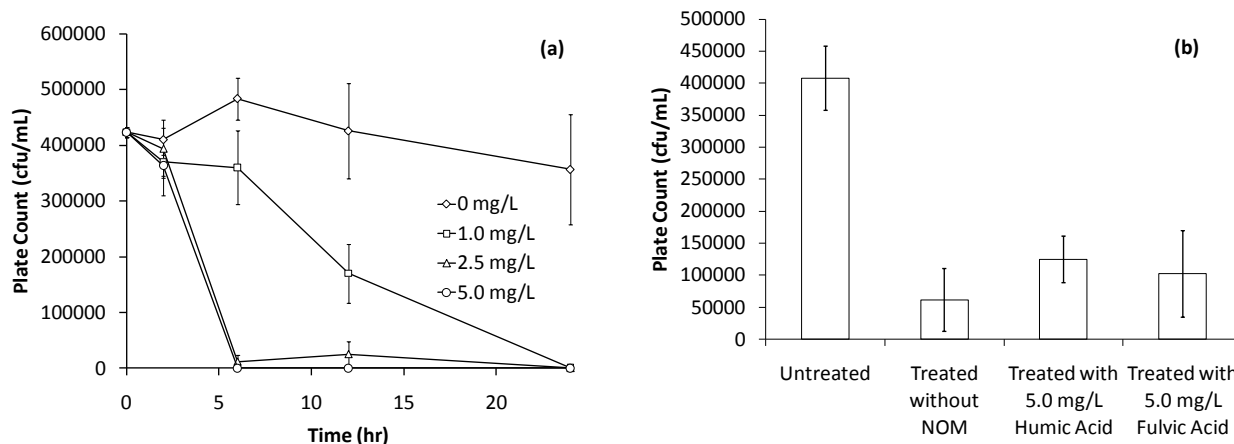


**Figure C-1.** The survival of *E. coli* DH5 $\alpha$  in the presence of THFC<sub>60</sub> in MMD broth (37°C, dark).

[(a) Effect of nano-C<sub>60</sub> dose, (b) effect of natural organic matter (NOM), treated with 2.0 mg/L nano-C<sub>60</sub> (except for “untreated”) and incubated for 10 h]. Error bars represent standard deviations ( $n = 3$ ).

Based on the result from the second toxicity test, an incubation time of 19 h was selected for the subsequent *E. coli* knockout (mutant) strain test. Also, *aquC*<sub>60</sub> was chosen for the test to eliminate any background effects due to residual THF in THFC<sub>60</sub> (Zhang et al., 2009; Johnston et al., 2010). Figure C-3 summarizes the result from the 46-mutant toxicity test.

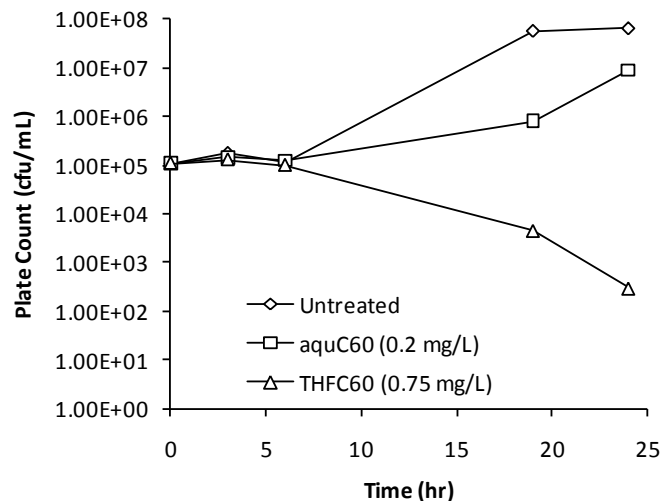


**Figure C-2.** The survival of *E. coli* K-12 BW25113 in the presence of *THFC*<sub>60</sub> and *aquC*<sub>60</sub> in MMD broth (37°C, dark).

It can be seen that the growth of most of the mutants, as well as the wild-type, were strongly inhibited in the presence of *aquC*<sub>60</sub>, with a few exceptions, including those mutants with *mdh*, *nuoK*, or *ppc* knocked-out (Figure C-3a, in the blue circle). Some strains were especially susceptible to the *aquC*<sub>60</sub> treatment, including *fumA*, *appC*, *appB*, and *nuoE* (Figure C-3b, in the purple circle). There were also a number of strains markedly more resistant to C<sub>60</sub> toxicity than the wild-type (Figure C-3a, in the green circles). See Table C-1 for the function of each gene.

It is interesting to note that both of the two "cytochrome bd-II oxidase" (*appB* and *appC*) knockout strains were more sensitive to *aquC*<sub>60</sub> treatment, which implies that cytochrome bd-II oxidase may help the cells to survive under the treatment. As nano-C<sub>60</sub> may induce an oxidative stress to cells (Sayes *et al.*, 2005), this is consistent with previous research indicating the role of cytochrome bd-II oxidase in protecting *E. coli* from oxidative stresses (Lindqvist *et al.*, 2000).

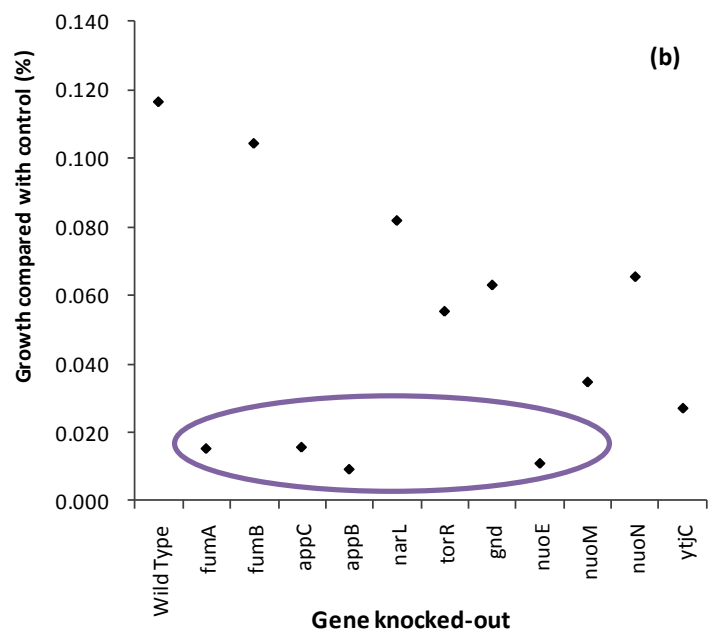
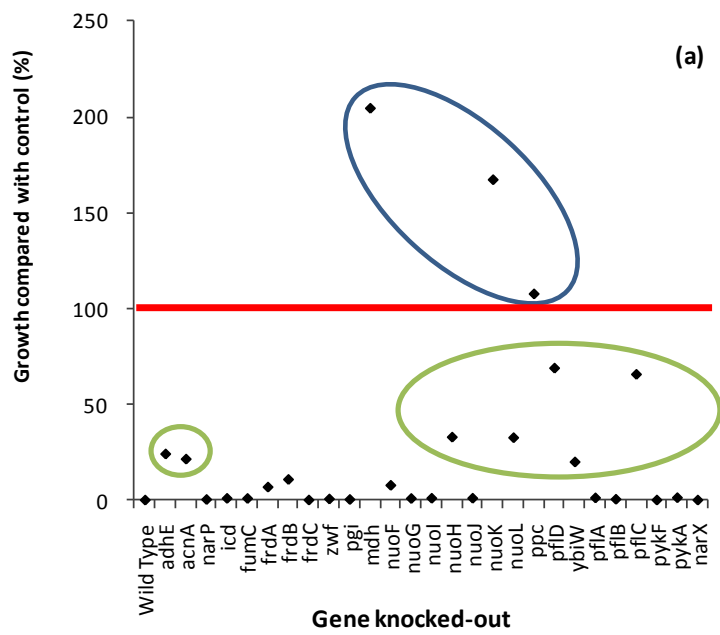


**Figure C-3.** Effects of *aquC*<sub>60</sub> treatment on the 46-knockout *E. coli* K-12 BW25113 mutants associated with carbon-source energy metabolism. [(a) Strains more resistant compared with the wild type, (b) Strains more sensitive compared with the wild type.]

**Table C-1.** Function of genes.

	<b>Gene</b>	<b>Function</b>
<b>Strains more sensitive compared with the wild type</b>	fumA	aerobic Class I fumarate hydratase (fumarase A)
	fumB	anaerobic class I fumarate hydratase (fumarase B)
	appC	cytochrome bd-II oxidase, subunit I
	appB	cytochrome bd-II oxidase, subunit II
	narL	DNA-binding response regulator in two-component regulatory system with NarX (or NarQ)
	torR	DNA-binding response regulator in two-component regulatory system with TorS
	gnd	gluconate-6-phosphate dehydrogenase, decarboxylating
	nuoE	NADH:ubiquinone oxidoreductase, chain E
	nuoM	NADH:ubiquinone oxidoreductase, membrane subunit M
	nuoN	NADH:ubiquinone oxidoreductase, membrane subunit N
ytjC	phosphoglyceromutase 2, co-factor independent	

**Table C-1.** Function of genes (continued).

	<b>Gene</b>	<b>Function</b>
	adhE	acetaldehyde-CoA dehydrogenase, NAD-dependent
	acnA	aconitate hydratase 1
	narP	DNA-binding response regulator in two-component regulatory system with NarQ or NarX
	icd	e14 prophage; isocitrate dehydrogenase, specific for NADP+
	fumC	fumarate hydratase (fumarase C), aerobic Class II
	frdA	fumarate reductase (anaerobic) catalytic and NAD/flavoprotein subunit
	frdB	fumarate reductase (anaerobic), Fe-S subunit
	frdC	fumarate reductase (anaerobic), membrane anchor subunit
	zwf	glucose-6-phosphate dehydrogenase
	pgi	glucosephosphate isomerise
<b>Strains more resistant compared with the wild type</b>	mdh	malate dehydrogenase, NAD(P)-binding
	nuoF	NADH:ubiquinone oxidoreductase, chain F
	nuoG	NADH:ubiquinone oxidoreductase, chain G
	nuoI	NADH:ubiquinone oxidoreductase, chain I, FeS
	nuoH	NADH:ubiquinone oxidoreductase, membrane subunit H
	nuoJ	NADH:ubiquinone oxidoreductase, membrane subunit J
	nuoK	NADH:ubiquinone oxidoreductase, membrane subunit K
	nuoL	NADH:ubiquinone oxidoreductase, membrane subunit L
	ppc	phosphoenolpyruvate carboxylase
	pflD	predicted formate acetyltransferase 2 (pyruvate formate lyase II)
	ybiW	predicted pyruvate formate lyase
	pflA	pyruvate formate lyase activating enzyme 1
	pflB	pyruvate formate lyase I
	pflC	pyruvate formate lyase II activase
	pykF	pyruvate kinase I
	pykA	pyruvate kinase II
	narX	sensory histidine kinase in two-component regulatory system with NarL

Also, it is possible that enzymes associated with tricarboxylic acid (TCA) cycle are targets of C<sub>60</sub>, especially in the steps of the TCA cycle involving NAD<sup>+</sup>/NADH and pyruvate. First of all, controls of mutants with these genes knocked out did not grow as well as the wild type strain, because of the reduction of energy production. However, compared with their own controls,

these mutants grew better than the wild-type strain under treatment (i.e., mutants in green circles), especially mutants with certain membrane subunits of "NADH:ubiquinone oxidoreductase" knocked out. This may indicate that some membrane subunits are targets of C<sub>60</sub> and that the lack of these targets helps the survival of *E. coli* under the *aquC*<sub>60</sub> treatment. In addition, the reduction of viability of the wild-type strain may result from the synergistic effects of several genes. In regard to the most resistant mutant strains, genes knocked out in these strains are actually closely associated with each other. For example, mutants with "malate dehydrogenase, NAD(P)-binding" (*mdh*) and "NADH:ubiquinone oxidoreductase" (*nuoK*) genes knocked out survived significantly better than the wild-type strain, and both of these two genes are involved in the recycle of NAD<sup>+</sup>/NADH. Lack of "NADH:ubiquinone oxidoreductase" can affect the recycle of NAD<sup>+</sup> and result in high ratio of NADH/NAD<sup>+</sup> (Friedrich, 1998). Consequently, deficiency in NAD<sup>+</sup> may lower the activity of NAD(P)-binding malate dehydrogenase, which further decrease the viability of the wild-type strain. There is also evidence in transferring of NADH from malate dehydrogenase to "NADH:ubiquinone oxidoreductase", which indicates that impacts on malate dehydrogenase may also result in lower activity of "NADH:ubiquinone oxidoreductase" (Amarneh and Vik, 2005).

## **Conclusions**

The antibacterial activity nano-C<sub>60</sub> against *E. coli* was investigated in this study. The nano-C<sub>60</sub> prepared by a solvent to water exchange method using THF as a dispersant was very toxic to *E. coli*, which is consistent with previous studies. A >2-log reduction in cell viability

was achieved with 1 mg/L of nano-C<sub>60</sub> within 24 hours. The addition of humic acid and fulvic acid had little or no impact on the C<sub>60</sub> toxicity. These results indicate that C<sub>60</sub> may pose a significant hazard to microorganisms in the environment.

Two potential target proteins of C<sub>60</sub> were identified, namely NADH:ubiquinone oxidoreductase and NAD(P)-binding malate dehydrogenase, by a systematic analysis of 46 mutant strains of *E. coli* K-12 BW25113 (the Keio Knockout Collection). These two enzymes are known to be involved in the TCA cycle. Thus, it may be speculated that an exposure to nano-C<sub>60</sub> disrupts the TCA cycle in *E. coli*, which results in the observed growth inhibition. Also, the high sensitivity of two cytochrome bd-II oxidase knockout strains toward nano-C<sub>60</sub> involvement supports the oxidative stress mediated mechanism of nano-C<sub>60</sub> toxicity.

Testing of additional knockout strains from the Keio Collection, combined with other systematic analyses of protein/gene targets, may yield more cellular targets of C<sub>60</sub> and further reveal the mechanisms of nano-C<sub>60</sub> toxicity and antibacterial activity.

## VITA

### Zhiya SHENG

---

#303 11435 41 Avenue NW, Edmonton, AB, T6J0T9; **Tel:** (780) 695 – 5190; **Email:**

[zhiya@ualberta.ca](mailto:zhiya@ualberta.ca)

### Education

---

- **PhD (ABD), Environmental Engineering** **Jan. 2011 – Present**  
University of Alberta – *Edmonton, AB, Canada* **GPA 3.9/4.0**
- **MSc, Environmental Engineering** **Sept. 2009 – Dec. 2010**  
University of Alberta – *Edmonton, AB, Canada* Transferred to PhD program in Jan. 2011
- **BSc, Biological Science** **Sept. 2002 – July 2006**  
China Agricultural University –*Beijing, China* **GPA 3.7/4.0**

### Relevant Work/Research Experience

---

- **University specialist, Environmental engineering** **Sept. 2007 – July. 2009**  
Gold Bar Wastewater Treatment Plant – *Edmonton, AB, Canada*
- **Technician, computational chemistry** **Sept. 2007 – July. 2009**  
Dr. Niu Huang's Lab, The National Institute of Biological Sciences, Beijing – *Beijing, China*
- **Research assistant, computational biology** **Sept. 2006 – Aug. 2007**  
Bioinformatics Center, China Agricultural University –*Beijing, China*

- **Graduation Project, computational biology** **Mar. 2006 – June 2006**

Structural Bioinformatics Laboratory, China Agricultural University –*Beijing, China*

- **Undergraduate Research Program (URP)** **Sept. 2004 – July 2005**

Academician Chen Wenxin's laboratory, China Agricultural University –*Beijing, China*

### **Academic Honors**

---

#### **May 2010 – Dec. 2010**

Alberta Innovates Graduate Student Scholarship, MSc, NANO (\$30,000 p.a. & \$5000 p.a. res. allow.)

#### **Jan. 2011 – Aug. 2014**

Alberta Innovates Graduate Student Scholarship, PhD, NANO (\$36,000 p.a. & \$5000 p.a. res. allow.)

#### **Sept. 2004–July 2006**

City of Beijing "tri-merit student" honor (rate 1/104); Excellent Youth League Leader

#### **Sept. 2003–Sept. 2004**

China Agricultural University "tri-merit student" honor (15%); State Training Base Scholarship (2/60); Scholarship for excellence in study (Second Prize) (15%); Honor for Progress in Study Prize for outstanding English

#### **Sept. 2002–Sept. 2003**

China Agricultural University "tri-merit student" honor (15%); Scholarship for excellence in study (Second Prize) (15%)

## **Publications**

---

### **Articles published in or submitted to refereed journals:**

1. Sheng, Z.; Mohammed, A.; Liu, Y. (2016). "Stability of full-scale engineered ecosystem under disturbance: Response of an activated sludge biological nutrient removal reactor to high flow rate condition." *International Biodeterioration & Biodegradation* 109: 88-95.
2. Sheng, Z.; Liu Y. (2015) Insights into the Effects of Silver Nanoparticles on Bacteria and Biological Wastewater Treatment. (submitted)
3. Sheng, Z.; J. D. Van Nostrand; Zhou J.; Liu Y (2015). The effects of silver nanoparticles on intact wastewater biofilms. *Frontiers in Microbiology* 6: 680.
4. Sheng, Z.; J. D. Van Nostrand; Zhou J.; Liu Y. (2014) Contradictory effects of silver nanoparticles on activated sludge wastewater treatment. (submitted)
5. Liu, H.; Tan, S.; Sheng, Z.; Liu, Y.; Yu, T. (2014) Bacterial community structure and activity: sulfate reducing bacteria in a membrane aerated biofilm analyzed by microsensor and molecular techniques. *Biotechnology and Bioengineering*, doi: 10.1002/bit.25277
6. Liu, H.; Tan, S.; Sheng, Z.; Liu, Y.; Yu, T. (2013) Distribution and activity of sulfate reducing bacteria in oxygen-based membrane aerated biofilm. (submitted and under revision)
7. Liu, H.; Tan, S.; Sheng, Z.; Yu, J.; Yu, T.; Liu, Y. (2013) Impact of oxygen on the co-existence of nitrification, denitrification, and sulfate reduction in oxygen based membrane aerated biofilm. (submitted)

8. Sun, X.; Sheng, Z.; Liu, Y. (2013) Effects of silver nanoparticles on microbial community structure in activated sludge. *Science of the Total Environment*, 443: 828-835
9. Hwang, G.; Dong, T.; Islam, M.; Sheng, Z.; Pérez-Estrada, L.; Liu, Y.; Gamal El-Din, M. (2013) The impacts of ozonation on oil sands process-affected water biodegradability and biofilm formation characteristics in bioreactors. *Bioresource Technology*, 130: 269–277
10. Sheng, Z.; Liu, Y. (2011) Effects of silver nanoparticles on wastewater biofilms. *Water Research*, 45(18): 6039-6050.
11. Zhang Z.; Tang Y.; Sheng Z.; Zhao D. (2009) An overview on de novo predicting the catalytic residues of an enzyme, *Current Bioinformatics*, 4: 197-206.
12. Tang Y.; Sheng Z.; Chen Y.; Zhang Z. (2008) An improved prediction of catalytic residues in enzyme structures, *Protein Engineering, Design and Selection*, 21: 295–302. (A piece of work published as co-first author, in which I did all the research from data collecting to predictor training and testing under Prof. Zhang's guidance, and wrote the manuscript. Yu-Rong Tang provided her software of GANN, a genetic algorithm integrated neural network, and advice on how to use it.)
13. Chen Y.; Tang Y.; Sheng Z.; Zhang Z. (2008) Prediction of mucin-type O-glycosylation sites in mammalian proteins using the composition of k-spaced amino acid pairs, *BMC Bioinformatics*, 18:101.
14. Wang H.; Sheng Z.; Sui X.; Chen W. (2006) Adoption of *gfp* marker gene method to study Soybean *Rhizobium* and the state of nodulation residence on soybean root, *Journal of Microbiology*, 26: 1-4.

### **Conference proceedings**

1. Sun, X.; Sheng, Z.; Liu, Y. Understanding the effect of silver nanoparticles on wastewater activated sludge microorganisms. 12th International Environmental Specialty Conference. Edmonton, AB, Canada. June 6-9, 2012, ENV-1009-1 to ENV-1009-7
2. Liu, H.; Tan, S.; Sheng, Z.; Liu, Y.; Yu, T. Distribution and Activity of Sulfate Reducing Bacteria in Membrane Aerated Biofilm Analyzed by Molecular Techniques and Microsensor Measurements. IWA Biofilm Conference 2011: Processes in Biofilms. Shanghai, China. October 27-30, 2011.
3. Ikehata, K.; Sun, R.N.; Sheng, Z.; Stuart, D.; Liu, Y. Biochemical investigation on the antibacterial activity of aqueous nano-C<sub>60</sub> against *Escherichia coli*, IWA World Water Congress and Exhibition, Montréal, QC, Canada, 2010, manuscript number: IWA- 3141R1.
4. Tang Y.; Chen Y.; Sheng Z.; Zhang Z. Predicting protein phosphorylation sites with neural-genetic network algorithm, in The 1st IEEE International Conference on Bioinformatics and Biomedical Engineering (ICBBE 2007), Wuhan, July 2007.

### **Poster and oral presentations:**

1. Sheng, Z.; Liu Y. Accumulation dynamics of silver nanoparticles in activated sludge and the corresponding effects. 248th ACS National Meeting & Exposition: ENVR, Division of Environmental Chemistry. San Francisco, CA, US. August 10-14, 2014. (Oral presentation)
2. Sheng, Z.; Liu Y., What is the magic? — Shift and recovery of microbial community in a full-scale wastewater treatment plant under a significantly increased flow rate. 248th ACS

- National Meeting & Exposition: ENVR, Division of Environmental Chemistry. San Francisco, CA, US. August 10-14, 2014. (Oral presentation)
3. Sun, X.; Sheng, Z.; Liu, Y., Understanding the effect of silver nanoparticles on wastewater activated sludge microorganisms. 12th International Environmental Specialty Conference: ENV-1009-1 to ENV-1009-7. Edmonton, AB, Canada. June 6-9, 2012. (Oral presentation)
  4. Liu, H.; Tan, S.; Sheng, Z.; Liu, Y.; Yu, T., Distribution and activity of sulfate reducing bacteria in membrane aerated biofilm analyzed by molecular techniques and microsensor measurements. IWA Biofilm Conference 2011: Processes in Biofilms. Shanghai, China. October 27-30, 2011. (Oral presentation)
  5. Sheng, Z.; Liu, Y., The effects of silver nanoparticles on wastewater biofilms. Goldschmidt 2011: Engineered Nanomaterials in the Environment — strategies to understand their behaviour and impact in environmental and biological media. Prague, Czech Republic. August 14-19, 2011. (Poster)
  6. Liu, H.; Tan, S.; Sheng, Z.; Liu, Y.; Yu, T., Distribution and activity of sulfate reducing bacteria in membrane aerated biofilm analyzed by molecular techniques and microsensor measurements. 2nd Faculty of Engineering Graduate Research symposium. Edmonton, AB, Canada. June 26, 2011. (Oral presentation)
  7. Liu, H.; Sheng, Z.; Yu, T.; Liu, Y., Analysis of the vertical distributions of sulfate reducing bacteria within MABR biofilms based on molecular techniques. The Edmonton Waste Management Centre of Excellence Annual Research Day. Edmonton, AB, Canada. February 24, 2011. (Oral presentation)

8. Ikehata, K.; Sun, R.N.; Sheng, Z.; Stuart, D.; Liu, Y. Biochemical investigation on the antibacterial activity of aqueous nano-C<sub>60</sub> against *Escherichia coli*. 2010 World Water Congress & Exhibition. Montréal, QC, Canada. October 19-24, 2010. (Poster)
9. Sheng Z.; Liu Y., Application of molecular biology techniques for analyzing the effects of nano-silver on wastewater biofilms. The 84th ACS Colloid and Surface Science Symposium: Nano and Colloidal Materials: Environmental Applications and Implications. Akron, OH, US. June 20-23, 2010. (Oral presentation)
10. Tang Y.; Sheng Z.; Chen Y.; Zhang Z. An Improved Prediction of Active Sites in Enzymes. The 6th “TICPS” International Conference of Protein Science. Shanghai, China. November 9-11, 2007. (Prepared and presented by me.)